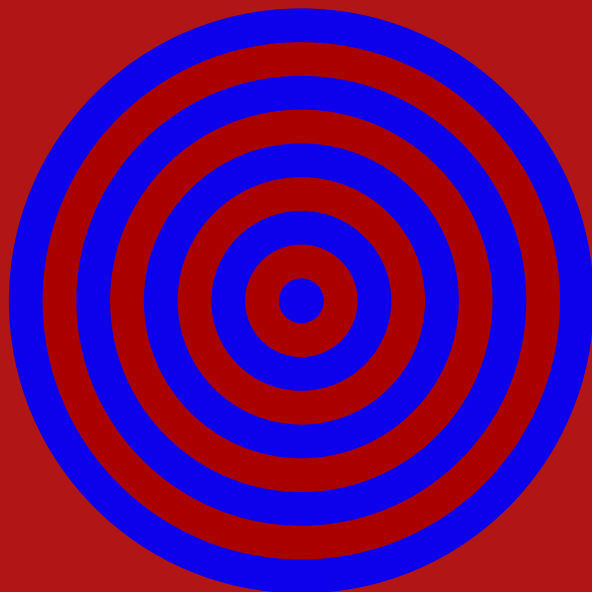


L. V. Tarasov

Laser Physics and Applications



MIR PUBLISHERS

Laser Physics and Applications

Л В. Тарасов
ЛАЗЕРЫ И ИХ ПРИМЕНЕНИЕ

Москва «Радио и связь»

L. TARASOV

Laser Physics and Applications



MIR PUBLISHERS MOSCOW

*First published 1986
Revised from the 1983 Russian edition*

Translated from the Russian by
M. Edelev

The Greek Alphabet

A α	Alpha	I ι	Iota	P ρ	Rho
Δ β	Beta	K κ	Kappa	Σ σ	Sigma
Γ γ	Gamma	Λ λ	Lambda	T τ	Tau
Δ δ	Delta	M μ	Mu	Υ υ	Upsilon
Ε ε	Epsilon	N ν	Nu	Φ φ	Phi
Z ζ	Zeta	Ξ ξ	Xi	X χ	Chi
Η η	Eta	O ο	Omicron	Ψ ψ	Psi
Θθυ	Theta	Π π	Pi	Ω ω	Omega

На английском языке

© Издательство «Радио и связь», 1983.
© English translation, Mir Publishers, 1986.

Printed in the Union of Soviet Socialist Republics

Contents

Preface	7
Chapter 1. BASIC LASER PRINCIPLES	9
1.1 Light Waves and Photons	9
1.2 Optical Coherence	14
1.3 Quantum Transitions in Absorption and Emission of Light	18
1.4 The Active Medium. Creating a Population Inversion	22
1.5 Laser Oscillation in Optical Resonant Cavity	27
1.6 Basic Laser Characteristics	33
1.7 A Historical Review of the Laser	41
Chapter 2. TYPES OF LASERS	45
2.1 A Laser Exposition. Pumping Methods	45
2.2 Solid State Lasers	47
2.3 Organic Dye Lasers	53
2.4 Photodissociation Lasers	55
2.5 Ion and Atomic Lasers	57
2.6 Molecular Lasers	65
2.7 Electroionization Lasers	70
2.8 Gas Dynamic Lasers	73
2.9 Chemical Lasers	76
2.10 Plasma Lasers	79
2.11 Semiconductor Lasers	81
2.12 Confinement of the Beam within the Resonator	89
Chapter 3. CONTROL OF THE LASER OUTPUT	94
3.1 Intracavity Control of Spectral Characteristics	94
3.2 Methods of <i>Q</i> -switching	100
3.3 Pulsed Lasing	106
3.4 Mode Locking for Ultrashort Pulses	111
3.5 Modifying the Spatial Structure of the Laser Output	116
3.6 Frequency Transformations in Nonlinear Media	118

3.7 Wavefront Correction of the Laser Output	129
3.8 Light Beam Manipulation	134
Chapter 4. APPLICATIONS OF LASERS	138
4.1 Material Working	139
4.2 Lasers in Medicine	145
4.3 Isotope Separation	148
4.4 Holography	150
4.5 Information Related Applications	157
4.6 Optical Communications	16
4.7 Ranging and Measurement	168
4.8 Environmental Measurements. Quality Control	173
4.9 Thermonuclear Fusion	178
Exercises	181
Performance Data for Selected Soviet-made Commercial Lasers	184
Index	188

Preface

Among the outstanding achievements of science and engineering in the 20th century, the laser occupies by right a major position. First lasers made in 1960 paved the way for the vehement development of laser technology. Today, lasers and laser systems find wide use in many fields of science and engineering. They are employed in communications systems, computers, navigation equipment, measuring instruments, and in complicated technological processes. Biology, medicine, and various chemical and physical investigations utilize lasers to advantage.

Wide use of lasers in science and technology is due to the specific properties of laser radiation. The laser is a generator of coherent light. Unlike other sources of light, such as incandescent lamps or arc lamps, the laser produces radiation with a highly regular light field, outstanding in its high coherence, monochromaticity and directivity.

The discussion of lasers in this book begins with the evaluation of the physics of processes resulting in coherent optical radiation in the laser. This is the subject to Chapter 1. Chapter 2 takes up the classification of lasers and the physical and engineering benefits of various types of lasers. Application of lasers puts in the forefront the control of laser radiation. This includes not only such aspects of beam control as deflection, scanning and modulation, but also the

variation of the regime of oscillation to produce radiation with the desired spatial, temporal, frequency and power characteristics. All these topics are treated in Chapter 3. Finally, Chapter 4 is concerned with diverse applications of lasers in science and engineering.

Chapter 1

Basic Laser Principles

1.1 Light Waves and Photons

Light Waves. The notions of light or optical radiation relate to electromagnetic waves whose wavelengths occupy the range from $0.01 \mu\text{m}$ to $100 \mu\text{m}$ ($1 \mu\text{m} = 10^{-6} \text{ m}$). These e.m. waves are referred to as light waves. Of these we can see only visible light ranging in wavelengths from $0.4 \mu\text{m}$ to $0.75 \mu\text{m}$. The adjacent range of lower wavelengths, $\lambda < 0.4 \mu\text{m}$, belongs to ultraviolet light, whereas that of longer wavelengths, $\lambda > 0.75 \mu\text{m}$, to infrared light.

Let us recall some properties of electromagnetic waves. The e.m. wave is a system of periodically varying electric

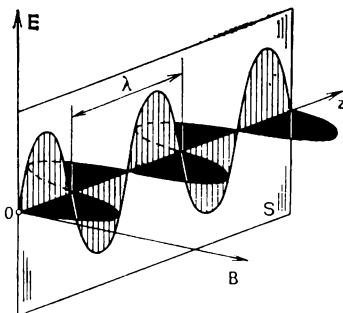


Fig. 1.1 Schematic presentation of a plane electromagnetic wave which is ideally monochromatic and polarized. Its plane wavefront is normal to the direction of travel (here the z axis)

and magnetic fields oscillating at right angles to each other and to the direction of propagation of the wave, travelling at the velocity of light. A snapshot of a section of such a system is shown in Fig. 1.1. It presents an e.m. wave propagating in the z direction. The electric field in the wave is defined by the vector of electric field strength E , and the magnetic field by the vector of magnetic induction B .

Another way of saying this is that the vectors **E** and **B** oscillate in an e.m. wave and these oscillations are in mutually perpendicular planes. The frequency ν of these oscillations is related with the wavelength by

$$\nu = v/\lambda \quad (1.1)$$

where v is the velocity of wave propagation (velocity of light) in the medium. It will be recalled that

$$v = c/n \quad (1.2)$$

where n is the refractive index of the medium, and c is the velocity of light in vacuum, numerically equal to 3×10^8 m/s.

Vectors **E** and **B** are of equal significance to the wave. However, photochemical, photoelectric, and physiologic effects of light are mainly due to the electric component **E**. Therefore, in what follows we shall confine ourselves to the discussion of vector **E**. The plane in which it oscillates (S in Fig. 1.1) will be referred to as the *plane of polarization* of the wave.

Figure 1.1 shows an idealized representation of an e.m. wave. It is strongly monochromatic, i.e., has a definite wavelength λ and a definite frequency ν , possesses a plane wavefront (perpendicular to the z direction) and is ideally polarized, that is, the oscillations of vector **E** occur in one plane. This is a *plane, monochromatic, polarized wave*. Such waves exist only in popular books and textbooks. An actual wave emitted by a real source of light always has a certain spread in frequency over an interval of values, and its wavefront is never ideally plane. In addition, actual light waves do not possess normally a plane of polarization, i.e., they are unpolarized waves. Such are in particular the light waves emitted by the sun, a flame, and an incandescent lamp.

The actual light wave may be treated as a collection of plane monochromatic polarized waves of various frequencies, directions of propagation, and polarization planes. This descriptive approach is often used, though it is formal to a some degree. It would be more correct physically to represent an actual light wave as a stream of microparcelles of light, called *photons*, which possess a certain structure

defined by the distribution of the photons among different energy states.

Photons. The photon has a definite place in the list of elementary particles. It has neither rest mass nor electric charge. In any reference frame the velocity of the photon is equal to the velocity of light in vacuum. Like any other elementary particle, the photon denies a three-dimensional representation. There is no point in asking how the photon looks like, or what its structure is alike. Therefore we confine ourselves to the simple question, namely, what should be determined for the photon to be defined?

To be able to do so, we need first of all to know the energy of the photon, ϵ , and its direction of motion. This implies that the photon may be defined by its momentum \mathbf{p} . The direction of vector \mathbf{p} indicates the direction of travel of the photon, the modulus of \mathbf{p} being the energy of the photon divided by the velocity of light in vacuum

$$p = \epsilon/c \quad (1.3)$$

In addition, we need to specify the polarization of the photon. Now we denote it by γ deferring its definition until later paragraphs. So far we note that this characteristic assumes only two values reflecting two possible photonic polarizations.

Thus, to define a photon, we need to specify four quantities: the three projections of the momentum (p_x , p_y , p_z) and the polarization γ . From expression (1.3) it is an easy matter to see that this definition also specifies the energy of the photon $\epsilon = pc = c(p_x^2 + p_y^2 + p_z^2)^{1/2}$. When two photons have identical sets of the quantities p_x , p_y , p_z , and γ then these photons are said to be in the same state. Accordingly, these four quantities may be viewed as the characteristics of photonic states. The conversion from one photon state to another involves altering at least one of these quantities in value.

Two photons are discernible only when they are in different states. All photons occupying the same state are indiscernible in principle.

It is important to note that the characteristics of a photon state correspond to the characteristics of a plane monochromatic polarized light wave. The direction of the photon's momentum coincides with that in which the wave pro-

pagates. The polarization of the photon corresponds to the polarization of the wave. Two possible values for photon polarization represent two independent states of wave polarization (we speak here of two states of wave polarization in two perpendicular planes). The statement "a photon is in the state of polarization $\gamma = \gamma_1$ " implies that the photon belongs to a light wave of exactly this polarization. In terms of frequency, the photon energy is as follows:

$$\epsilon = h\nu \quad (1.4)$$

where h is the Planck constant, $h = 6.626 \times 10^{-34}$ J s. Upon substitution of (1.4) into (1.3) we get

$$p = h\nu/c = h/\lambda \quad (1.5)$$

Equations (1.4) and (1.5) reflect the dual nature of radiation. These relationships combine the characteristics of a microparticle (corpuscle or quantum) ϵ and p with the wave characteristics ν and λ . Essentially, these are two models to explain the phenomenon of light. According to Bohr, they are complementary, and connected mathematically by means of Planck's constant h .

Thus, a plane, monochromatic, polarized, light wave is an ensemble of photons occupying the same state. To various states of photons there correspond various plane monochromatic waves.

Fermions and bosons. All microparticles existent in nature may be divided into two groups according to their behaviour in the ensemble of the like, or, as physicists say, according to their statistical properties. In one group, microparticles behave as extreme individuals—if one state is occupied by one microparticle it is denied to all the other particles of this ensemble. In other words, one state can be populated by one such particle only.

In the other group, microparticles behave in the ensemble differently—they not only populate one and the same state in an unlimited number, but the probability of them occupying a state is the greater the more such particles are already in this state. Stated another way, these microparticles tend to accumulate in separate states.

The microparticles of the first group are called *fermions* (in deference to E. Fermi, an outstanding Italian physicist),

whereas the microparticles of the other group are called *bosons* (after the Indian physicist S.N. Bose). Electrons, for example, belong to fermions. Note, that it is this statistics of electrons, called the Fermi-Dirac statistics, that caused the familiar distribution of electrons in electron orbitals of the atom, where, moving away from the nucleus, the number of electrons in the filled electron shells increases as 2, 8, 18 . . . The thing is that each electron orbital is able to lend to electrons only a definite number of electron states, namely, 2, 8, 18, and so on. If electrons could populate one state in a number higher than unity, all electrons in all atoms would occupy the level with the least possible energy. As a result, all the variety of chemical elements would disappear.

Photon ensembles obey other laws than electrons, as they belong to bosons. The more photons are in a given state the higher the probability that new photons will occupy this particular state. In the following paragraphs we shall see that the boson nature of the photon statistics is of extreme importance for optical phenomena.

Photons and light waves. Consider a photon state of momentum p and polarization γ ; we shall call it the $p\gamma$ -state. To this state there corresponds a plane, monochromatic, polarized, light wave; we shall call it the $p\gamma$ -wave. Let $N_{p\gamma}$ be the number of photons occupying the $p\gamma$ -state within an elementary volume. When

$$N_{p\gamma} \gg 1 \quad (1.6)$$

that is, the given photon state contains very many photons, we may neglect the discrete, quantum, structure of the radiation and treat it as "continuous medium", or a plane, monochromatic, polarized wave of light (a polarized $p\gamma$ -wave). Until the condition (1.6) is met, however, the discrete structure of the radiation field may not be neglected.

Thus, the possibility of the existence of light waves is associated with how densely photons populate their states. It is a simple matter to see that the existence of light waves immediately follows from the boson nature of the photon statistics. If photons were fermions, each photon state could accommodate only one photon.

1.2 Optical Coherence

“Disordered” light waves. Wave trains. Actual light consists of many photons in a variety of states. These are emitted by various atoms of emitting substance, which radiate independently so that the emitted photons differ in their energy, direction of momentum, and polarization. In loose terms, a radiation combined of such photons may be

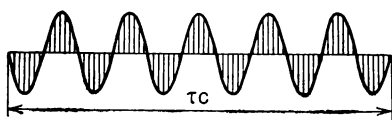


Fig. 1.2 A wave train may be imagined as a piece of a monochromatic wave. A wave train corresponds to a certain photonic state

called “disordered”. It cannot be represented by a plane monochromatic wave. Light waves from such random emitters exhibit a wide spread of photons over various states.

A disordered light wave is often modelled as a set of the so-called wave packets, or trains. Assume that the photons that make up a radiation are distributed (imaginary, of course) into groups each of which contains a rather large number of photons in the same state. Each such group represents a wave train. For simplicity of consideration a wave train is shown graphically as a piece of a plane monochromatic wave whose characteristics are those of the given photon state. The population of this state, i.e., the number of photons in the train, is represented conditionally as the length of the wave train. To the greater number of photons in a considered state there corresponds a longer wave train. Fig. 1.2 schematizes a wave train of duration τ and spatial length τc .

Coherence of light waves. The more disordered a light wave, the less it suits for producing an interference pattern in Young’s experiment with two illuminated pinholes. The ability of a wave to produce interference fringes may be categorized by measuring the fringe contrast, called the fringe visibility, and defined as the ratio

$$V = (I_{\max} - I_{\min})/(I_{\max} + I_{\min}) \quad (1.7)$$

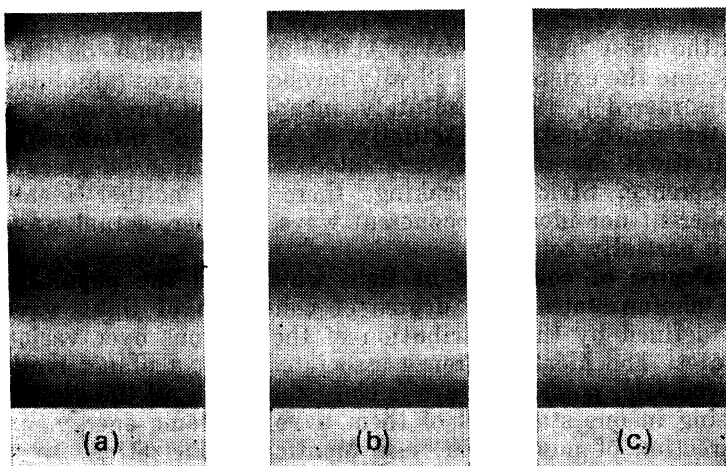


Fig. 1.3 Interference patterns demonstrating various visibilities, the degree of coherence of the beam decreasing from (a) to (c)

where I_{\max} is the irradiance* at the centre of a light fringe, and I_{\min} is the irradiance at the centre of a dark fringe. The maximum visibility $V = 1$ takes place when $I_{\min} = 0$. The minimum visibility is observed at $I_{\max} = I_{\min}$, when simply no interference pattern is evident. The higher the "capacity" of a wave to produce interference fringes, the higher the visibility, that is, the closer is its value to unity. Comparison of interference patterns is presented in Fig. 1.3 where the visibility declines from (a) to (c).

In order to measure the ability of light waves to produce interference fringes an important characteristic is introduced—the degree of coherence of a light wave. The higher the degree of coherence, the more likely will the wave provide a contrast interference pattern. A decrease in the degree of coherence of a light beam corresponds to an increase in its internal "disorder".

The plane, monochromatic, polarized, light wave is an ideally coherent wave. It possesses the greatest capacity to

* The quantity that describes the power incident on a unit area, popularly known as the "intensity" of the light, is properly called the *irradiance* in radiometry and measured in watts/m². Here we shall adhere to this term.

produce interference fringes in Young's experiment. This is the most "regular" wave. At the other extreme, one may assume the existence of ideally incoherent waves (absolutely "disordered"), i.e., absolutely incapable of producing an interference pattern. Actually, a variety of intermediate situations are realized, associated with various degrees of coherence. Strictly speaking, there exist neither ideally coherent nor ideally incoherent waves, rather, actual waves are partially coherent.

Degree of coherence of light waves and the population of photon states. The degree of coherence of light waves is defined by the distribution of the photons over various states. The ideal coherence associated with a plane, monochromatic, polarized wave is consistent with all the photons being in one state: all of them have the same energy, one direction of momentum, and identical polarization. In an actual light wave photons occupy different states, some of them being more populated, others less. The higher this selectivity (inhomogeneity) of population of photon states, that is, the more some states are populated at the expense of the others (which remain completely or almost free), the higher the degree of coherence of the radiation. For actual light beams this means that the degree of coherence is higher, the higher the monochromaticity, and the lower the degree of divergence, and the higher the degree of polarization.

The degree of non-monochromaticity of a wave may be defined as the relative bandwidth

$$\xi = \Delta v / v_0 \quad (1.8)$$

where v_0 is the central frequency of the wave, and Δv the interval of frequencies describing the spread of frequencies about the mean value (it is associated with the spread of photon energies $\Delta \epsilon = h \Delta v$). The degree of divergence is measured as the angle of the cone confining the light wave, also called the angle of divergence. The closer the wave-front's shape to a plane, the smaller the angle of divergence. The degree of polarization of a light wave is determined experimentally by a polarizer, say, a special crystal which passes through those waves whose electrical vector oscillates in a certain plane. By rotating the crystal, the experimenter can measure the irradiance of light passed through the crystal in its various orientations to find the maximum

(I_{\max}) and minimum (I_{\min}) irradiance values. The degree of polarization then may be defined as

$$P = (I_{\max} - I_{\min})/(I_{\max} + I_{\min}) \quad (1.9)$$

The degree of non-monochromaticity and the time interval τ consistent with the length of the wave trains of this wave are related as

$$\xi \approx 1/\tau v_0 \quad (1.10a)$$

Observing (1.8) we may recast this expression as

$$\Delta\nu \approx 1/\tau \quad (1.10b)$$

The quantity τ is referred to as coherence time. The longer the coherence time the higher the coherence of the beam of light.

Coherent phenomena in the prelaser optics. The optics of prelaser time is often called incoherent optics. This name is

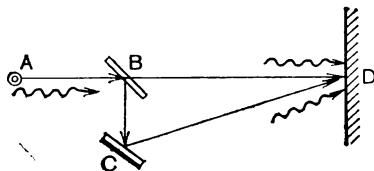


Fig. 1.4 Experimental arrangement to observe interference between parts of the same wave train

fairly conditional—one should speak of a small degree of coherence. However small is this degree, this coherence can, in principle, always be used to produce an interference pattern. It is not surprising, therefore, that interference of light was observed in the prelaser optics with ordinary light sources.

Let us refer to the representation of light waves by means of wave trains. Various trains emitted by a source of light though interfere with each other fail to produce a stable visible interference pattern. One can, however, produce a constructive interference pattern by making portions of the same train meet on the interference plane. The arrangement of an experiment producing such an interference pattern is shown in Fig. 1.4. In this figure, A is a source of light, B a semitransparent mirror, known as a beamsplitter,

C a totally reflecting mirror, and *D* the interference plane—just a white screen. Beamsplitter *B* splits a wave train, while mirror *C* reflects the divergent train into the point where the transmitted train is to arrive. In order that the portions of the same train, rather than different trains, meet at the interference screen, the condition must be satisfied

$$L < \tau c \quad (1.11)$$

where τc is the train length, L the pathlength difference which the portions of the train acquire in their travel to *D*, being in our experiment $L = BC + CD - BD$. When this condition is met, a stable interference pattern is observed.

The idea presented in Fig. 1.4 has been realized in the prelaser optics in various experimental arrangements, say, with the Fresnel biprism, Michelson interferometer, interferometric arrangements to observe Newton's rings, and nonuniform thin films. In all these experiments an interference pattern can be observed because the pathlength difference L turns out to be very small—in the order of one millimetre at most. This implication is important because for ordinary light sources the length of wave trains τc (the coherence length) never exceeds one centimetre.

High coherence of laser radiation. The discovery of laser made a revolution in optics. The laser has supplied man with optical radiation of high coherence. The coherence time of laser radiation may be as high as 10^{-3} s. This implies that the coherence length τc may be as long as 10^5 m, that is up to 100 km long. This value is seven orders of magnitude higher than the coherence length of ordinary light sources. Moreover, the divergence angle of the laser beam may be as low as one minute.

1.3 Quantum Transitions in Absorption and Emission of Light

Now that we have introduced the notion of coherence of light we look at the principles of laser action. We start the discussion with the major processes of the interaction of radiation with atoms and molecules in a medium.

Energy levels of atoms and molecules. The energy of an atom or a molecule can take on only definite (discrete) values. These are the energy levels of the atom (molecule). The tran-

sition of an atom or molecule from one energy level to another occurs in jump and is called the quantum transition. Quantum transitions may be induced by various causes. In particular they can occur when atoms interact with optical radiation.

The atoms of each chemical element have their own characteristic system of energy levels. In energy units, the typical spacing between levels of an atom ranges between 1 and 5 electronvolts (eV). The system of energy levels of an atom governs the behaviour of electrons performing transitions in this atom.

The structure of energy levels of a molecule reflects three types of motion taking place in the molecule: motions of the electrons, vibrations of the atoms in the molecule, and rotation of the molecule itself. Accordingly, in addition to the levels associated with motions of electrons, the system contains vibrational levels (spaced about 0.1 eV apart) and rotational levels (distant from each other by at most 0.1 eV). The energy-level system of a molecule is therefore much more complicated than that of an atom.

Note. A unit often used to measure separation between levels is electronvolt (eV). It is equal to the energy which an electron acquires in an electric field created by a potential difference of one volt. To convert it in SI units, $1 \text{ eV} = 1.6 \times 10^{-19} \text{ J}$. Making use of the expression $\epsilon = h\nu = hc/\lambda$ and recalling that $h = 6.626 \times 10^{-34} \text{ J s}$ and $c = 3 \times 10^8 \text{ m/s}$, we obtain that to the photon energy 1 eV there corresponds the wavelengths of light equal to $1.24 \mu\text{m}$.

Absorption of light. To make our consideration simpler, we shall focus our attention on two levels of an atom only. Let the energy of the lower level be E_1 and that of the upper level E_2 . Assume that the atom is in the lower level and a photon of energy $\epsilon_{12} = E_2 - E_1$ travels near the atom. The atom can absorb this photon and rise from level E_1 to E_2 (Fig. 1.5), thus making a transition upon the absorption of a quantum of light.

Let W be the probability of absorption of light by $E_1 \rightarrow E_2$ transitions in atoms per unit time, in other words, the rate of absorption. This probability is obviously proportional to the number of incident photons and can be written as

$$W = BN\epsilon_{12} \quad (1.12)$$

where N is the number of photons in unit volume (all of energy ϵ_{12}), B is a coefficient characteristic of the $E_1 \rightarrow E_2$ transition.

Stimulated emission of light. When the atom lies in the upper energy level, then the same incident photon may play the role of a trigger, and induce the transition from E_2 to E_1 .

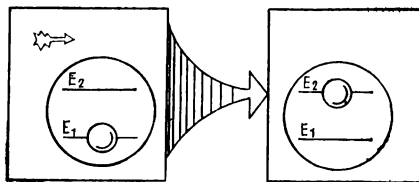


Fig. 1.5 Absorption of light

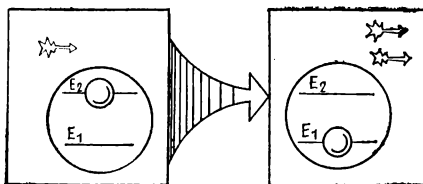


Fig. 1.6 Stimulated emission

whereby the atom falls into the lower level. The transition causes an emission of a photon (Fig. 1.6). Both the inducing and the induced photons have the energy $\epsilon_{12} = E_2 - E_1$. Moreover, both of them have identical direction of their momenta and identical polarization. In other words, the secondary photon finds itself in the same state as the primary photon. This result is a sequel of the bosonic behaviour of photons—they tend to accumulate in the same state.

This is the phenomenon of stimulated emission of light. The more primary photons are incident on our elementary volume, the higher the probability that the atom lying in level E_2 will be forced to undergo a transition to E_1 . Here we should recognize a certain similarity between the stimulated emission and stimulated absorption processes, namely, the probabilities of both processes are proportional to the

number of primary photons. The probability of stimulated emission W_{st} referred to unit time (rate of emission) is

$$W_{st} = BN\varepsilon_{12} \quad (1.13)$$

This expression is seen to coincide with (1.12).

To summarize, if an atom is in the ground state of energy E_1 , a photon of energy $\varepsilon_{12} = E_2 - E_1$ incident on the atom induces its transition to E_2 and is absorbed by the atom; if the atom is in the level of energy E_2 , then this photon is

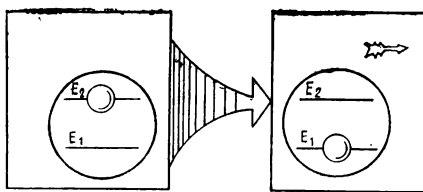


Fig. 1.7 Spontaneous emission

able, with the same probability as in the absorption process above, to stimulate the atom to fall from E_2 to E_1 with the emission of another photon.

Let us assume that there are many atoms in level E_2 of the material. An e.m. wave of the frequency consistent with ε_{12} incident on the material is capable of inducing the $E_2 \rightarrow E_1$ transition in many atoms, i.e. one primary photon may initiate an avalanche of secondary photons. All of them will be emitted in the same state as the stimulating primary photon. Therefore, one photon can initiate the radiation of a wave train whose length, conditioned by the number of the secondary photons, can, in principle, be of any large value.

Spontaneous emission. An atom lying in level E_2 will tend to decay to level E_1 spontaneously, that is without any stimulus, say, in the form of a photon, applied to it from outside just to assume a more stable state or lower energy (Fig. 1.7). The photon emitted in the spontaneous $E_2 \rightarrow E_1$ emission has the energy $\varepsilon_{12} = E_2 - E_1$, while its other characteristics (momentum direction, polarization) are arbitrary. The probability of the spontaneous emission of a photon is determined only by the properties of the transition

and is defined as

$$W_{sp} = A \quad (1.14)$$

The coefficients A and B entering the expressions for the probabilities of emission and absorption are called the *Einstein coefficients*. It is important to note that for a given transition (and the energy of incident photons) these coefficients are independent of any external conditions, such as temperature, pressure, power of the radiant flux, and so on.

Thus, two types of emission of light by atoms are possible, namely, stimulated and spontaneous emission. The former may be viewed as a controllable process, as it is stimulated by the primary photon which not only induces the transition, but also governs the characteristics of the new emitted photon. The second process proceeds spontaneously, it is random in nature. The instant of the transition, direction of the emitted photon, and its polarization, all are random quantities. Strictly speaking, an element of chance is present in the processes of stimulated emission too as the primary photon may and may not initiate the transition. That is why we have always spoken about the probability of the transition processes.

We should note in passing that spontaneous processes are spread rather widely in the microworld. Suffice it to mention the radioactivity of atomic nuclei and spontaneous transformations of various elementary particles. In spite of the principally random nature, all these processes have their own cause (as do all the processes in nature). We shall not consider here the phenomena causing spontaneous processes, but limit ourselves to noticing that each object of the micro-world interacts with the environment. This interaction is specific and cannot be reduced to ordinary force interactions.

1.4 The Active Medium. Creating a Population Inversion

The active medium. The heart of the laser is a certain medium—solid, liquid, or gaseous—called an active medium for it contains atoms, ions, or molecules capable of decaying from their high energy states in a radiative manner, i.e. by emitting e.m. waves. These atoms (ions or molecules) are sometimes called *active species* or *centres*. In the medium,

these may account for only a small fraction of all the atoms (molecules). One cubic centimetre of gaseous media has about 10^{16} to 10^{17} of such species, while that of solid and liquid media 10^{19} to 10^{20} .

We shall consider only those levels of the active species which are of consequence for laser action. First of all we single out two levels whose transition produces radiation. We shall call it the *lasing transition*. As before, one of them is the upper level, while the other is the lower level. Let $\varepsilon_{12} = E_2 - E_1$ be the energy difference of these levels, then $v_{12} = \varepsilon_{12}/h$ is the frequency of the transition, that is the frequency of emitted radiation. Let n_1 and n_2 be the number of active species (per unit volume) lying in the upper and lower levels respectively. These quantities are known as the *populations* of these levels.

Light amplification in an inverted active medium. As we already know, a photon of energy ε_{12} can, with an identical probability, induce either the $E_1 \rightarrow E_2$ transition or the $E_2 \rightarrow E_1$ transition. Which of them will result depends on the energy level in which the active centre lies. If the lower level of the medium is more populated than the upper level, the absorption processes will dominate. Conversely, if the upper level is more populated than the lower, the processes of stimulated emission will prevail.

Under normal conditions, specifically in thermodynamic equilibrium, the populations of energy levels decline as the level energy increases, so that normally $n_2 < n_1$, and the processes of absorption of light are dominant.

To produce radiation, however, we need that the processes of stimulated emission will be dominant. Consequently, we should take care of the higher population of the upper level, that is, to ensure that

$$n_2 > n_1 \quad (1.15)$$

When this condition is met we say that a population inversion takes place in the medium.

Let us assume that such an inverted active medium be prepared. Let a collimated light beam of frequency v_{12} and irradiance I be incident on the medium (Fig. 1.8).

We would like to dwell a bit on the notion of irradiance. It is measured as the energy of a light beam incident on unit area per unit time, therefore, the dimension of this

quantity is $\text{J m}^{-2} \text{s}^{-1}$, of W/m^2 . If we denote by ρ the energy density of the light field (the energy in unit volume), then the irradiance may be represented as the product ρv , where v is the velocity of light in the given medium. We have introduced earlier the quantity N being the number of photons in unit volume. It is quite obvious that $\rho = \epsilon N = h\nu N$, consequently

$$I = h\nu N v \quad (1.16)$$

It should be noted that the quantities I , ρ , and N are all considered for a certain frequency of e.m. radiation. We will

assume below that this frequency is equal to the laser transition frequency $\nu_{12} = (E_2 - E_1)/h$.

An e.m. wave of atomic frequency incident on an active medium with a population inversion can be amplified because of the stimulated emission processes being dominant here over the processes of absorption. Moreover,

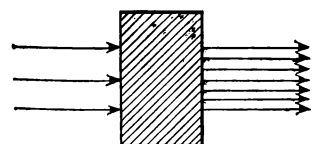


Fig. 1.8 A light beam may get amplified in passing through an active medium

the photons amplifying the incident beam are produced in the same state as the photons of the initial beam.

Let P be the light energy generated at frequency ν_{12} in unit volume of the active medium per unit time (that is, the light power density). It is an easy matter to demonstrate that

$$P = (n_2 - n_1) BN h^2 \nu_{12}^2 \quad (1.17)$$

To prove, we recall that $n_2 W_{\text{st}}$ stimulated transitions $E_2 \rightarrow E_1$ and $n_1 W_{\text{ab}}$ absorptions take place in unit volume per unit time. Each transition either emits or absorbs a photon of energy $h\nu_{12}$. Therefore, $P = (n_2 W_{\text{st}} - n_1 W_{\text{ab}}) \times h\nu_{12}$. Observing (1.12) and (1.13) we arrive at (1.17).

In view of (1.16) we may recast (1.17) to the form

$$P = (Bh\nu_{12}/v) (n_2 - n_1) I \quad (1.18)$$

The quantity

$$\sigma_{12} = Bh\nu_{12}/v \quad (1.19)$$

is called the *stimulated emission cross section* and represents the ratio of the process probability $BNh\nu_{12}$ to the irradiance Nv of the flux of photons that have induced this process. By

virtue of (1.19)

$$P = \sigma_{12} (n_2 - n_1) I \quad (1.20)$$

The methods of creating a population inversion. To produce a population inversion, we should take care of the upper energy level being populated more intensely than the lower level, or to provide a way for the lower level to be depopulated faster than the upper level. Each time our aim is to create higher populated upper levels in the medium.

The physical mechanisms of populating and depopulating energy levels are many and diverse. Accordingly, there exist various means of rendering the medium active, collectively known as the processes of pumping.

In *optical pumping*, the predominant population of the upper level is achieved by means of light energy delivered from appropriately selected sources such as gaseous discharge flashtubes, or continuously burning tubes. *Electrical pumping* is accomplished by means of a sufficiently intense electrical discharge in the medium and is particularly suited to gas media. The discharge converts the gas into a plasma where active centres collide inelastically with free electrons and cause the predominant population of the upper pumping level. Inelastic collisions of active centres with other atoms and molecules purposefully introduced into the gas are also of importance for pumping as they provide resonance energy exchange. *Chemical pumping* raises active centres into the higher level by means of suitable exothermal chemical reactions in the active material. Of other methods of pumping we may mention also *heat pumping* in which the active material is at first brought to a high temperature and then rapidly cooled down. In more detail the suitability of the pumping methods to various active media will be taken up in Chapter 2.

The principal pumping schemes. Atoms, ions, or molecules used as active centres often exhibit rather complicated systems of energy levels. However, for all the variety of these structures, the actual pumping schemes may be boiled down to a few rather simple diagrams correctly depicting the pumping process although neglecting some minor details. These diagrams involve three or four levels only. Fig. 1.9 showing these diagrams uses the following nomenclature: (0) the ground level, (1) the lower lasing level, (2) the upper

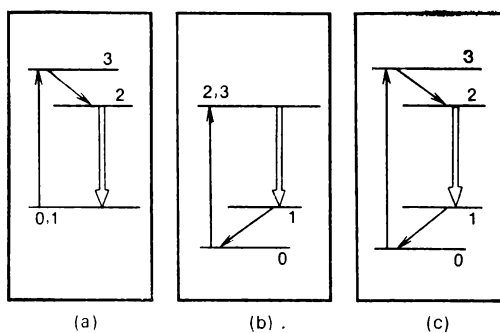


Fig. 1.9 Simplified energy level diagrams of active species. The lasing transition in all the diagrams is between levels 2 and 1

lasing level, and (3) the pumping level. The upward arrow implies the pumping transition, the downward arrow the lasing transition, and the slant arrows the auxiliary fast decays.

Consider the three-level pumping scheme shown in Fig. 1.9a. Active species excited by some pumping process, say, by optical pumping, are raised from the ground level 0 to the pumping level 3. Assume that more than half the active species undergo this transition. Then a very fast (during about 10^{-8} s) decay follows from level 3 to the upper lasing level 2. This is a nonradiative transition which gives its energy to the crystal lattice, if the material is a solid. The decayed atoms reside in level 2 (for about 10^{-4} to 10^{-2} s) and because more active centres are now in this level than in the ground state the inversion of the material takes place.

In the three-level laser scheme shown in this diagram, the ground state is simultaneously the lower lasing level and therefore is labelled 0 and 1. Such sharing of functions is a disadvantage in the sense that the lower lasing level should be depopulated, or better still, empty, which is not the case with the ground level being populated rather densely under normal conditions. Since it can be depopulated by the pumping process only, to produce an inversion more than half the active centres should be raised from this level.

This disadvantage is circumvented in the three-level scheme shown in Fig. 1.9b. This arrangement takes care of the lower lasing level being always virtually empty, as a fast decay

is provided for electrons to fall from this level to the ground state. This scheme is, however, limited by another setback, a substantial one, namely, its upper lasing level being simultaneously its pumping level. In order to use efficiently the pumping energy, this level should be rather wide, that is, be essentially an energy band. From the lasing viewpoint, however, this level must be very narrow so that the lifetime of atoms in it may be sufficiently long. In one level these conflicting requirements are incompatible.

More advantageous in the circumstances seems to be the four-level laser scheme shown in Fig. 1.9c, although it has one more auxiliary transition as compared to the three-level schemes and we must remember that each extra transition implies additional energy losses.

To sum up, all the considered schemes have their own advantages and disadvantages. All require that the lifetime in the upper lasing level is relatively long or else the desired accumulation of active centres in this state, necessary for population inversion, fails to occur. Such accumulating levels are called metastable levels.

To complete our discussion of laser schemes, we should mention that the two-level scheme cannot be used for lasing in principle. In such a scheme, pumping radiation would, on the one hand, move the ground state atoms to the upper level and, on the other hand, initiate transitions from the upper level to the ground level. In other words, pumping would simultaneously populate and deplete the upper level and, because the ground state is normally more populated than the upper level, all that we may hope to achieve by pumping in this scheme is a system of equally populated levels, whereas a population inversion is in achievable. That is why all the actual lasing schemes operate with different frequencies of pumping and lasing transitions.

1.5 Laser Oscillation in Optical Resonant Cavity

From spontaneous emission to laser oscillation. We have learned already that a light beam incident on an active medium can be amplified because stimulated emission dominates over absorption in an inverted medium. This is

the basic idea of the quantum optical amplifier. Now we would like to look at the laser.

As contrasted to such an amplifier, the laser does not include a primary coherent light beam to induce stimulated emission. To provide a better insight into how laser oscillation begins, we turn to the processes of spontaneous emission. In the laser, the role of primary photons which stimulate the emission of new photons and thereby initiate laser oscillation is played by the photons spontaneously radiated by some active species. Each spontaneous photon can initiate in the active medium many other stimulated transitions, which in turn may cause an avalanche of secondary photons occupying the same state as the primary spontaneous photon.

Such spontaneous photons are emitted by active centres independently and in various directions. Therefore, their secondary avalanches will also travel in various directions. In other words, the spread of these spontaneous photons over different states causes the respective spread of states of the avalanches they produced. It is quite obvious that a radiation consisting of such photonic avalanches will not exhibit high coherence properties.

To arrive at a coherent radiation, the above spread should somehow be narrowed. One way to do so is to restrict the number of possible photon states, that is to take care of their selectivity. Assume that for certain selected (and relatively small in number) photon states there have been established favourable conditions to develop stimulated emission, whereas for other photon states no such conditions exist. Spontaneous photons emitted in these selected states give rise to a large number of secondary photons in these states as the result of the stimulated emissions of active species. The photons emitted in other states die out very rapidly without contributing much to the flux of secondary photons.

This flux of secondary photons in the selected states is the desired laser radiation. The less the number of the selected photon states and the better they are selected, the more rigorous the selectivity and, consequently, the higher the degree of coherence of such a lasing device. If only one state could be selected, the laser would generate an ideally coherent light wave, i.e. a plane monochromatic wave of certain polarization.

Optical resonant cavity. The selection of some photon states and the suppression of other states can be realized by means of an *optical resonator*, a principal component of each laser. In its simplest version the optical resonant cavity is a pair of mirrors set on an optic axis which defines the direction of the laser beam. The active material is placed in-between these mirrors. Solid active materials are often in the shape of a cylinder whose axis is aligned with the axis of the optic resonator, the length of the cylinder being about ten its diameters. At least one of the mirrors of the resonant cavity is made semitransparent to serve as an output element passing the light out of the resonator.

Figure 1.10 shows the schematic arrangement of a simple resonator with an active material inside it. The photons produced spontaneously in the *OO* direction or sufficiently close to it will travel within the active material a relatively long way, which is elongated by multiple reflections from the resonator's mirrors. These photons interact with excited active centres to eventually initiate a powerful avalanche of stimulated photons constituting the laser beam. The photons emitted in other directions (and their stimulated avalanches) will traverse a relatively short pathlength in the material and die out soon. This process is vividly illustrated in Fig. 1.10.

Thus, the optical resonant cavity provides the desired selectivity of photon states by primarily confining the possible direction of photon propagation. As a result, lasing action occurs in this direction.

The optical resonator can provide selectivity in other properties of radiation. Of course, the selectivity in photon energy is secured by the choice of active centres with an appropriate system of energy levels. However, an actual system of levels is much more complicated than the laser schemes illustrated in Fig. 1.9. Actual active centres can have a few lasing transitions rather than one. To exclude undesired transitions, the resonant cavity may be provided with mirrors whose reflectivity is a function of frequency, so that the undesired transitions will be damped out, and the necessary selectivity will be ensured for photon states.

The resonant cavity plays, therefore, a key role: it as if guides the processes of stimulated emission induced by spontaneous photons in the active medium so that a laser

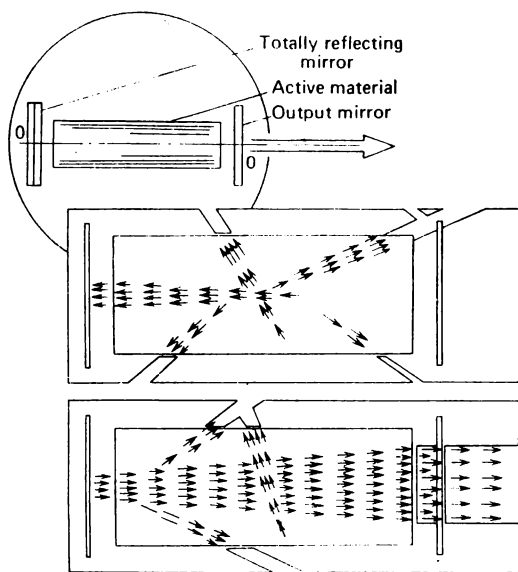


Fig. 1.10 The optical resonator determines the direction of laser action (along the resonator axis) and favours the processes of stimulated emission exactly in this direction

radiation of high coherence properties results. Later we shall learn that the resonator forms radiation not only of high coherence but also of a certain structure of the light field. This implies that the resonator also performs control of laser radiation.

The quality factor. Now we look at certain characteristics of the optical resonant cavity, of which the most important is its Q , the *quality factor*.

Let $U(t)$ be the energy of a radiant field (at the frequency of lasing) inside the resonator at a time t . Imagine that the active species present in the material are inoperative, as if they had suddenly disappeared: such a resonator is said to become passive. This energy will decay with time because of various losses inside the resonator. Let ΔU be the decline in the energy in the time interval from t to $t + \Delta t$. It is proportional to the length of the time interval Δt and the energy at time t

$$U = -U(t) \Delta t / \tau_c \quad (1.21)$$

The minus sign implies that U declines and $\Delta U < 0$. This equation can be shown to lead to the exponential law for energy decay with time

$$U(t) = U(0) e^{-t/\tau_c} \quad (1.22)$$

The parameter $1/\tau_c$ defines the rate of decay of the field energy in the passive resonant cavity. Fig. 1.11 illustrates this law showing that over the time τ_c the initial energy decreases e times (where $e = 2.71828$ is the base of the natural system of logarithms).

The dimensionless quantity

$$Q = 2\pi v \tau_c \quad (1.23)$$

is called the Q -factor of the resonator and used to show the ability of the cavity to store energy. The slower the energy of a radiation field falls off, i.e. the smaller the losses in the resonator, the smaller $1/\tau_c$ and, consequently, the higher the resonator's Q .

Losses inside the cavity. In a passive resonant cavity, the light beam irradiance gradually declines with travel distance owing to various losses in the medium inside the cavity or escapes through the side surface. The irradiance of the light beam declines again by an exponential law:

$$I(z) = I(0) e^{-\alpha z} \quad (1.24)$$

where the light beam travels along the z direction aligned with the cavity's axis, and α is the loss factor having the dimension of reverse length.

The relation between α and τ_c can be established in a rather straightforward manner. In the time interval τ_c the light flux covers the distance $v\tau_c$. In agreement with (1.22) the field energy inside the cavity falls off e times during this interval. It would be natural to assume that the flux irradiance also decreases e times. But according to (1.24), it suffers the same decrease over the pathlength of $1/\alpha$. Consequently,

$$\tau_c v = 1/\alpha \quad (1.25)$$

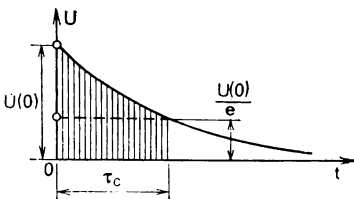


Fig. 1.11 Exponential decay of a radiation field inside a passive resonator

Substituting (1.1) and (1.23) in this equation we get

$$1/Q = \lambda\alpha/2\pi \quad (1.26)$$

If the causes of loss are many, say, absorption and radiation through the side surface, we may associate with each type of loss its own loss factor α_i and its own Q -factor, Q_i , so that

$$1/Q_i = \lambda\alpha_i/2\pi \quad (1.27)$$

If these losses are independent of each other, then the resultant change in the field energy inside the cavity may be

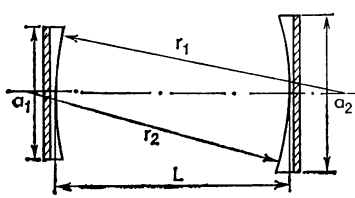


Fig. 1.12 Resonant cavity formed by two spherical mirrors of different curvature radii and apertures

presented as the sum of contributions due to various losses, $\Delta U = \sum \Delta U_i$. With reference to (1.21), we then have $1/\tau_c = \sum 1/\tau_{c,i}$ and by virtue of (1.25) and (1.26)

$$\alpha = \sum \alpha_i \quad (1.28)$$

$$1/Q = \sum 1/Q_i$$

This expressions imply that in taking account of various losses, we may sum up the loss

factors associated with those losses, or, which is equivalent, add the inverse Q 's associated with these losses.

Radiant losses. A proportion of the field energy leaves the cavity through the output mirror as laser radiation. For the laser as a source of radiation, this beam is just another type of loss referred to as radiant loss. This loss may be accounted in (1.28) as another term in the sum. The loss factor due to this loss, α_{rad} , has the form

$$\alpha_{rad} = \ln(1/R)/2L \quad (1.29)$$

where L is the resonator length (shown in Fig. 1.12), and R the reflectivity (reflection factor) of the output mirror (the ratio of the light flux reflected by the mirror to the incident flux).

Diffraction losses. These are an important class of losses caused by the fact that the apertures (lateral dimensions) of the resonator's mirror, as well as other components, are of limited dimension. A light beam incident on a mirror of finite aperture suffers diffraction on the mirror edge, which

entails a loss of a proportion of the flux. The collimated light beam of mirror size can be well aligned with the mirror, yet owing to the wave properties of light a portion of beam energy will walk off the mirror edges, as it were, and leave the cavity, incurring the aforementioned additional losses. These are called diffraction losses.

Diffraction losses increase as the mirror diameter a decreases and the wavelength and resonator length increase. In order that a resonator be low in diffraction losses at wavelength λ , it should be so long that

$$a^2/4\lambda L \gg 1 \quad (1.30)$$

The dimensionless parameter on the left-hand side is called the Fresnel number

$$N_F = a^2/4\lambda L \quad (1.31)$$

This number is not the only criterion used in estimating diffraction losses. Other features of resonator geometry should also be taken into account. These are determined by resonator length and mirror radii of curvature as laser resonators normally use spherical rather than flat mirrors. So, two resonators of the same Fresnel number may incur different diffraction losses due to different geometry.

Figure 1.12 shows a resonator produced by two spherical mirrors. Assume for generality that the mirrors have different apertures (a_1 and a_2) and different radii of curvature (r_1 and r_2). Such a resonator is defined by three principal parameters:

$$\begin{aligned} N_F &= a_1 a_2 / 4\lambda L \\ G_1 &= (a_1/a_2) (1 - L/r_1) \\ G_2 &= (a_2/a_1) (1 - L/r_2) \end{aligned} \quad (1.32)$$

Two resonators will have equal diffraction losses, if they are identical in these parameters. Such resonators are called equivalent resonators.

1.6 Basic Laser Characteristics

This section will be concerned with certain important laser characteristics essential to understand laser behaviour. Basic laser components are shown in the functional diagram in Fig. 1.13. In what follows we assume for simplicity that

the laser is operating in continuous regime, that is, the process of generation is stationary.

Gain coefficient. Consider a light flux at the lasing frequency travelling along the z direction in an active material. A layer of the material Δz thick located at a point z receives a flux of irradiance $I(z)$ and emits a more intense flux

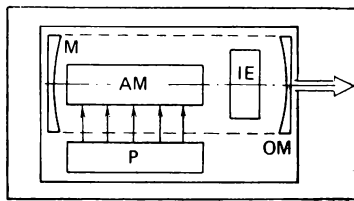


Fig. 1.13 Functional scheme of the laser. AM active material, P pumping system; M totally reflecting resonator mirror, OM output mirror, IE additional intracavity elements

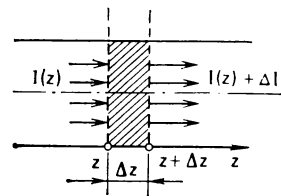


Fig. 1.14 Amplification of a radiation flux in a thin layer of an active material

$I(z) + \Delta I$ (Fig. 1.14). This increment of the flux is proportional to the initial irradiance $I(z)$ and the thickness of the amplifying layer

$$\Delta I = \beta I(z) \Delta z \quad (1.33)$$

The coefficient β is called the (small-signal) gain coefficient; it has the dimension of inverse length.

On the other hand, the increment of flux irradiance over the beam cross section s is equal to the power generated in the slab of material $s\Delta z$ (due to stimulated emission dominating over absorption), so that

$$\Delta Is = P(z) s \Delta z \quad (1.34)$$

where P denotes the power generated in unit volume of the material. Comparing (1.33) and (1.34) leads to

$$P(z) = \beta I(z) \quad (1.35)$$

Finally, from the comparison of (1.35) with (1.20) we get

$$\beta = \sigma_{12} (n_2 - n_1) \quad (1.36)$$

It will be noted that the relationships derived above involve functions dependent on the spatial z coordinate, and both P and I have been considered for the lasing transition, which will also be assumed in what follows.

It is important that the difference $n_2 - n_1$ is not a constant. As I grows in value the transitions from E_1 to E_2 and back become more frequent and the populations of these levels gradually equalize, that is, $n_2 - n_1$ decreases as I increases. Assume that at $I = 0$ the populations of the lasing levels are n_{10} and n_{20} , then it may be shown that

$$n_2 - n_1 = \frac{n_{20} - n_{10}}{1 + (\kappa/v) I} \quad (1.37)$$

where κ is a parameter accounting for the nonlinear behaviour of the transition, and v is the velocity of light in the medium. Denoting $\beta_0 = \sigma_{12} (n_{20} - n_{10})$, referred to as the initial gain coefficient, we recast (1.36) by virtue of (1.37) as

$$\beta = \frac{\beta_0}{1 + (\kappa/v) I(z)} \quad (1.38)$$

Note. To avoid possible confusion, we would like to emphasize that it should be distinguished between the absorption of radiation by the lasing transitions of active species and the absorption by other non-lasing atoms and molecules inside the cavity. The first absorption is always considered together with stimulated emission and is taken into account in the small-signal gain coefficient β . The second absorption is related to losses and enters the respective loss coefficient α .

Equations (1.33) and (1.34) have been written for loss-free active materials experiencing only stimulated emission and absorption in the lasing transitions of the active centres. For inverted materials with nonzero losses, (1.33) should be replaced with

$$\Delta I = (\beta - \alpha) I(z) \Delta z \quad (1.39)$$

This expression is rather indicative of the fact that two conditions should be satisfied in order for the inverted medium to amplify a light signal. First, the processes of stimulated emission must dominate over those of absorption for lasing transitions, so that $\beta > 0$. Second, the gain must exceed the losses, $\beta > \alpha$.

Should we include the losses in our consideration, we would introduce the loss power density $P_1(z)$ and write in

place of (1.34)

$$\Delta I = [P(z) - P_1(z)] \Delta z \quad (1.40)$$

Observing that $P_1(z) = \alpha I(z)$ carries (1.40) to

$$\Delta I = [P(z) - \alpha I(z)] \Delta z \quad (1.41)$$

Comparing (1.39) and (1.41) yields the same result as (1.35).

Output power. Conditions for laser oscillation. We can eliminate I between (1.35) and (1.38) to express the power density P through the coefficients pertinent to laser gain

$$P(z) = (v/\kappa)(\beta_0 - \beta) \quad (1.42)$$

Let V be a volume of active material being hit by the incident radiation. The light power generated in this volume may be expressed, subject to (1.42), as

$$P' = (v/\kappa) V (\beta_0 - \beta_{av}) \quad (1.43)$$

where β_{av} is the gain per unit length averaged over the length of the active material. To produce sustained laser action, upon completing a round trip about the resonator—from one mirror to the other and back—the light flux must be at its initial irradiance. Accordingly (we quote this without proof), the average gain coefficient must be equal to the overall loss coefficient

$$\beta_{av} = \alpha + \alpha_{out} \quad (1.44)$$

Notice, that we have separated here the radiant losses due to useful output, lost on the cavity into an individual term. Substituting this expression for β_{av} in (1.43) yields

$$P' = (v/\kappa) V [\beta_0 - (\alpha + \alpha_{out})] \quad (1.45)$$

It is quite obvious that not all of the light power generated in the active material leaves the resonator through the output mirror. A proportion of generated photons is lost non-radiatively. Only a proportion $\alpha_{out}/(\alpha + \alpha_{out})$ of the power leaves the resonator as laser output. In terms of power

$$P_{out} = P' \alpha_{out}/(\alpha + \alpha_{out}) \quad (1.46)$$

Substituting here P' from (1.45) we arrive at an expression for the useful output light power

$$P_{out} = \frac{v}{\kappa} v [\beta_0 - (\alpha + \alpha_{out})] \frac{\alpha_{out}}{\alpha + \alpha_{out}} \quad (1.47)$$

An obvious condition for laser oscillation to occur can be easily drawn from the aforementioned expressions, namely,

$$\beta_0 > \alpha + \alpha_{\text{out}} \quad (1.48)$$

Repeating this in words, for laser action to occur the initial gain must exceed the sum of the losses in the cavity.

Optimal value of the radiant loss coefficient. The radiant losses of a laser can be controlled by appropriately selecting the reflectivity R of the output mirror [see (1.29)]. If we wish to make the losses smaller in order to improve the condition for laser action, we can try to lower α_{out} by enhancing R . The quality factor of the resonator will improve, but the passage condition for the radiation leaving the cavity will be impeded—the ratio $\alpha_{\text{out}}/(\alpha + \alpha_{\text{out}})$ will decrease. This will cut down the output power. If, on the other hand, we try to improve α_{out} at the expence of lower R , this will hamper the generation to develop because of increasing losses. Stated mathematically, a decrease in α_{out} increases the factor P' in (1.46) but decreases $\alpha_{\text{out}}/(\alpha + \alpha_{\text{out}})$, and vice versa.

From this it follows that there should be an optimal value of the coefficient of radiant losses, $\alpha_{\text{out}}^{\text{op}}$, at which the output power is a maximum. That such a value exists could be readily proved by plotting P_{out} as a function of α_{out} in accordance with (1.47). This function, depicted in Fig. 1.15, reaches a maximum at

$$\alpha_{\text{out}}^{\text{op}} = \sqrt{\beta_0 \alpha} - \alpha \quad (1.49)$$

where

$$P_{\text{out}}^{\text{max}} = (\nu/\kappa) V (\sqrt{\beta_0} - \sqrt{\alpha})^2 \quad (1.50)$$

Now we can refer to (1.29) to obtain with (1.49) the optimal reflectivity for the output mirror

$$R_{\text{op}} = e^{-2L(\sqrt{\beta_0 \alpha} - \alpha)} \quad (1.51)$$

Forestalling the later material in this book, we note that at rather high gains typical of neodymium lasers with pulsed pumping, R_{op} can be relatively small (10% to 20%). For the He-Ne laser of small gain, R_{op} reaches as high a value as 99%.

Laser gain curve. So far we have considered systems with ideal energy levels. In actual systems, however, each

energy level is associated with a certain interval of values so that it would be physically more correct to speak of level broadening or of the width of a level, and the concept of energy level becomes somewhat conditional. This broadening of laser levels entails a spread in the frequencies of the tran-

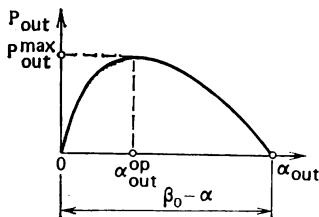


Fig. 1.15 Dependence of laser output power on radiative losses conditioned by the reflectivity of the output mirror

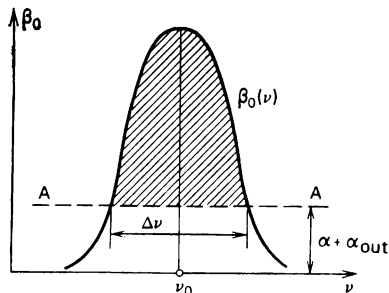


Fig. 1.16 Gain curve and loss level superimposed. The higher the loss threshold, the smaller the amplitude of the net gain profile

sition, as a result of which we have to deal with a certain frequency interval, called bandwidth, corresponding to a given transition, rather than with a single frequency.

The Einstein coefficients defining transitions have been treated as constants in previous sections. Actually they are functions of radiation frequency over the bandwidth associated with the transition. This implies specifically that both the cross-section and the initial gain coefficient β_0 are also functions of frequency.

Figure 1.16 shows a typical *gain profile* of $\beta_0(v)$, also termed the laser *transition (emission or fluorescent) line*. This function is defined by

$$\beta_0(v) = C \frac{v\Delta_0}{(v-v_0)^2 + \Delta_0^2} \quad (1.52)$$

where v_0 is the *central or resonance frequency* of the transition (consistent with the maximum of the function), Δ_0 is the halfwidth of the function measured as the full width at half-maximum power (FWHM), and C a constant.

The line AA drawn in this figure indicates the cavity loss level. The plot above this line confines the area of the net

gain defined by (1.48) for the oscillating laser. The width of the gain curve, Δv , is measured at this loss level. For Nd lasers $\Delta v \approx 10^{10}$ Hz, therefore the relative linewidth $\Delta v/v_0 \approx \approx 0.005\%$. For organic dye lasers, $\Delta v/v_0$ runs into a few percent as here $\Delta v = 10^{12}$ to 10^{13} Hz.

Cavity resonance frequencies. The main task of the optical resonator is to select a set of resonance frequencies within the laser emission (gain) linewidth. Assume that the radiation field inside the resonator consists of plane e.m. waves propagating strictly along the resonator axis. The cavity will be resonant for those of them that fit an integer number of half-wavelength between the mirrors, or mathematically

$$L = q\lambda_q/2 \quad (1.53)$$

where L is the resonator length, q positive integers far larger than unity, and λ_q are resonant wavelengths. This resonance condition may be recast in terms of resonant frequencies by virtue of (1.1) and (1.2) as follows

$$\nu_q = qc/2Ln \quad (1.54)$$

where n is the refractive index of the medium filling the cavity.

As can be seen from (1.54) the lines in the resonant spectrum are equidistant, since the spacing between the neighbouring frequencies is constant and equal to

$$\Delta\nu' = c/2Ln \quad (1.55)$$

By selecting a set of resonance frequencies, the resonator transforms the transition lineshape shown in Fig. 1.16 into a series of narrower spectral lines of the resonator shown in Fig. 1.17. The peaks of these lines correspond to the resonance frequencies. The width of these lines, $\Delta\nu_c$, is conditioned by the losses in the resonant cavity. Assuming that $\Delta\nu_c \approx \approx 1/\tau_c$ we obtain from (1.23)

$$\Delta\nu_c \approx 2\pi\nu_0/Q$$

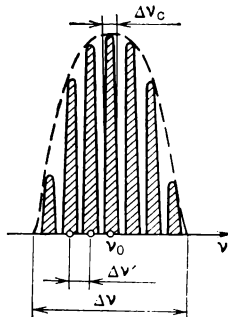


Fig. 1.17 Optical resonator fills the laser transition line gain profile with cavity modes

where Q is the resonator quality factor. It is an easy matter to see that at relatively high losses (low Q) and in inhomogeneous media the spectral lines of the resonator will overlap.

Modes of the optical resonator. In the previous sections we have learned that the resonant cavity of a laser is able to exert considerable influence on the output power and on the spectral behaviour of the laser. But the actual effect of the resonator on laser radiation is even more pronounced and crucial. It is so because the resonator is able to form definite states of e.m. field in the cavity; these are referred to as the resonator modes.

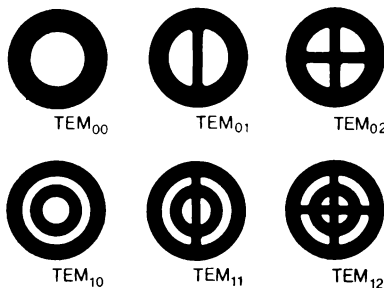


Fig. 1.18 Low-order transverse-mode patterns in cylindrical symmetry. The first integer defining the mode number indicates the number of nulls as one passes across the beam in a radial direction. The second integer specifies half the number of nulls in an azimuthal direction

The different modes are designated by the notation $\text{TEM}_{m n q}$ where TEM denotes Transverse Electro-Magnetic, m and n are the transverse indexes (or numbers), and q is the longitudinal index of a mode; the same q that appears in (1.53) and (1.54). A mode has a characteristic spatial structure of the e.m. field, that is, a certain distribution of the field amplitude and phase. In the plane perpendicular to the resonator axis, specifically on the mirror surface, this distribution is described by transverse indexes m and n .

To each combination of m and n , there correspond a number of modes having various q . These are *longitudinal*, or *axial, modes*. In the emission spectrum of a laser, each longitudinal mode is consistent with a spectral line of the resonator. By way of example, Fig. 1.17 shows seven longitudinal

modes; that at the frequency ν_0 is the central longitudinal mode.

When one refers to a given *transverse mode*, it means that one is considering a mode with given values of the transverse indexes (m, n), regardless of the value of q , which is dropped from the designation, therefore the transverse mode is denoted as TEM_{mn} . Since transverse indexes m and n specify the e.m. field variation in the transverse direction, each type of mode has a characteristic light pattern on the resonator mirror. Fig. 1.18 shows the patterns observed on a round (dark) mirror for a few simplest (low-order) transverse modes. It is seen that the lower the values of the transverse indexes, the denser the light field of the mode concentrates at the mirror's centre.

The transverse mode TEM_{00} is the lowest-order, symmetric mode, called the *fundamental mode*. It presents the simplest structure of the light spot.

Light spots observed in actual conditions often result from the superposition of a few transverse modes (multimode oscillation). The spectrum of a laser normally contains a few spectral lines (multiple oscillation).

1.7 A Historical Review of the Laser

The first steps on the way to the laser. The name laser is an acronym of Light Amplification by Stimulated Emission of Radiation. Thus the term reflects the crucial role of the processes of stimulated emission for quantum generators and amplifiers of coherent light. Therefore, the history of laser development should be traced as far back as 1917 when Albert Einstein showed that the process of stimulated emission must exist.

This was the first step toward the laser. The next one was due to the Soviet physicist V.A. Fabrikant who pointed out in 1939 to the possibility of exploiting stimulated emission to amplify e.m. radiation travelling through a medium. More specifically, he came up with the idea of using microsystems with inverse population of levels. Later, after the Second World War, he returned to this idea and summarized his research in a patent, filed in 1951 together with M.M. Vudynsky and F.A. Butayeva, for the invention of a means to amplify radiation by stimulated emission. This

patent was granted with the formulation of the invention as follows. 'A method to amplify electromagnetic radiation (ultraviolet, visible, infrared, and radio frequency bands) outstanding in that the radiation to be amplified is passed through a medium where an additional radiation or other means creates excessive populations, over the equilibrium one, of atoms, other species or their systems in the upper energy states corresponding to excited states.'

The development of the maser. If the transition frequency of a device operating in accordance with the principles outlined above falls in the microwave region, this type of amplifier is called a maser amplifier. This term appeared earlier than the laser as the idea was first realized in the microwave region. In May 1952, Soviet physicists N.G. Basov and A.M. Prokhorov reported to the All-Union Conference on Radiospectroscopy about the possibility of developing the amplifier of microwave radiation. They referred to it as a molecular-beam generator as it supposed to operate with a beam of ammonium molecules. The idea of employing stimulated emission to amplify and generate millimetre waves was expressed practically at the same time by the American physicist C.H. Townes of the Columbia University.

In 1954, the molecular-beam generator, soon named the maser, became a reality. It was developed independently and simultaneously by the team leaded by Basov and Prokhorov at the Lebedev Physical Institute of the USSR Academy of Sciences and by a group headed by Townes at the Columbia University in the United States.

Later the letter *m* in the term maser, related to 'microwave', was replaced by *l*, due to 'light', to give birth to the term 'laser'. Both devices, maser and laser, harness the same principle formulated by V.A. Fabrikant in 1951. Maser realization signified the birth of a new field of science and technology. In the Soviet Union this field was initially called quantum radio physics—the term retained by some Soviet journals and texts—and later acquired a new name, quantum electronics, in wide use elsewhere.

Six years of intense studies. In 1964, ten years after the maser had been developed, in his Nobel winner speech A.M. Prokhorov said: 'When masers were developed they seem to be followed soon by quantum oscillators in the

optical range. But we had to wait for them to appear for as long as five or six years. What was the reason for this delay? There were two principal difficulties to handle. One was the absence of resonators for the optical region of wavelengths; the other was due to the absence of practical systems and methods of realizing inverse population in the optical region.'

The six years mentioned were indeed devoted to research which ultimately led the way from the maser to the laser. In 1955, Basov and Prokhorov substantiated optical pumping as a method of population inversion. In 1957, Basov came up with the idea of using semiconductor materials for quantum oscillators and make the resonant cavity of the polished faces of the semiconductor chip. In that same year V.A. Fabrikant and F.A. Butayeva observed the effect of optical quantum amplification in experimenting with electrical discharge through a mix of mercury vapours and small amounts of hydrogen and helium. In 1958, A.M. Prokhorov in the USSR and A. Schawlow and C. Townes in the USA suggested independently that the stimulated emission phenomenon, which had been utilized in the maser, could also be used in the infrared and optical portions of the spectrum. Together with R.H. Dicke of Princeton University they also proposed to use open (rather than closed as in the microwaves) resonators in the optical region. Physically such resonators consist of only end-face mirrors aligned along the resonator axis and dimensioned so that their spacing exceeds the wavelength a great deal.

In 1959, N.G. Basov, B.M. Vul, and Yu.M. Popov published a paper where they established the idea of semiconductor quantum oscillator on theoretical grounds and analysed the requirements that should be met for their development. Finally, in 1960 there appeared a substantial publication of N.G. Basov, O.N. Krokhin, and Yu.M. Popov, which gave a thorough investigation to the development principles and theory of quantum oscillators and amplifiers in the infrared and visible portions of the spectrum. The authors concluded the paper with the words: "The absence of principal limitations gives us hope that generators and amplifiers in the visible and infrared portions of the spectrum will be realized in the nearest future."

The first lasers. The extensive theoretical and experi-

mental studies in the Soviet Union and the United States had brought scientists close to the first laser which was operated in mid-1960 by Theodore Maiman, an American physicist. He reported in two scientific journals in 1960 a successful experiment on light generation with a ruby rod in the optical region. So the world learned about the first "optical maser", the ruby laser. This device has a rather modest appearance by today's standards: a small ruby rod about 5 cm long had its two opposite ends silver coated to play the role of a resonator. It was fitted inside a helical high power flashlamp which periodically pumped the ruby by green light. The red pulses radiated by the ruby emanated as a beam through a small opening in one of the silvered faces.

Historically, the next development came in 1960 when Javan, Bennett, and Herriott demonstrated laser action in a gaseous discharge of helium and neon. This was the first gas laser the appearance of which actually had been prepared by the experimental studies of Fabrikant and Butayeva performed as early as 1957.

Beginning in 1961 various types of lasers (solid state and gaseous) gained a strong foothold in optical laboratories. New active media were introduced and the laser technology was improved rapidly. In 1962-63 the first semiconductor lasers were demonstrated in the United States and in the Soviet Union.

The laser is now in its third decade. During this period it has developed into one of the most important technological developments of this half-century. It has brought about a rebirth of the science and technology of optics and has led to the development of whole new industries.

Chapter 2

Types of Lasers

2.1 A Laser Exposition. Pumping Methods

The table in Fig. 2.1 lists the most commonly used types of lasers together with their active media and pumping methods. Lasers are normally classed by their active media and means employed for excitation (pumping). This chapter, therefore, will be devoted to the physical properties of media utilized as active materials and the methods of pumping allowing laser action to occur. We will also discuss the system of interconnections between various pumping techniques illustrated in Fig. 2.1. It might look sophisticated at first glance, but we recommend to return to this figure after reading this chapter to see it again from the angle of what is said in this chapter.

Of the pumping methods presented in the figure two are of major consequence—optical pumping and electrical pumping. *Optical pumping* is the most versatile pumping process. It suits to excite a variety of active media including dielectric crystals, glasses, semiconductor materials, liquids, and gas mixtures. Other pumping processes may integrate optical pumping as a component as well. *Electrical pumping* is accomplished by means of a sufficiently intense self-sustained electrical discharge and is particularly suited to gaseous active media at pressures of 1 to 10 torr (mm of mercury). The pertinent types of laser, using atomic, ion, or molecular transitions, are not infrequently joined by the common name of *gas-discharge laser*. These lasers as well as solid-state, liquid, and semiconductor lasers find their way into various fields of science and engineering.

The pumping process may be continuous or pulsed. So, optical pumping employs gaseous-discharge flashtubes and continuously emitting lamps. In electrical pumping, the discharge may be pulsed and stationary or quasistationary.

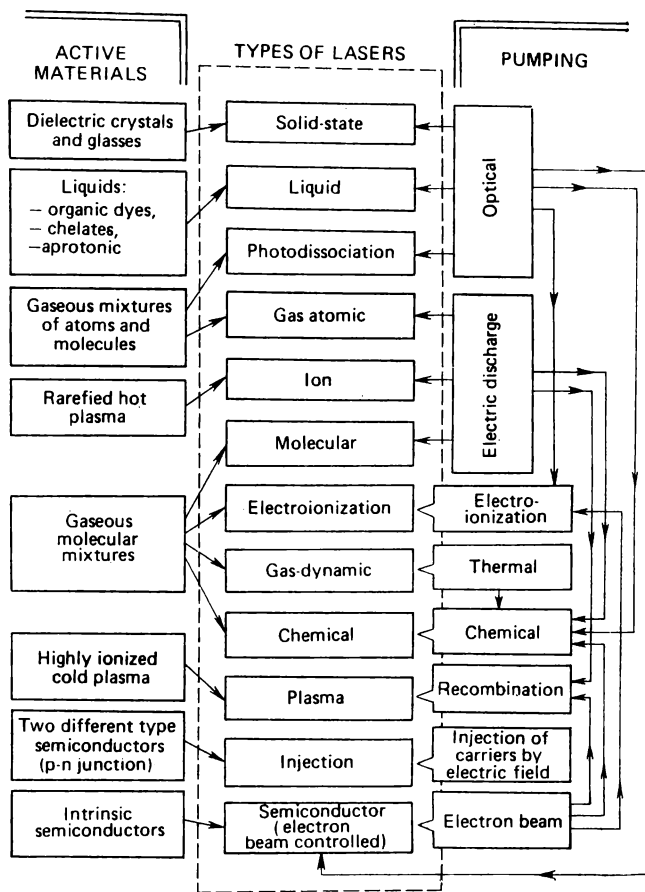


Fig. 2.1 Laser classification and functional relationship

Pulsed pumping supplies excitation energy in portions, whereas continuous pumping gives it up continuously.

Pulse pumping offers a number of advantages over its continuous counterpart. When a population inversion occurs only for certain time intervals, the requirement for a fast depopulating lower laser level may turn out to be less severe. Assume that on applying a pump pulse the population rate of the upper laser level exceeds that for the lower laser level.

Then lasing action may occur due to the population inversion that takes place at the initial phase of the excitation pulse. This situation is illustrated graphically in Fig. 2.2. It can be readily seen that an inversion occurs during time t_1 at the beginning of the pulse. It is quite obvious that the rate at which the lower level is depopulated is immaterial.

This example makes it clear why pulse pumping makes oscillation possible in a larger number of active media and in a greater number of transitions within a medium than it could be possible with continuous pumping. Another advantage of pulse pumping concerns its easier implementation. It is more difficult technically to provide a continuous pump power supply on a stable basis to the active medium than to realize a pulsed pump operation. In addition, forced cooling is no longer needed with pulse pumping.

Pulse pumping is favourable in that it enables various pulsed oscillation regimes to be realized, with the lasing in the form of single light pulses or pulse trains. These regimes afford exceedingly strong concentration in time and space of radiated energy emitted as gigawatt picosecond pulses. For example, regimes are realized for producing powerful exceedingly short light pulses with 10^{12} W of power within 10^{-11} to 10^{-12} s.

2.2 Solid State Lasers

The *solid state laser*, also called the *doped insulator laser* to avoid connotation of semiconductor, is built around active media prepared as insulating material (dielectric crystal or glass) doped with ions of impurity in its host structure. These lasers are rugged, simple to maintain, and capable of generating high peak powers. They employ optical pumping only.

Optical pumping. Optical pumping excites active centres through the absorption of light from specially selected sour-

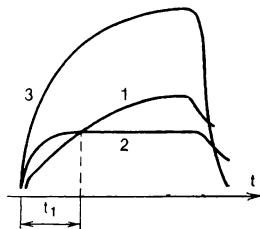


Fig. 2.2 Production of a population inversion between the population of the lower laser level (1) and upper laser level (2) during the risetime (t_1) of a pump pulse (3)

ces. These sources may be discharge flashtubes, continuously operating lamps (discharge or incandescent), spark gaps, flame, etc. An auxiliary laser may also be used as a pump source.

Two conditions need be met to make optical pumping efficient. First, the pumping level of the active centre must be sufficiently wide. In other words, the absorption line of pump transition must exhibit a relatively large bandwidth. Second, the peak of this absorption lineshape must be in the highest-irradiance portion of the pump source spectrum. Unless these conditions are satisfied the proportion of usefully expended power of the source will be exceedingly small.

Both aforelisted conditions are satisfied in solid-state lasers. Doped-insulator active media offer absorption bandwidths in the order of $0.1 \mu\text{m}$. Available pumping sources provide radiation spectra which can be selected for a particular laser so as to excite the active centre to the pump level, or to a group of levels performing as the "pump level" and often referred to as energy bands.

The solid state laser. In most cases, the active material of a solid state (doped-insulator) laser consists of an impurity or dopant in a crystalline or glass insulator. The crystal atoms do not participate directly in the lasing action, but serve as a host lattice in which the dopant resides. Today about 300 dielectric crystals doped by transition element ions exhibit the effect of stimulated emission. Oxide crystals of regular structure are most widely used. They include in particular Al_2O_3 crystal (corundum) doped by triply ionized chromium atom (Cr^{3+}), and $\text{Y}_3\text{Al}_5\text{O}_{12}$ crystal (commonly called YAG, an acronym for yttrium aluminium garnet) in which some of the Y^{3+} ions are replaced by neodymium ions (Nd^{3+}). The substitution of chromium ions in corundum converts it into ruby, so the first crystal is used as active material for ruby lasers, whereas the second ion, Nd^{3+} , brings about the active materials for the family of neodymium lasers (Nd:YAG, Nd:glass). These lasers are the most popular type of solid-state lasers.

Figure 2.3 illustrates how optical pumping is realized in a solid-state laser. The pump source, say a discharge flash-lamp, is the shape of a right cylinder placed parallel and adjacent to the rod of active material. The arrangement

shown takes advantage of the focusing properties of an ellipse. The laser rod and flashlamp are placed inside a cylindrical reflector of elliptical cross section, with the rod at one focus and the lamp at the other focus. Any light leaving one focus of the ellipse will pass through the other focus after reflection from the silvered surface of the pump cavity. As a result all of the pump radiation is maximally focused on the active material. The geometry of the pumping

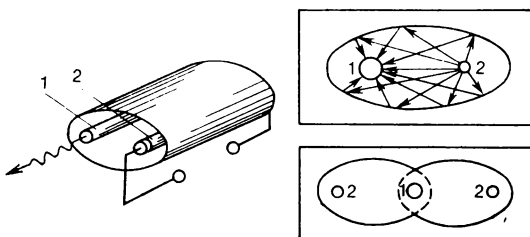


Fig. 2.3 Practical configurations of pump cavities for optically pumped solid lasers

cavity varies a great deal with the particular application. For example, two or four ellipses are used in the cross section of the pump cavity, with the rod in the common focus. This geometry of the cavity enhances the output power of the laser.

The end faces of the rod are polished and silvered to play the part of the optical resonator mirrors. Therefore, in this laser the length of the resonant cavity is the length of the rod.

The ruby laser. This type of laser was the first to be made to operate and still continues to be used on a wide scale owing to a high mechanical strength and thermal conductivity of ruby crystals which can be grown to high optical quality.

Ruby, which has been known for hundreds of years as a naturally occurring precious stone, is a crystal of Al_2O_3 (corundum) in which some of the Al^{3+} ions are replaced by Cr^{3+} ions. Laser rods are normally prepared of pink ruby which contains 0.05% chromium (1.6×10^{19} chromium ions in one cubic centimetre). These ions perform as active

centres in a ruby crystal. Fig. 2.4 shows the levels of the chromium ion in ruby. The vertical axis shows energy in terms of spatial frequency (reciprocal wavelength). To be converted to common energy units, the wave number should be multiplied by hc , i.e., $E = hc/\lambda$. Optical pumping raises an electron in the chromium ion to the broad upper levels (denoted 4F_1 and 4F_2 in spectroscopic notation, see note below). The height of the bar in the figure provides some idea on the spread of the respective level. These excited states give up a proportion of their energy to the thermal oscillations of the ruby crystal lattice and fall comparatively fast from the states 4F_1 and 4F_2 onto two adjacent metastable (having relatively long lifetimes) levels denoted as $2\bar{A}$ and \bar{E} . These latter levels play the part of the upper laser level.

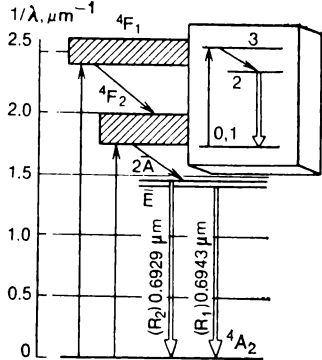


Fig. 2.4 Energy levels of the chromium ion in ruby and the principal transitions

The lower laser level 4A_2 is the ground level for this system. Therefore, the ruby laser fits into the definition of the three-level laser scheme presented in Fig. 1.9a.

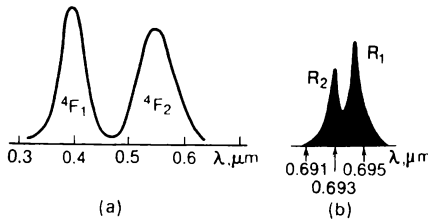


Fig. 2.5 Absorption (a) and fluorescence (b) spectra of the chromium ion in ruby

The absorption spectrum of the chromium ion in a ruby crystal is shown in Fig. 2.5a. It shows up two maxima for the transitions to 4F_1 and 4F_2 lying at $\lambda' = 0.41 \mu\text{m}$ (blue absorption band) and $\lambda'' = 0.55 \mu\text{m}$ (yellow-green absorption

band). Each of the bands is about 0.1 μm wide. The optical pump of this laser is effected by a gas discharge xenon lamp.

The emission spectrum of the radiation spontaneously emitted by the chromium ions in lasing (the fluorescence spectrum of the chromium ion in ruby) is presented in Fig. 2.5b. It consists of two bands: one at 0.6943 μm (the so-called R_1 -line), the other at 0.6929 μm (R_2 -line). The laser action occurs practically on the R_1 -line only.

Note. In atomic spectroscopy, there exists certain nomenclature for succinct identification of the states of atoms, ions and molecules. We have no room in this text to discuss this nomenclature at length and invite the reader to treat the term symbols, such as 4F_1 and 4F_2 , as certain labels of the atomic levels. We will return to this nomenclature in Sec. 2.5.

The Nd:YAG laser. The neodymium-doped yttrium aluminium garnet laser is the most popular type of solid state laser. It has a rather low excitation threshold and a high thermal conductivity, therefore lends itself for generation of light pulses at a high repetition rate or for continuous operation (called continuous wave or *cw* operation in the laser jargon). The efficiency of this laser is also comparatively high, running to a few percent.

The atomic levels of the neodymium ion in YAG crystal are presented in Fig. 2.6. In fact, the figure shows energy bands of various width rather than thin levels. Each of this bands contains a group of energy levels identified each by its own atomic term symbol.

The optical pumping raises the ground state Nd atoms (the atomic term $^4I_{9/2}$) to a few states identified by the terms $^4G_{7/2}$, $^2G_{7/2}$, $^4S_{3/2} + ^4F_{7/2}$, $^4F_{5/2} + ^2H_{9/2}$, and $^4F_{3/2}$. These five groups of states give rise to five bands in the Nd:YAG absorption spectrum plotted in Fig. 2.7a. The bands are seen to reveal fine structure which reflects the fact that the energy bands consist of individual levels.

The upper laser level is the state $^4F_{3/2}$. The laser action occurs when the neodymium ions decay from this level to the states $^4I_{11/2}$, $^4I_{9/2}$, $^4I_{13/2}$, and $^4I_{15/2}$. Since each of these terms is associated with a few energy levels, the total number of lasing transitions runs into two decades. The major portion of the energy is emitted in the $^4F_{3/2} \rightarrow ^4I_{11/2}$

transitions (about 60%), therefore the $^4I_{11/2}$ state is normally taken as the lower laser level.

Figure 2.7b shows the Nd:YAG fluorescence spectrum for the $^4F_{3/2} \rightarrow ^4I_{11/2}$ transitions. The spectrum contains seven

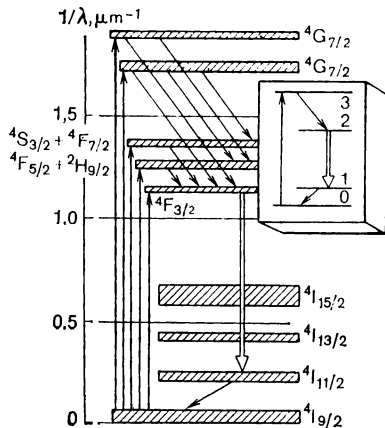


Fig. 2.6 Energy-level diagram of the neodymium ion in yttrium aluminium garnet

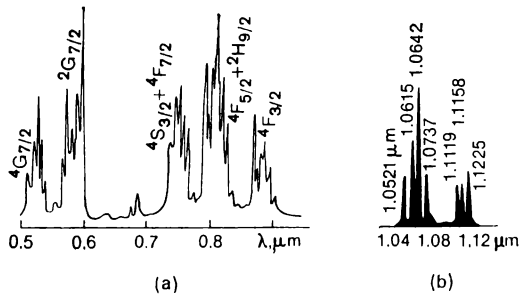


Fig. 2.7 Absorption (a) and fluorescence $^4F_{3/2} \rightarrow ^4I_{11/2}$ (b) spectra of Nd:YAG

lines. The most intense lines are those at 1.0615 and 1.0642 μm in the infrared. In addition to these transitions, a certain contribution to the output is made by the transitions $^4F_{3/2} \rightarrow ^4I_{13/2}$ (1.3 μm oscillation) and $^4F_{3/2} \rightarrow ^4I_{9/2}$ (at 0.9 μm).

It is quite obvious from Fig. 2.6 that the multitude of the Nd:YAG laser levels corresponds to the four-level laser scheme shown in Fig. 1.9c.

In high-power continuous operation, the laser is excited with krypton lamps. At times, the YAG crystal lattice is doped by chromium ions in addition to Nd³⁺ so that xenon lamps could be used for pumping. The chromium ion in YAG exhibits two rather wide absorption bands (at 0.43 and 0.59 μm) well within the spectrum of xenon lamps. The excited chromium ions transfer their excitation energy to the neodymium ions of the material and enhance the output.

Glass lasers. In these lasers, the active material is glass doped by ions of rare-earth elements, specifically, by neodymium. They also operate by the four-level scheme as Nd:YAG lasers. The Nd:glass laser emits at a wavelength of $\lambda = 1.06 \mu\text{m}$ and is a rather popular device.

Various types of glass are used for these lasers: borate glasses based on boron oxides, lead glasses based on lead oxides, phosphate glasses based on phosphorous oxides, fluoroberillate glasses, silica glasses, and such. The glass materials are relatively cheap to fabricate in the form of long rods (more than 1 m long), optically homogeneous and lend themselves for doping in high concentrations of impurities. The major disadvantage of glasses relates to their low thermal conductivity, therefore glass lasers may be operated in a pulsed mode only at a relatively low pulse repetition rate.

2.3 Organic Dye Lasers

Liquid lasers are called so because their active media are either liquid solutions of organic dyes or specially prepared liquids doped with rare-earth ions, say, with Eu³⁺ or Nd³⁺. These special liquids may be of two types: organometallic (chelate) and inorganic (aprotonic) liquids. These lasers are optically excited devices.

Organic dyes for active media. A large proportion of liquid lasers are organic dye lasers. Their active medium is a solution of an organic dye, which gives active species in some liquid solvent, such as water, ethanol, methanol, toluene, benzene, aceton, etc.

The organic dyes are complex organic compounds offering wide absorption bands in the visible and near ultraviolet

portions of the spectrum. The chemical structure of dye molecules typically contains a number of benzene, pyridine, azine and other rings attached to each other in one plane. The most effectively lasing dyes are classed into the following eight groups: *xanthenes*, *polymethines*, *oxazines*, *coumarins*, *anthracenes*, *acridines*, *azines*, and *phthalozianines*. Today laser action is obtained for more than 200 dyes. The lasing range

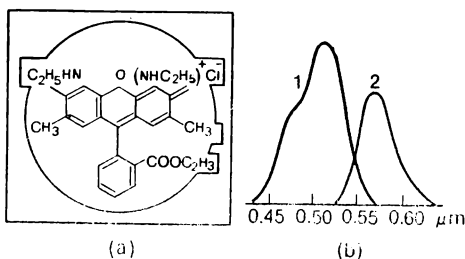


Fig. 2.8 Structural formula of Rhodamine 6G (a) and the spectra of absorption (1) and fluorescence (2) of this dye

covered by various dyes runs from 0.3 to 1.3 μm . By selecting a suitable dye, one may obtain coherent radiation of any wavelength from this range.

Rhodamine 6G is a practically important lasing dye of the xanthene group. Fig. 2.8a shows its structural formula based on a system of benzene rings. Xanthene dyes absorb pumping radiation and fluoresce in the visible portion of the spectrum. Fig. 2.8b shows the absorption and emission spectra of rhodamine 6G. Like solid-state lasers, the linewidth of the absorption band is about 0.1 μm for this dye. The emission band of this dye has the same linewidth which is about 10 to 100 times broader than the fluorescence linewidth of the dopants in solid-state lasers. This unusually large emission linewidth and, as a consequence the gain curve linewidth, is one of the most interesting features of organic dye molecules utilized as active centres.

Optical pumping of dye lasers. Auxiliary lasers and lamp sources are used to excite dye lasers. In the laser pumping, the pump radiation is at the frequency of the pumping laser or at a frequency two or three times as high. In the latter case it is said that the second or third harmonic of the auxiliary laser transition is used for excitation.

Most often the pump laser is a neodymium doped glass laser or a Nd:YAG laser operated in a pulsed mode. The pumping beam enters the dye cavity either along the axis or transverse to it. Fig. 2.9 shows, by way of example, an arrangement with longitudinal excitation of the material. The dye cell is inside the cavity where one of the mirrors is replaced with a total reflection prism. The output mirror

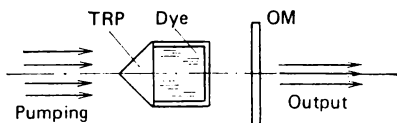


Fig. 2.9 Parallel pumping arrangement in a dye laser. *TRP* total reflection prism, *OM* output mirror

of the resonant cavity is 100% reflectant for the pump radiation which enters the cavity through the prism and strikes the dye cell to excite the dye. The dye fluorescent output leaves the cavity through the output mirror.

Continuous laser pumping is also employed to excite these lasers. This is frequently done with the argon ion laser (discussed in Sec. 2.5). Because this pumping would heat the dye exceedingly if in an ordinary arrangement, the pump beam this time is arranged transverse to the dye medium. It is focused into a $10 \mu\text{m}$ diameter spot on a dye stream rapidly pumped through the excitation area. This flow arrangement is not for cooling only, it is also essential for removing photo-decay products from the generation zone.

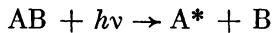
2.4 Photodissociation Lasers

Optical pumping in gaseous media. We have already mentioned that the efficiency of optical pumping of solid-state and liquid lasers is primarily conditioned by a sufficiently large absorption linewidth, being about $0.1 \mu\text{m}$. In gaseous media, the absorption lines of active centres exhibit substantially narrower widths, never exceeding $10^{-6} \mu\text{m}$. Optical excitation in this case can be achieved, provided the pump radiation has a line spectrum of very narrow lines and the peak of at least one intense line coincides with the maximum of an active-centre absorption line.

This is a rather severe condition. One of the rare examples, when it is met, is the *cesium vapour laser*. The cesium atoms are excited by a helium lamp whose spectrum contains a narrow intense line at the wavelength $0.3888 \text{ } \mu\text{m}$ which is exactly the wavelength of the laser transition of the cesium atom.

Wideband pumping is obviously of low efficiency for gaseous media, as only a negligible portion of pump source energy would reach the active centre through the narrow absorption lines. The major portion of pump energy would then go for heating the gas and structural members of the laser. This reason makes wideband optical pumping prohibitively useless for gas lasers.

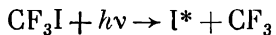
Wideband-excited photodissociation gas lasers. An exception to the aforementioned rule are the gaseous media that contain molecules dissociating upon absorption of light quanta so that one of the splitting products appears in an excited state (marked with an asterisk)



The process of molecular splitting as a result of light absorption is known as *photodissociation*. An interesting consequence of photodissociation that the absorption linewidth of the gas molecule turns out to be as wide as the absorption linewidths in solid and liquid active media. This fact allows the use of wideband optical pumping. The excitation power is absorbed by dissociating molecules which brings about an excited product to be used for lasing. This type of gas lasers is termed *photodissociation lasers*.

Two classes of photodissociation lasers are known. One uses the excited dissociation product as the active centre. This excitation is said to have occurred in primary photo-processes. The second class obtains excited active species as a result of a series of chemical reactions with the products of dissociation, that is, gets them from secondary chemical reactions. Therefore, this type of laser is referred to as the *photochemical laser*.

The iodine laser is an example of photodissociation laser. A wideband optical pumping at $\lambda \approx 0.3 \text{ } \mu\text{m}$ dissociates CF_3I molecules



The excited iodine atoms emerge in the $^2P_{1/2}$ state. Laser action occurs when these atoms radiatively decay to the $^2P_{3/2}$ state, emitting at the wavelength $\lambda = 1.315 \mu\text{m}$.

The photodissociation laser has an efficiency of 0.5%. Higher efficiency is possible by means of expanding the absorption linewidth of the dissociation molecules and by means of introducing special secondary chemical reactions.

2.5 Ion and Atomic Lasers

Gas-discharge lasers. These lasers operate with rarefied gases as their active media (at pressures of 1 to 10 torr) excited by an electric discharge. They include three more specific types: (i) *ion lasers* lasing on the transitions between the energy levels of ions in ionized gases, (ii) *neutral atom lasers* which fluoresce on the transitions between the energy levels of neutral atoms; and (iii) *molecular lasers* oscillating on transitions in molecules.

Ion lasers fluoresce mostly in the visible and near ultraviolet region of the e.m. spectrum (from 0.3 to 1.0 μm). Neutral atom lasers oscillate over a wider range of wavelengths, from 0.4 to 100 μm , most lasing transitions lying in the range from 1 to 20 μm .

Molecular lasers cover a wider frequency range of all the three groups. The lasers whose lasing action takes place between rotational levels belonging to the same electronic and vibrational state of the molecule (purely rotational transitions) emit in the infrared, from 10 μm to a few hundred micrometres. When the lasing transition is between vibrational levels (vibrational-rotational transitions), the lasing is mainly in the range from 5 to 50 μm in the infrared. Molecular lasers can also oscillate on the transitions between electronic states of a molecule. Then the fluorescence is in the visible or ultraviolet portions of the spectrum (approximately from 1 to 0.2 μm).

The active medium of the gas-discharge laser is a plasma produced by an electric discharge. If the rise time of the firing current pulse is shorter than the time taken to establish steady-state conditions in the plasma, then the discharge is said to be of pulse variety. Another variety includes stationary (quasi-stationary) discharges. With reference to lasers, these may be of the arc discharge type (in ion

lasers) and of the flow discharge type (in atomic lasers and molecular lasers). The arc discharge operates at high currents and temperatures and produces high degrees of plasma ionization (measured as the ratio of free electrons to heavy particle concentrations in the plasma). The current density in the discharge is as high as 100 to 1000 A/cm², the discharge temperature is 1000 K, and the degree of ionization is more

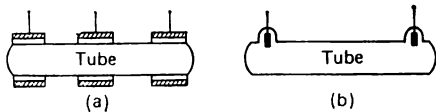


Fig. 2.10 Placement of electrodes for (a) high frequency and (b) dc voltage excitation of discharge

than unity. The glow discharge operates at rather weak current densities of 0.001 to 0.1 A/cm², at room temperature, and results in a low degree of ionization of 0.001.

Stationary discharges may be fired by high frequency and direct current voltage. The former are excited by ac voltage of 10 to 50 MHz via electrodes placed outside the discharge tube, as shown in Fig. 2.10a. The latter are fired by dc voltage with the electrodes introduced inside the tube, as in Fig. 2.10b.

The helium-neon laser. This laser using a mixture of helium and neon for its active medium will be considered as a typical example of a laser exploiting atomic transitions. It oscillates on the transitions between the levels of neon atoms acting as active centres. Helium which is a component of the gas mixture will be shown to play an important role in the excitation of the neon. The mixture is at a pressure of about 1 torr, the partial pressure of the helium gas being 5 to 10 times that of the neon. The He-Ne laser is excited by a stationary glow discharge fired by dc current.

Figure 2.11 shows a He-Ne laser with the discharge tube aligned with the resonator axis. When the potential difference between the anode and cathode in this tube rises to about 1000 V, a glow discharge is initiated in the working capillary of a few millimetre diametre. The output windows of the tube set oblique to the axis rather than normal to it. The normals to these Brewster windows make the so-called Brewster angle with the resonator axis.

The *Brewster, or polarizing, angle* is an angle of incidence α of a light ray such that satisfies the condition $\tan \alpha = n$, where n is the refractive index of the glass material. In this case, the ray reflected from the surface is polarized normally to the plane of incidence, whereas the refracted ray is predominantly polarized in the plane of incidence. This situation

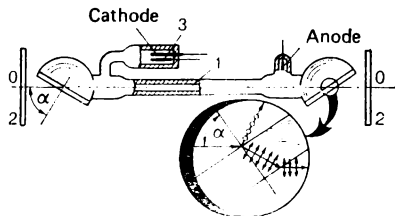


Fig. 2.11 A helium-neon laser design with Brewster windows. 1 laser bore of the gas discharge tube, 2 resonator mirrors, 3 heated gas scavenger to absorb deleterious gases

is illustrated in the insert in Fig. 2.11. The short arrows there indicate that the electric field vector oscillates in the plane of the page (the plane of incidence), while the circles show the oscillations in the plane perpendicular to the page. It will be noted that at this angle of incidence the refracted ray makes an angle of 90° with the reflected ray (*Brewster's law*).

Note. As we noted in Sec. 1.5, the optical resonator selects in space a direction in which laser action takes place. By placing the output windows at the Brewster angle to the resonator axis, we also select a certain polarization for the lasing beam—in other words, we introduce a device to select photons of certain polarization. Let an unpolarized light wave be incident on a plane Brewster window of the laser tube after travelling along the axis of this tube. The wave may be represented as a combination of two polarized waves, of which one is polarized in the plane of incidence and the other perpendicular to this plane. The first wave will suffer refraction at the interface and enter the window, then will be refracted again leaving the plate and will keep travelling along the resonator axis. The second wave will undergo reflection from the window and will be lost to the resonator. Thus, the photon states with the polarization in the plane of

incidence turn out to be selected (in terms of Sec. 1.5), whereas the states with the perpendicular polarization do not. It is an easy matter to see that the light wave reflected from the window will not contribute to the oscillation in the laser as it is lost to the cavity. The laser will take up for oscillation the wave passing through the window, i.e., the one polarized in the plane of incidence which includes the resonator axis and the normal to the window. So, the Brewster windows help us to kill two birds with one stone. First, we obtain a polarized laser output, and, second, exclude losses suffered in the reflection from the tube windows.

Electronic configurations and atomic terms. Before we go on discussing the processes causing inversion in gas-discharge lasers a few words are in order on the state of active species in a gaseous medium. Such a state includes a group of energy levels defined in atomic spectroscopy by respective atomic term symbols. These symbols, as we have already noted, indicate the electronic state of the atom to which the contributions are made by the electrons orbiting this atom and producing respective electronic configurations. Each stable electronic energy state is described quantum-mechanically by four quantum numbers and their specific symbols. More specifically, these are the principal quantum number, n , called so because the differences in energy are greatest for electrons in quantum states with different n values, as it defines the average distance of the electron from the nucleus; the orbital quantum number, l , associated with different amounts of orbital angular momentum (corresponds to much smaller differences in energy than n does); the magnetic quantum number, m , defining the z-component of angular momentum (together with l this number determines the extent to which the electronic orbit deviates from a perfect sphere), and the spin quantum number, s , contributes to the atom's energy when in a magnetic field.

In multi-electron atoms each electron is associated with a set of quantum numbers. The quantum number n may assume integer values 1, 2, 3, etc. The orbital quantum number l may take values from 0, 1, 2 . . . to $n - 1$, but for historical reasons this quantum number is usually represented by a letter, as s , p , d , f , g , etc. The magnetic quantum number m takes values from $-l$ to l , and the spin s may be

either $+1/2$ or $-1/2$. Atoms with the same values of n and l but different values of m and s often have the same total energy. Such quantum states are described, therefore, as degenerate energy states. When atoms in these states are placed in a magnetic field, the energy of each degenerate state increases or decreases by an amount that depends on the values of m and s .

In the absence of a magnetic field, a symbolic notation for atomic states results. For example, $3p$ signifies the state $n = 3$, $l = 1$; $2s$ signifies $n = 2$, $l = 0$. When electrons in the atom are many, we arrive at a combined electronic configuration. For example, $2p^64s$ stands for five p -electrons ($l = 1$) with $n = 2$ and one s -electron ($l = 0$) with $n = 4$. As will be recalled, electrons in an atom are filled in orbitals, or shells, so that the closest orbital to the nucleus $1s$ can accommodate no more than two electrons, the next orbital no more than eight, then eighteen, and so on. Filled up orbitals such as $1s^2$ and $2s^22p^6$ are called closed shells. In the case of a single electron outside a closed shell the orbital angular momentum of the whole atom is the same as the orbital momentum of the single outermost electron. This is because the closed shell possesses no net orbital motion.

This fact is of significance in deriving atomic term symbols which are just a short way to convey the information on the atomic states. These are denoted by upper-case letters (e.g., S , P , D) indicating the total orbital angular momentum of the atom (the rules of conversion from figures to letters are the same as for l in electronic configurations). The left superscript in the term symbol (e.g., 2 in ${}^2P_{3/2}$) gives the number of possible orientations of the total spin of the atom. For example if the atom contains a single unpaired electron, its total spin is $1/2$ and there are two permitted orientations. Therefore 2 is used in the left-superscript position. The right subscript in the term symbol (e.g., the $3/2$ in ${}^2P_{3/2}$) indicates the values of the total angular momentum quantum number J . If there are several electrons outside the closed shell the values of J and the total spin S are determined by special rules. It is important to note, however, that one electronic configuration may correspond to a few atomic term symbols. So, to the configuration $2p^64s$ there correspond four terms, while to the configurations $2p^53p$ and $3p^44p$ ten and fifteen terms, respectively.

In solid state and gas-discharge lasers, the state of the active centre (atom or ion) is represented by energy bands each with its own bandwidth. However, the bands in these lasers are of different origin. In the solid state laser, each band corresponds to one or two atomic terms (see Figs. 2.4 and 2.6). The energy levels identified by individual terms spread into an energy band as a result of the interaction of the active centre with the host crystal lattice. In the gas-discharge laser, the active medium is a rarefied gas where the active centre behaves almost without interaction with

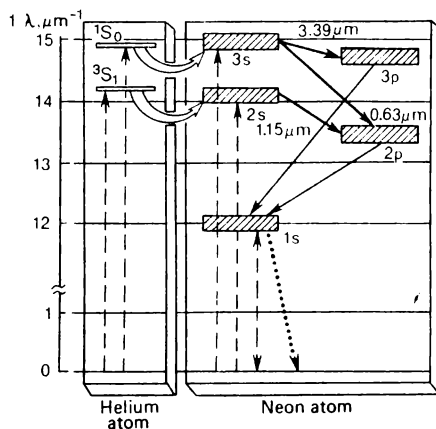


Fig. 2.12 Energy-level diagram of the He-Ne laser. The solid straight arrows indicate the lasing transitions

the rest of the medium. Therefore, each atomic term represents a narrow energy level. Here, the energy band appears as the result of a few atomic states, identified by the term symbols of the same electronic configuration, tending to unite into a single level of some energy spread.

The population inversion mechanism in the He-Ne laser. Fig. 2.12 illustrates the basic transitions that occur in the medium of a helium-neon laser. On the left, there are transitions of the helium atom, on the right those of the neon atom. The excited states of the neon are shown by energy bands identified according to the following table

designation	$1s$	$2s$	$3s$	$2p$	$3p$
el. configuration	$2p^53s$	$2p^54s$	$2p^55s$	$2p^53p$	$2p^54p$

You may also come across a different (and a new one) notation for these states elsewhere, namely, by the quantum numbers of their single excited state electron — $3s$, $4s$, $5s$, $3p$ and $4p$ —which takes advantage of the fact that the other nine electrons in the neon atom retain their ground-state quantum numbers.

Each s -band consists of four levels (four terms), while each p -band, of ten levels. The $3s$ and $2s$ bands play the role of the upper levels, whereas the $3p$ and $2p$ bands, that of the lower laser levels. Laser action occurs on the three transitions: $3s \rightarrow 3p$ at $3.39 \mu\text{m}$, $2s \rightarrow 2p$ at $1.15 \mu\text{m}$, and $3s \rightarrow 2p$ at $0.63 \mu\text{m}$ (red).

The inverted population in the He-Ne laser occurs as a result of the population rate of the upper levels being considerably higher than that for the lower levels. Free electrons of the gas discharge collide with the helium and neon atoms to excite them by impact energy transfer. Absorptive transitions due to the electron impacts are shown by dashed arrows. The electrons excite the 1S_0 and 3S_0 states in the helium atoms and a variety of neon bands corresponding to both the upper and lower lasing levels. The excited helium atoms collide with the neon atoms and give up their energy in the process known as *resonant collision energy transfer*. This process is depicted by curved light arrows. The resonant transfer of energy from the helium to neon is crucial for the more intense population build-up of the upper neon levels than the lower levels. Three factors contribute favourably to this process. These are the close match, in energy, of the pertinent helium and neon levels, the metastable behaviour of the excited helium levels (their deactivation through spontaneous emission is relatively slow), and a higher partial pressure of the helium in the gas mixture, that decreases the probability of energy transfer in the reverse direction—from neon to helium.

The spontaneous emission in the lines $3s \rightarrow 1s$ and $2s \rightarrow 1s$ proceeds slower than in the $3p \rightarrow 1s$ and $2p \rightarrow 1s$ lines, therefore the lower lasing levels of the neon atoms depopulate faster than the upper levels. The emptying of the $1s$ -band levels is the bottleneck of the He-Ne lasing process. The relaxation proceeds through electronic deexcitation, in which the excited neon atom gives up its energy to free electrons, and through atomic collision of the Ne

with the tube walls. The latter contribution is of high significance, for the output of this laser falls off as the laser bore of the tube increases in diameter.

The argon laser. With the exception of neon, none of the neutral noble gases is very useful as a practical laser medium. The other noble gases, when used as laser media, must be

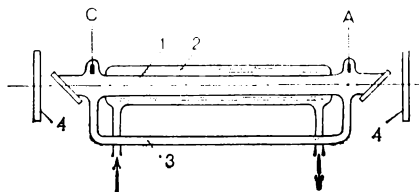


Fig. 2.13 An argon laser system. *A* anode, *C* cathode, *1* lasing volume of discharge tube, *2* water cooling system, *3* return path, *4* resonator mirrors

ionized by electron collisions. The resulting ion is excited by further electron collisions and an inverted population of the ion energy levels occurs.

As an example of such a laser we take up the argon laser fluorescing in the singly ionized argon (Ar^*) lines. The tube design of this laser, schematized in Fig. 2.13, is much more complicated than that of the helium-neon laser. The Ar^+ system exploits a continuous dc arc discharge of high current density. This entails intense heating and a water cooling system is a requirement. During operation, the high current causes a pumping of the argon ions toward the cathode and the electrons toward the anode. Because of the low mobility of the ions they tend to pile up at the cathode where they are neutralized and diffuse slowly back into the discharge. To equalize their distribution over the tube a gas return path is provided between anode and cathode. It balances out the pressure gradient caused by the pumping, preventing the discharge from being extinguished.

The principal transitions of the argon ion are depicted in Fig. 2.14. The dashed arrows indicate the transitions due to electron impact, the solid line arrows show visible emission lines. The hatched bars in the figure represent five atomic states (energy bands), each consistent with its own electronic configuration. We will again, as with the helium-neon

laser, use short-hand notation for these states. The state of the $3p^44p$ configuration will be termed the $4p$ band; this is the upper level of the laser. The state of the $3p^44s$ configuration will be termed the $4s$ band; this is the lower laser level. It will be recalled that we use the term "level" conditionally, as actually each band includes a number of energy levels of the argon ion (a few atomic terms). For example, the $4p$ -band includes 15 terms, and the $4s$ -band 8 terms. Therefore, the $4p$ - $4s$ laser transition includes a set of spectral lines. The most intense of them are the blue line at $\lambda = 0.488 \mu\text{m}$ (45% of the output) and the green line at $\lambda = 0.515 \mu\text{m}$ (35%).

The upper laser level ($4p$ -band) builds up its population with the help of a few processes: by the direct electron impact through the $3p \rightarrow 4p$ transition, by the radiative cascade pump $3p \rightarrow 4d \rightarrow 4p$, and by the step-by-step electron excitation $3p \rightarrow 3d \rightarrow 4p$. It is remarkable that the electronic excitation rate for the upper laser level turns out to be about half as intense as that for the lower laser level. A population inversion occurs owing to the fact that the lifetime of the upper level is ten times that of the lower level, therefore the lower level decays very fast by spontaneous emission. As a result, the argon laser builds up its population inversion not by predominantly populating the upper level (as the case is with the He-Ne laser) but through the predominant clearing of its lower laser level.

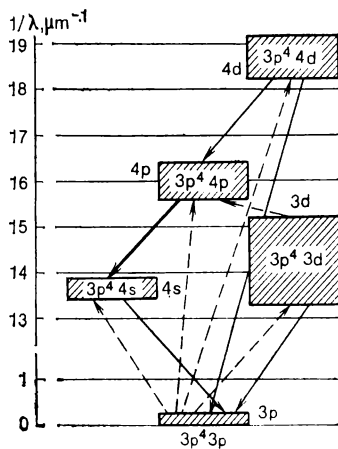


Fig. 2.14 Energy levels involved in some transitions of the Ar⁺ laser. The lasing transition is shown by the heavy arrow

2.6 Molecular Lasers

The CO₂ laser. From the standpoint of potential industrial applications, the carbon dioxide laser unquestionably ranks first. It is capable of continuously generating as high powers

as 10 kW at a relatively high efficiency (up to 40%). The active medium of the laser is a gas mixture consisting of carbon dioxide, molecular nitrogen, and diverse additives, such as helium and water vapour. The active centres here are the CO_2 molecules lasing on the transitions between the vibrational levels of the electronic ground state. The nitrogen in the CO_2 discharge takes the role that helium plays in the

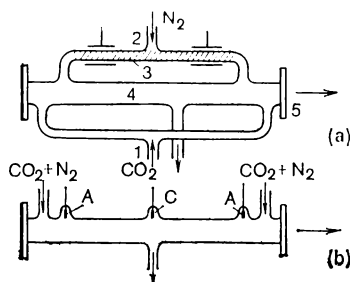


Fig. 2.15 Two discharge tube configurations for the CO_2 laser. (a) with the discharge and laser volumes separated: 1 CO_2 flow system, 2 N_2 flow system, 3 hf glow discharge, 4 laser working volume, 5 output mirror; (b) with the discharge and the laser in one chamber: A anode; C cathode

helium-neon laser; excited nitrogen molecules transfer energy to the CO_2 molecules by resonant collisions. Carbon dioxide lasers normally use a glow discharge for their excitation.

Figure 2.15a schematizes one of the first designs of the CO_2 laser using a high frequency glow discharge. The system has two flow loops for pumping carbon dioxide and nitrogen. The nitrogen molecules first enter the area of discharge and become excited by collisions with the electrons of the discharge and then flow into the laser volume where they mix up with the unexcited CO_2 molecules. When these molecular species collide, the nitrogen molecule imparts a proportion of its energy to the CO_2 molecule by resonant energy transfer. It is an important feature of this particular design that the discharge electrons excite nitrogen molecules only, which then transfer this energy to the active centres in another area of the system.

Subsequent designs of the CO_2 laser have fired a discharge in the $\text{CO}_2 + \text{N}_2$ mixture. This has been as a rule a dc

glow discharge. The arrangement of such a system is schematized in Fig. 2.15b. Similar to the previous arrangement, this system employs pumping of the gas mixture through the lasing volume. This pumping is a way to avoid an undesired change in the chemical composition of the active medium, which could occur, in particular, as a result of the reaction $2\text{CO}_2 \rightarrow 2\text{CO} + \text{O}_2$. Today, sealed-off CO_2 lasers (with no flow of the gas mixture) are in wide use. The life of such devices could be as long as 1000 hours and more.

Vibrational modes of carbon dioxide. Thus far in our discussion, the energy levels of interest for laser transitions

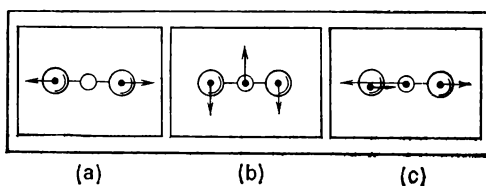


Fig. 2.16 Vibrational modes of a CO_2 molecule. (a) symmetric stretching, (b) bending, and (c) asymmetric stretching

have been electronic energy levels of an atom or an ion. Molecules have a more complicated structure and have energy levels that correspond to rotating or vibrating motions of the entire molecular structure. The carbon dioxide molecule, composed of two oxygen atoms and a carbon atom between them, undergoes three different types of vibrational oscillation, as shown in Fig. 2.16. These three fundamental vibrational configurations are called *vibrational modes*. In the *symmetric stretch mode*, the oxygen atoms oscillate along the axis of the molecule, by simultaneously departing and approaching the carbon atom in between. In the *asymmetric stretching mode*, the oxygen atoms also move along the axis of the molecule, but both in one direction relative to the carbon atom itself moving to the other side. In the *bending mode*, all the three atoms of the molecule undergo vibrational oscillations by moving perpendicularly to the molecular axis. We denote the frequencies of the symmetric stretching, bending, and asymmetric stretching modes by v_1 , v_2 , and v_3 , respectively. The energy contents of these vibrations are

as follows: $h\nu_1 = 0.163$ eV, $h\nu_2 = 0.078$ eV, and $h\nu_3 = 0.276$ eV.

According to quantum theory, the energy of oscillation of a molecule in any one mode can have only discrete values, which are all integer multiples of some fundamental value. At any one time, a carbon molecule can be vibrating in a linear combination of the three fundamental modes. The energy state of the molecule can then be represented by three numbers, (ijk) . These numbers represent the amount of energy, or the number of energy quanta, associated with

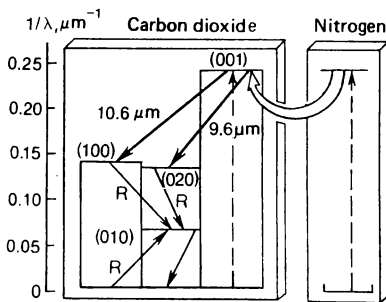


Fig. 2.17 Energy levels in the CO_2 laser

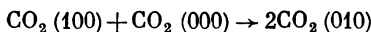
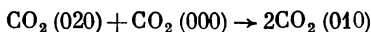
each mode. For example, the number (020) means that the molecule in this energy state is in the pure bending mode with two units of energy (i.e., no units of energy associated with the symmetric and asymmetric stretch modes).

In addition to vibrational states, rotational states, associated with rotation of the molecule about the centre of mass, are also possible. The energies associated with the rotational states, however, are generally small compared to those of the vibrational states, and are observed as splittings of the vibrational levels into a number of much finer sublevels. The separations between vibrational-rotational states are usually much smaller on the energy scale than separations between electronic states.

The mechanism of population inversion in the CO_2 laser. Fig. 2.17 shows the lowest vibrational levels of the ground electronic state of a CO_2 molecule and an N_2 molecule. In the CO_2 portion of the figure the levels correspond to vari-

ous vibrational modes. The upper laser level is state (001), the lower laser level is provided by states (020) and (100). The transition $(001) \rightarrow (100)$ yields a line at the wavelength $\lambda = 10.6 \mu\text{m}$, whereas the $(001) \rightarrow (020)$ yields a line at $\lambda = 9.6 \mu\text{m}$. The population of the (001) state builds up through inelastic collisions of the CO_2 molecules with electrons (electron impact) produced in the plasma of the discharge and with the excited nitrogen molecules (resonant energy transfer).

States (020) and (100) decay into the ground state mainly by resonant energy transfer to the unexcited CO_2 molecules so that these accumulate in the (010) state



The respective transitions are labelled in the figure by the letter R . The depopulation of state (010) is the bottleneck of the process. To hasten the relaxation of this level to the ground state, special additives, such as helium and water vapour, are introduced into the gas mixture. The level degrades as a result of collisions with the additives to which it transfers the excitation energy.

To achieve a population inversion in this case, it is important that the probability of the electronic excitation of the nitrogen and state (001) of the CO_2 molecule be sufficiently high, while the probabilities of the electronic excitation of states (100), (020) and (010) be rather small. These population rates may be controlled by varying the ratio E/p of the electric field intensity in the discharge, E , and the pressure of the gas mixture, p . For example, the optimal values of E/p for the case of equal partial pressures of CO_2 and N_2 range from 5 to 10 V/cm torr.

Excimer lasers. An interesting and important class of molecular lasers involving transitions between different electronic states is that of the excimer lasers. As a rule, these lasers use a beam of electrons from an accelerator, rather than an electric discharge, for their excitation. Since the laser action occurs between the electronic states of excimer molecules, the emission falls in the ultraviolet end of the e.m. spectrum. The active medium of these lasers consists of the so-called bound-free systems. These are diatomic molecules that can be bound into a single system when in the excited

state only. When in the ground state, the constituents of such a system repel one another at interatomic distances characteristic of most diatomic molecules. For some atoms, an excitation or ionization sufficiently modifies the state of the atom, so that there is an attractive force with other atoms in the gas. The two atoms are then bound together at a small separation distance, creating an *excited-state dimer*, or *excimer* for short.

The atoms of inert gases are known to defy bounding into molecules. They can in fact be bound into molecules only after being imparted an energy, they occur only in excited state. If one or both of the excited-state atoms in the system are rare-gas atoms, the amount of excitation is extremely large. Hence the metastable excimer state is an important system for storing high energies.

The possibility of storing high energies in excimers makes them very attractive propositions for lasing. The upper laser level in such a molecule is its electronic excited state, and the lower level coincides with the electronic ground state. It is quite obvious that a population inversion in this system will occur as soon as some molecules are excited to bound in the upper state. Once a molecule decays to the lower level, it leaves it immediately because of dissociation into atoms. Therefore, the lower level in excimer lasers is always empty.

The active medium in an excimer laser can be an excited rare-gas dimer (Ar_2^* , Kr_2^* , Xe_2^* ; * denotes excited state), a rare-gas oxide (ArO^* , KrO^* , XeO^*), or a rare-gas atom in combination with a halide atom (ArF^* , KrF^* , XeCl^*). Excimer lasers are responsible for the emissions with the shortest wavelengths. For example, lasing has been obtained at $\lambda = 175 \text{ nm}$ (ArCl) and at $\lambda = 126 \text{ nm}$ (Ar_2).

2.7 Electroionization Lasers

Rising pressure in the gas laser. We have already noted that the gas lasers operate at low pressures of active media, being in the range from 1 to 10 torrs. This implies a relatively low concentration of the active centres ($10^{15}\text{-}10^{16} \text{ cm}^{-3}$) which is a few orders of magnitude lower than the figures of solid state or liquid lasers ($10^{19}\text{-}10^{20} \text{ cm}^{-3}$). Higher gas pressure in gas lasers means enhanced output powers, The-

before, much research has been done to make them operate at higher pressures.

Two circumstances exist, however, that oppose this pressure-increasing trend in gas lasers. First, an attempt at increasing pressure up to a few ten torrs turns the self-maintained electric discharge practically unuseful for exciting appropriately large gas volumes because the discharge loses its stability (arches), sticks to the walls and leaves the core volume of the tube. Second, for a higher pressure an optimal E/p ratio obviously calls for a higher electric field intensity. This leads to a greater electron density in the plasma, being a negative factor as excess electrons enhances the number of quenching collisions, specifically those causing deactivation of the upper levels and population of the lower lasing levels.

Electroionizing pumping of high-pressure gas lasers. This technique has made possible solving the aforementioned pressure problems. It does not refer to the self-maintained discharge at all, instead it produces fast electrons capable of efficiently exciting the active material by an ionizing radiation which is applied together with an electric field. The ionizing radiation knocks out free electrons and the electric field takes care of their acceleration. The further processes are essentially the same as in a gas discharge laser — the fast electrons excite certain molecules (atoms) to bring about a population inversion provided appropriate conditions exist. Fig. 2.18 shows schematically the process of electroionization pumping.

To produce one free electron, it takes an energy of about several ten electronvolts. This energy is supplied with the ionizing radiation. The electron suffers up to 10^5 collisions with the particles of active material, until it recombines or leaves the working volume. In these collisions the electron gives up about 10^4 eV of energy to the active medium, which is about three orders of magnitude above the energy expended to produce this electron. This large amount of ener-

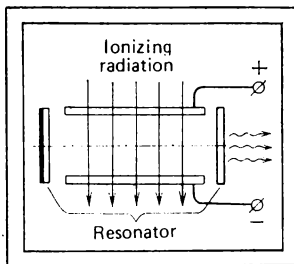


Fig. 2.18 Electroionization pumping

gy is gained from the external electric field. This technique, therefore, is a rather efficient (up to 30%) direct conversion of electric energy into a coherent optical radiation.

This technique lends itself for an easy control of the optimal electric field to pressure ratio at higher pressures, since the concentration of free electrons now is independent of the electric field intensity E , and is controlled by the intensity of the ionizing radiation. As a consequence, pressures as high as 100 atm has been realized in the systems known as high-pressure gas lasers.

The passage of electric current through the ionized gas is rather stable over a wide pressure interval. A non-self-sustained discharge initiated in the working volume exhibits a stable behaviour for a wide range of volume capacities (up to 100 litres).

Generally, to sustain a discharge, the gas must be ionized; to obtain a population inversion, the active material must be excited. In a gas discharge laser, the same electrons perform both these functions and the energy distribution of these electrons cannot be optimal simultaneously for both the ionization and excitation. The electroionization laser has these functions separated — the gas is ionized by radiation and the electrons provide the excitation of the medium only.

The electroionization CO_2 laser. The physical mechanism of population inversion in CO_2 high-pressure lasers excited with the electroionization technique is the same as in a gas discharge CO_2 laser (see Fig. 2.17). The only difference is that the fast electrons exciting vibrational states of the nitrogen and carbon dioxide molecules are produced here by an ionizing radiation and an accelerating external electric field rather than by a self-sustained discharge. The ionizing radiation is a beam of electrons produced in an electron accelerator (gun). The beam carries electrons of energies from 100 to 500 keV, its current density being in the order of 10^{-4} A/cm^2 .

A simplified diagram of the electroionization CO_2 laser is shown in Fig. 2.19. The intense electron beam passes through a metal and enters into the working volume confined between two electrodes. The foil separates the vacuum of the electron gun from the high pressure of the working volume. The laser beam leaves the working volume through the out-

put mirror of the resonator. Compared with an ordinary CO₂ laser, the power generated by this laser per unit volume of the active medium increases five to six orders of magnitude.

To conclude the discussion, we note that the ionization may also be achieved with ultraviolet radiation (photoioniza-

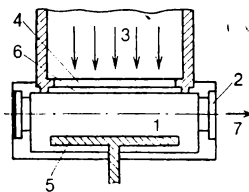


Fig. 2.19 Schematic of an electroionization laser arrangement. 1 laser volume, 2 output mirror, 3 fast electron beam, 4 upper electrode, 5 lower electrode, 6 metal foil transparent for the electron beam, 7 laser output

tion). The optical excitation then acts as a component of the electroionization pumping. Finally, the gas can be ionized with heavy particle products of nuclear reactions.

2.8 Gas Dynamic Lasers

Thermodynamic methods of population inversion. A sufficiently high population of the vibrational and rotational states of a molecule may be achieved by thermal excitation. To this end, a gas mixture should be heated to temperatures in the range of 1000-2000 K. This simple rise of temperature cannot, of course, produce a population inversion, as in equilibrium the level is populated less, the higher its energy. In other words, whatever high the temperature of the gas, the lower-lying levels of a molecule will be more populated than the higher-lying levels.

Now assume that the gas is heated to a temperature T_2 and then rapidly cooled down to another temperature T_1 . Let τ denote the time it takes the gas to be cooled from T_2 to T_1 , and E_1 and E_2 be the lower and the upper level energy, respectively. Assume that the cooldown of the gas mixture sweeps out level E_2 at a lower rate than level E_1 . Denote the lifetimes of these levels by τ_2 and τ_1 . Suppose that our cooldown is a rapid process and $\tau_1 < \tau \ll \tau_2$. With this time

setting, the population of level E_1 will follow the drop in temperature, whereas that of level E_2 will lag the temperature profile and remain virtually at the high temperature population. This population behaviour will produce an inversion between levels E_2 and E_1 .

A fast cooldown may most conveniently be achieved with the adiabatic expansion of the gas as it passes through a narrow slit or a nozzle under pressure. It is this thermodynamic principle that underlies the operation of gas dynamic lasers.

It should be noted that a population inversion can also be achieved by rapidly heating the gas provided that the excitation buildup of the higher-lying level is more intense than that of the lower lasing level. A sufficiently fast heating of the gas [mixture may be achieved by means of shock waves.

The gas dynamic CO₂ laser. This laser uses a mixture of carbon dioxide, nitrogen and water vapour as its active

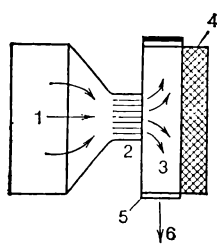


Fig. 2.20 Idea of the gas dynamic laser. 1 prechamber, 2 nozzle, 3 working volume of the resonator, 4 diffusor, 5 output mirror, 6 laser output

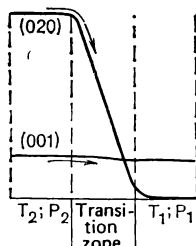


Fig. 2.21 Transition behaviour of the upper (001) and lower (020) laser level populations of the CO₂ molecule in the gas stream

medium. The mixture typically contains 8% CO₂, 90% N₂ and 2% H₂O. The active centres are the CO₂ molecules.

The idea of the gas dynamic laser design is illustrated in Fig. 2.20. Upstream of the nozzle, the gas mixture is brought to the operational condition of the temperature $T_2 = 1500$ K and pressure $p_2 = 20-30$ atm. Behind the nozzle block — a set of slits each 1 mm wide — the gas expands so that its temperature falls to $T_1 = 250-300$ K and pressure to $p_1 = 0.05-0.1$ atm. The flow rate downstream of the nozzle

is as high as 1200 to 1500 m/s. The excited CO₂ molecules lase in the working chamber. Then the gas flow meets the diffuser provided for decelerating the flow and matching its pressure with the atmosphere.

Available gas dynamic CO₂ lasers yield record continuous output powers of up to 100 kW. Unfortunately, the efficiency of these lasers is fairly low, never exceeding 1%. The latter fact is due to a number of reasons. First of all, the kinetic energy of the gas flow is useless for the laser. Moreover, the flow sweeps out of the resonator a number of excited nitrogen molecules which have had not enough time to transfer their excitation energy to the CO₂ molecules, and also a certain amount of CO₂ molecules which have failed to lase.

The inversion production mechanism in the gas dynamic CO₂ laser. Similar to other types of CO₂ lasers, here the population inversion is obtained between the (001) and (100) states and (001) and (020) states of the CO₂ molecule. The processes of resonant energy transfer from the N₂ molecules take an important part in populating the (001) upper laser level. Water molecules introduced into the mixture aid in rapid sweeping out lasing molecules in the (010) state.

The thermodynamic pumping is remarkable in that now the vibrational states of the N₂ and CO₂ molecules are populated through thermal, rather than electronic, excitation. It is essential that the excited vibrational level of the N₂ molecule and state (001) of the CO₂ molecule depopulate slower than states (100), (020), and (010).

Assume that the CO₂ + N₂ gas mixture heated to 1500 K rapidly expands in passing through a nozzle. Downstream from the nozzle, where the gas velocity runs into the supersonic 1500 m/s, the kinetic energy of the molecules increases considerably. This translation energy increases at the expense of the vibrational motion in the molecules. Therefore, behind the nozzle the vibrational states are swept out in the ground state rapidly. It is important that not all the levels undergo rapid decay, but exactly those having shorter lifetimes, that is, the lower laser levels of the CO₂ molecule. As for the (001) state of the CO₂ molecule and the vibrational level of the N₂ molecule, there is simply not enough time for them to somewhat relaxate in the rapid gas expansion. When in the laser volume, with a sufficiently rarefied gas medium, these levels fail to deactivate by collisions practi-

cally altogether, and the vibrational state of the nitrogen molecules and state (001) of the CO₂ molecules are said to be "frozen".

The behaviour of the population for states (001) and (020) of the CO₂ molecule passing from the prechamber (at T₂ and p₂) to the working volume (at T₁ and p₁) is presented in Fig. 2.21. In the transition region around the nozzle, the (020) level is almost completely removed to the ground state, while state (001) suffers only insignificant loss of its population. As a result, a population inversion occurs between these states.

Thus, CO₂ molecules arrive at the working volume having practically unpopulated lower lasing levels (more precisely, having the population of these levels at T₁). The upper laser level turns out to be populated as if the gas remained at temperature T₂. It is of consequence that the population of the vibrational level of the N₂ molecules is also frozen. These excited molecules will give their energy to the CO₂ molecules through resonant collisions and maintain the relatively high population of the (001) level. Recall that the nitrogen is the prevalent component in the gas mixture (about 90%). Therefore, its vibrational energy is believed to be a chief source of energy for the coherent radiation.

To sum up, the gas dynamic laser spends the energy stored in the vibrational degrees of freedom of the molecules arriving at the nozzle as follows. The fraction of the energy stored in the symmetric stretching and bending oscillations of the CO₂ molecules converts into the translation energy of the flow leaving the nozzle. The energy stored in the asymmetric stretching oscillations of the CO₂ molecules and, what is more important, in oscillations of the nitrogen molecules converts (minus losses in the resonator) into the energy of the coherent radiation of the laser.

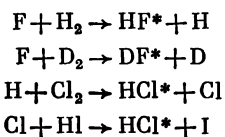
2.9 Chemical Lasers

Chemical compounds are able to store large amounts of energy that may be partially released in exothermal chemical reactions, i.e. the ones proceeding with liberation of energy. It has been rather attractive to convert this energy into coherent optical radiation. The chemical lasers are exactly the systems where such a conversion has been realized. The

current chemical lasers oscillate on the vibrational (more exactly, on vibrational-rotational) transitions of molecules. They can lase at wavelengths as short as 2 μm (near infrared). Research is under way to produce chemical lasers radiating in the visible region of the spectrum, i.e., oscillating in the lines between the electronic states of molecules.

Initiation and acceleration of chemical reactions. Most often chemical lasers use the energy of substitution reactions which produce diatomic molecules in excited vibrational states. These molecules either fluoresce themselves or transfer their excitation energy to other molecules that lase. In the first case the population inversion is produced directly, whereas in the last case it is achieved in an indirect way resulting in chemical transfer lasers.

Here are some examples of the substitution reactions useful for lasing action (* indicates an excited state)



Although these reactions produce species in the excited state, the dissociation of the hydrogen, fluorine, or chlorine atoms from their initial molecular states (H_2 , F_2 , Cl_2) must be accomplished with an additional energy source (say a flashlamp or a thermal source). Apart from that, the chemical reaction must be made fast running in order to quickly fill the upper laser level of radiative molecules. The rate of a chemical reaction is proportional to the concentrations of the reacting species, therefore an ample amount of species must be provided to make it go fast.

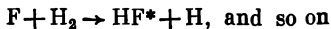
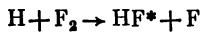
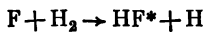
There is a number of means for initiating and accelerating chemical reactions. One of them is dissociation which for the laser purposes takes the form of photodissociation, dissociation with an electron beam, although it may be achieved by a pulsed discharge, or by a heat source.

Photoinitiation in chemical lasers is obtained by flash-lamps. Where a pump of a shorter wavelength is required (shorter than 0.2 μm) various types of gap discharge may be employed, say a spark. One of the simplest techniques to initiate chemical reactions is with an electric discharge in the

gas. It is suitable, however, for relatively low pressures and small lasing volumes only. Therefore, more promising appears to be the energy influx by an electron beam. The electron beam is able to initiate a reaction within very short time of 10^{-7} - 10^{-8} s (in a self-sustained discharge the duration of a pulse cannot be made shorter than 10^{-6} s). Thermal initiation uses some source of heat to dissociate the molecules of the reaction. This technique lends itself for gas dynamic types of laser.

Chemically active species can also be provided by certain chemical reactions. An example may be the reaction $\text{NO} + \text{F}_2 \rightarrow \text{NOF} + \text{F}$. Nitrogen monoxide existing as a stable radical at ambient temperatures reacts with molecular fluorine yielding chemically active atomic fluorine.

Chain reactions for chemical lasers. The reactions utilized in chemical lasers are cyclic, i.e., once initiated the reaction keeps producing the active centre (atom or radical) by its own means. Assume that a gaseous mixture containing molecules of H_2 and F_2 receives a package of chemically active species, say, fluorine atoms. Then this mixture is expected to give rise to the following chain process



When these chemically active species build up in a sufficiently large amount, the process will proceed rather fast and the condition for lasing in some transitions of the HF^* species will occur. Since in a cyclic process the amount of chemically active species remains unaltered, due to replenishment, there appears a possibility to involve, by chain process, an enormous number of hydrogen and fluorine molecules into the reaction and build up the number of the active centres HF^* . The amount of chemical energy that can in this way be converted into the coherent optical radiation will by far exceed the energy expended in creating the chemically active centres.

An actual chain process is not endless of course. The chemically active species decrease in number by recombination ($\text{H} + \text{H} \rightarrow \text{H}_2$, $\text{F} + \text{F} \rightarrow \text{F}_2$). Therefore, the chemical reaction should be not only initiated but also maintained by creating new chemically active species instead of those

eliminated from the chain. The number of lasing species also declines through the processes deactivating the upper laser level.

To extend the life of lasing chemical chains, they should be of the branched type rather than of a single line variety. Branched chain reactions, as their name implies, multiply chemically active species in a fan-like scheme. For example, at certain pressure and temperature conditions, the fluorine-hydrogen gas mixture yields the reactions $F_2 + HF \rightarrow HF + F + F$ which can initiate branching of the chains.

The deuterium fluoride chemical transfer laser. Here we give a short exposition to a chemical transfer laser operating in CO_2 lines excited by the reaction between deuterium and fluoride. The reactor chamber of the laser, shown in Fig. 2.22, receives through one port a mixture of helium (carrier gas) and molecular fluorine, and through another port a mixture of nitrogen monoxide and carbon dioxide. The reaction $NO + F_2 \rightarrow NOF + F$ yields the atomic fluorine necessary to initiate reactions with deuterium, introduced through a separate channel: $F + D_2 \rightarrow DF^* + D$, $D + F_2 \rightarrow DF^* + F$. The excited DF^* molecules transfer their energy to the CO_2 molecules that lase in the optical resonator where they enter with the gas flow. An inert carrier gas — helium in this case — flows through the entire system to prevent overheating and self-ignition of the fluorine-deuterium mixture, as well as for sweeping out the lower laser levels of the CO_2 molecules.

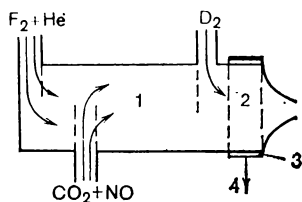


Fig. 2.22 Schematic of a hydrogen-fluoride chemical transfer laser. 1 chemical reactor chamber, 2 resonator volume, 3 output mirror, 4 laser output

2.10 Plasma Lasers

Recombination plasma as the active medium. When free electrons collide with positively charged ions in a discharge plasma, they may be captured by these ions, i.e., recombinations take place. In the act of recombination, energy is liberated equal to the binding of the electron in the atom. This

energy may lead to the buildup of atoms (ions) in excited states. Accordingly, an actively recombining plasma can be used as an active medium. The lasers build on this idea are termed plasma lasers in the Soviet literature on the subject.

The plasma of such lasers differs considerably from the plasma of gas discharge lasers. To draw a terminological dividing line, the first plasma is said to operate in the recombination mode, while the last in the ionization mode. A consideration of plasma behaviour involves in addition to the discharge temperature T , defined through the average kinetic energy of the heavy plasma species (ions, atoms and molecules), the electron temperature T_e , defined through the mean energy of the free electrons in the plasma.

In the ionization mode, $T_e \gg T$, with $T_e/T \approx 100$ in a glow discharge and $T_e/T \approx 10$ in an arc discharge, which means that free electrons in such a plasma move much faster than the ions. The probability of recombination collisions under these conditions is rather low. For recombination, it is essential that the free electron moves at a low velocity so that the inequality $T_e < T$ held true. The probability of recombination will, obviously, be higher, the greater the concentration of free electrons, i.e., the more ionized is the plasma. Whereas in a glow discharge this concentration is 10^{11} cm^{-3} and in an arc discharge 10^{13} cm^{-3} , the recombination plasma must have at least $10^{15}\text{--}10^{16}$ electrons per cubic centimetre. Thus the plasma in the recombination mode is a dense, highly ionized plasma with "supercooled" electrons, called accordingly *cold plasma*. By contrast, a plasma in the ionization mode is a rarefied gas of a relatively low ionization degree and "overheated" electrons, hence the name *hot plasma*.

A recombination plasma is very attractive as an active medium. Unlike other media, it does not alter its phase at arbitrary high density of the energy influx. This opens up principally new possibilities for high power lasers. In addition, the recombination plasma offers certain potentialities for lasing in the ultraviolet and x-ray portions of the e.m. spectrum.

Comparison of plasma and gas discharge lasers. The principal difference between these systems is due to the properties of plasma in the recombination mode in one and in the

ionization mode in the other laser. In operation, the degree of plasma ionization increases in the gas discharge laser and decreases in the plasma laser. Accordingly, the gas discharge laser may be said to operate on the gas to plasma transition, whereas its plasma counterpart operates on the plasma to gas transition.

A pulse gas discharge laser starts oscillating upon some rather high current pulse intensity is reached in the discharge, already during the pulse risetime. In a pulse plasma laser, oscillations set in when the current pulse is over, the plasma is highly ionized and the free electrons are cooled down. In other words, the plasma laser emits in the discharge's afterglow.

The pulse plasma laser. To ionize the active medium, these lasers are pumped by rapidly falling electric pulses which are typically as large as 20 kV and 300 A within 0.1 to 1 μm of pulse duration. The oscillation pulse develops in the discharge afterglow. The active medium is a mixture of an easily ionizable laser-active component and a hardly ionizable auxiliary (buffer) component. The latter is needed mainly for fast cooldown of free electrons in the plasma.

The available pulse plasma lasers use in particular the ionized vapours of alkali-earth metals, such as Mg, Ca, Sr, Ba, as the active medium. Consider as an example the strontium-helium plasma laser oscillating on the transitions between the levels of singly ionized strontium ions (Sr^+). The helium plays the role of a buffer gas. A pumping pulse generates a plasma with a high concentration of doubly ionized strontium ions (Sr^{2+}). The processes of recombination lead to the formation of excited singly ionized strontium ions acting as the active centres. The system lases in a few transitions of these ions. The major lines are in the violet portion of the spectrum at 0.416 μm and 0.431 μm .

2.11 Semiconductor Lasers

Electronic states in intrinsic semiconductors. The energy of electrons in the atom (ion or molecule) takes on discrete values identified as the electronic levels. When atoms form a crystal lattice in a solid they donate their outermost electrons into the crystalline structure. The energy of these elec-

trons can as a result vary continuously within a certain energy interval, called an energy band or zone. Each energy band is consistent with a finite (although very large — in the order of 10^{23} to 10^{24}) number of electronic states. It will be recalled that electrons belong to fermions, that is, obey the Pauli exclusion principle, which states that only one electron is allowed in each possible quantum state. This means, first, that only two electrons can occupy the lowest possible energy state (the two have opposite spins and, therefore, do not violate the exclusion principle), and second, that an electron cannot be excited to a higher state unless it is unoccupied. Therefore, an energy band is either occupied by electrons partially or is completely filled. Electrons occupy levels, considerably the lowest energy levels, filling them in succession from the lowest-lying energy levels upwards in energy.

The electronic properties of a solid are determined largely by the periodic crystal lattice arrangement of the atoms that make up the solid itself. A quantum mechanical calculation of the allowed energy levels for electrons in a periodic lattice predicts that the allowed electronic states occur within well defined bands of energy. Between these bands are energy gaps, which are energy intervals that no electron in the solid can possess. The highest filled band in the electronic energy distribution is the *valence band*. The next highest energy band partially or completely unoccupied by electrons is the *conduction band* of the solid. It is the size of the energy gap, known as the "*band gap*", between the valence band and the lowest conduction band that determines whether a solid is an insulator, a metal or a semiconductor.

If the valence band is completely occupied and the conduction band is empty, the material is an insulator. This is because conduction is due to the movement of "free" charge carriers from one state in a band to another state in the band under the influence of an electric field. In an insulator the valence band is filled and the nearest available states in energy are in the lowest conduction band separated from the valence band by the gap so large that thermal excitation is insufficient to excite electrons into the conduction band. In contrast, metals are good conductors because either there is an overlap between the valence and conduction bands, or the conduction band is partially filled. Under the influence of an

electric field, the electrons are free to move because there are nearby empty states available.

If the band gap for a material is sufficiently small (about 2-3 eV or less) that thermal excitation can excite electrons in the valence band to states in the conduction band, the conductivity is intermediate between that of a metal and that of an insulator. The material behaves as a semiconductor. When an electron in the valence band of a semiconductor is excited thermally to the conduction band, an unfilled energy state in the valence band occurs. This unfilled state, called a hole, has many of the same properties as an electron, except that a positive charge is assigned to it. In the presence of an electric field, the hole moves in the direction of the field, just as a positive charge would.

A semiconductor with no impurities, called an *intrinsic semiconductor*, has an equal number of conduction electrons and holes, since for every conduction electron produced there must be a corresponding hole generated. A quantum transition of an electron through the band gap into the lowest conduction band may be viewed as the generation of an electron-hole pair. The electron brought to the conduction band tends to occupy the lowest state in this band whereas the hole tends to ascend to the top of the valence band. Along with the transitions through the band gap into the conduction band the reverse transitions from the conduction into the valence band are also possible. When an electron undergoes the transition from the conduction band into the valence band it meets a hole there, so the process may be viewed as a recombination of an electron and a hole.

Optical transitions in semiconductors. Assume that a semiconductor material is illuminated by photons whose energy exactly fits the width of the band gap in this material (or is slightly higher than this width). Such a photon can be absorbed by an electron occupying a level close to the upper boundary of the valence band. The excited electron will then move to the conduction band (Fig. 2.23a). Practically the same probability exists for the photon to initiate the opposite process, i.e., the transfer of an electron lying at the bottom of the conduction band down to the valence band. When this electron recombines with a hole in the valence band, a quantum of radiation with energy equal to the energy difference between the two states is released. This secondary

photon is in the same state as the primary photon (Fig. 2.23b). In the first case, the semiconductor absorbs light, while in the second case, the stimulated emission of light takes place. Spontaneous emission of light is also possible when electrons spontaneously fall from the conduction band to the valence band.

Thermal excitation of a semiconductor moves a relatively small number of electrons from the valence band into the conduction band. So, the concentration of electrons in the

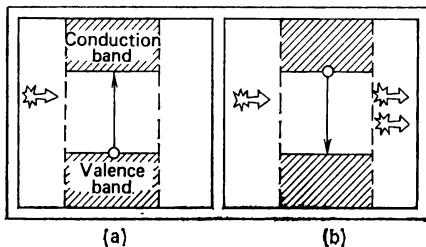


Fig. 2.23 Absorption (a) and emission (b) transitions in optically stimulated intrinsic semiconductor

conduction band — even at its lowest boundary — is sizeably lower than that in the valence band. Therefore, at reasonable temperatures the processes of light absorption dominate over those of stimulated emission and the outside effect will be the absorption of radiation by the semiconductor.

In order that a semiconductor material may amplify an incident flux of photons, it must be inverted, with the concentration of electrons at the bottom of the conduction band being higher than that at the top of the valence band. Then the processes of stimulated emission of light will dominate over those of absorption of light. The inverted semiconductor is characterized by a sufficiently high concentration of electrons in the conduction band and, respectively, a high concentration of holes in the upper levels of the valence band. The semiconductors in which these properties are created are referred to as *degenerate* semiconductors. A semiconductor can be made degenerate in *p*-type carriers (*p* stands for positive) that is in holes, or in *n*-type carriers (electrons). Semiconductors with no impurities, intrinsic semiconductors, can be made degenerate in both *n*-and *p*-carriers only simultaneously.

Semiconductor lasers pumped by an electron beam. An intrinsic semiconductor can be inverted by optical pumping in which the semiconductor chip is irradiated by photons whose energy exceeds the width of the band gap. More often, however, an electron beam is used for this purpose. Fast electrons (50 to 100 keV strong) traverse the semiconductor chip and initiate electron transitions from the valence band into the conduction band. Among the electronic materials employed in such devices are gallium arsenide (GaAs), cadmium sulphide (CdS), cadmium selenide (CdSe), to name a few.

More than half of the electron beam energy is lost in heating the chip. Therefore, the pumping is mainly fed in short pulses of electrons and a heat sink is essential. Cooling is crucial for semiconductor lasers. The point is that high temperatures raise the electrons in the conduction band to ever higher energy levels, degrading the concentration of electrons at the bottom of the band. The same process increases the concentration of electrons at the top of the valence band. Both trends lower the degree of inversion, which results in decreasing gain, and the increasing losses imply a higher oscillation threshold. For many semiconductors this threshold is so high that they are able to emit at rather low temperatures only. For example, to operate at reasonable efficiencies, gallium arsenide lasers are normally cooled to 80 K. For the same reasons, cadmium sulphide and selenide lasers operate at liquid helium temperature (4.2 K) in some systems.

In this type of semiconductor lasers the pumping electron beam may be introduced in perpendicular and longitudinal arrangements. In the first arrangement, the electron beam and the emitted radiation propagate at right angles. The electron beam is incident normally on one face of the semiconductor chip made in the form of a right parallelepiped; two other opposite faces of the chip are cleaved along natural crystalline planes or polished to serve as the mirrors of the optical resonator (Fig. 2.24a).

The longitudinal-pumped laser uses external mirrors for the resonant cavity. The active medium is a thin layer of semiconductor material deposited on a transparent substrate of high thermal conductivity, say, a sapphire plate. Fig. 2.24b shows the idea of this arrangement, where the electron beam

is parallel to the resonator axis and, therefore, concurrent with the emitted radiation. Still another arrangement is presented in Fig. 2.24c, where the electron beam is incident on a cooled semiconductor layer at an angle to the resonator axis. Both these arrangements improve heat abstraction from the semiconductor and increase its active volume.

The cadmium sulphide laser oscillates at a wavelength of $\lambda = 0.49 \mu\text{m}$ with an efficiency of 25%. Its threshold current density is 0.4 A/cm^2 at 80 K and 0.03 A/cm^2 at 4.2 K , with an electron beam energy of 60 keV.

Degenerate n- and p-type semiconductors. Until now we have considered laser action in intrinsic, that is non-doped,

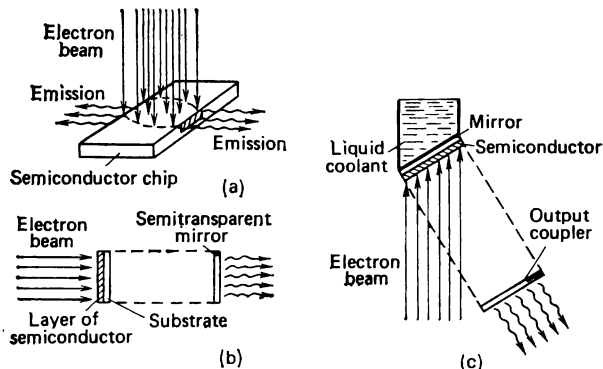


Fig. 2.24 Electron beam controlled semiconductor lasers. (a) transverse pumping, and (b, c) longitudinal pumping arrangements

semiconductor materials. Doping may considerably alter the electronic behaviour of a semiconductor. The dopants are of two types. One of them easily donate one of their electrons into the conduction band of the crystalline lattice, hence the name for them — donors or *n*-type impurities. Others tend to accept one electron from those electrons which the atoms of host material have donated for crystal bonding into the valence band; this type of impurities is therefore called *acceptors*.

In the energy-level diagram of the host crystal, the dopant atoms give rise to an energy level within the band gap. Fig. 2.25a shows the system of levels for an *n*-type material, i.e., a semiconductor with a donor impurity. The donor

energy level is seen to occur in the band gap, spaced ΔE below the bottom of the conduction band. The energy separation ΔE is on the order of 0.01 eV which is about one hundredth of the band gap width E_g . That ΔE is small implies a weak bonding of one of the electrons with the atom, there-

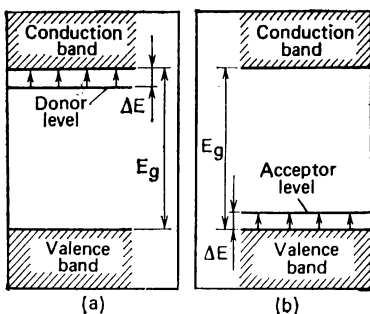


Fig. 2.25 Energy-band diagrams for (a) *n*-type and (b) *p*-type semiconductors

fore a small heat excitation would be enough for this electron to escape the atom and be raised from the donor level into the conduction band.

Assume now that an *n*-type semiconductor is gradually raised in temperature from 0 K. Since $\Delta E < E_g$, the first to occur will be the transitions from the donor energy level to the conduction band, whereas the transitions of electrons from the valence band to the conduction band will be virtually nonexistent. Normally, at around 20 to 50 K the donor energy level is depleted, which means that all the donor atoms have already donated their electrons into the conduction band. If the concentration of impurities in the material is sufficiently high (at least 10^{18} atoms/cm³) the semiconductor is said to be *heavily doped* or *highly degenerate n-type* material as already at the above temperatures it acquires a degenerate situation in the conduction electrons.

The energy level situation with an acceptor-doped semiconductor is depicted in Fig. 2.25b. Here the acceptor atoms are seen to produce the acceptor level ΔE above the valence band. Now a small heat excitation is capable of raising electrons from the valence band onto the acceptor energy level.

This level, therefore, is saturated already at 20 to 50 K. The electrons raised to this level leave behind a certain concentration of holes, which makes this semiconductor a highly degenerate *p*-type material at the impurity concentrations being at least 10^{18} atoms/cm³.

[Injection lasers.] The most common way to the population inversion in semiconductor materials is by joining a *p*-type and an *n*-type material together. The contact that occurs is

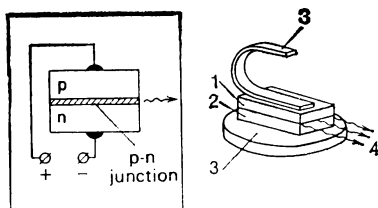


Fig. 2.26 Injection laser. (a) schematic diagram and (b) device configuration: 1 *p*-type semiconductor, 2 *n*-type semiconductor, 3 metal leads, 4 laser output

known as the *p-n* junction. Imagine that a dc voltage is applied to a semiconductor chip having a *p-n* junction as shown in Fig. 2.26a. This is referred to as forward biasing of the junction. Under the influence of the electric field conduction electrons will be injected from the *n*-side into the junction area, while holes will enter the junction from the *p*-side. The *p-n* junction will experience transitions of electrons from the conduction band into the valence band, that is the electrons and holes will recombine there, emitting the surplus energy as radiation. Consequently, a laser action may be realized provided the material is within a suitable optical resonator.

The semiconductor diodes lasing from their forward biased *p-n* junction are referred to as *injection lasers*. The most popular device of this type is built around a GaAs chip. Its highly degenerate *n* region is achieved by heavily doping gallium arsenide with tellurium in a concentration of 3×10^{18} to 5×10^{18} atoms/cm³, while the degenerate *p* region is achieved by doping the material with zinc in concentrations around 10^{19} cm⁻³. This laser oscillates at wavelengths from 0.82 to 0.9 μm in the infrared.

The semiconductor lasers of injection type are the cheapest and smallest lasers available. They are commercially significant because they can be mass-produced and easily fabricated into arrays using the same techniques developed for transistors. Fig. 2.26b renders the idea of this laser design. The polished ends of the chip, cut at right angles to the *p-n* junction layer, take up the role of the resonator mirrors as the GaAs to air reflectivity is rather high. This is a miniature device with the dimensions of its ends only 1 mm. The thickness of the *p-n* junction layer is within 2 μm . Output powers about 10 mW are lased in continuous operation, while in pulsed operation the peak power runs into 100 W. The largest output and the best efficiency can be obtained with the GaAs chip kept at the temperature of liquid helium 4.2 K. For some injection laser systems oscillation is observed at room temperatures, of course with lower powers and efficiencies. In general, the injection lasers are advantageous in a rather high efficiency of 50 to 60%.

2.12 Confinement of the Beam within the Resonator

The many types of lasers we have considered differ in their active media and pumping techniques. They may as well be placed in various optical resonators. The role the optical resonator plays in the confinement of laser beam and the optical feedback will be considered in this section.

Linear and ring resonators. By their outline the optical resonators may be broadly categorized into linear, and ring or offset configurations. In the linear resonator, the mirrors are on one line which is the optic axis of the resonator and the mirrors. In the ring resonator, light is reflected into a closed loop. This arrangement is normally achieved by a system of three or more mirrors, as shown in Fig. 2.27a. A two-mirror ring resonator is also possible as can be seen from Fig. 2.27b, where the active material is offset from the direction of the output beam. The curvilinear configurations may, however, be treated as modifications of linear resonators, the more so that ring and offset configurations emerge in discussing some special topics only. Accordingly, in what follows we confine ourselves to evaluating the properties of linear resonators.

Stable and unstable resonators. The stability condition. An optical resonator is referred to as stable, if light rays bouncing back and forth between the mirrors are reentrant and all the radiation is confined within the cavity, otherwise it is unstable. The stability of a resonator is determined by its geometry, i.e., by the curvature of the mirrors (plane parallel, concave, convex) and the ratio of the resonator length to the mirrors' radii of curvature. The stability analysis for a resonator is performed by the ray-tracing technique which evaluates the behaviour of a ray travelling close

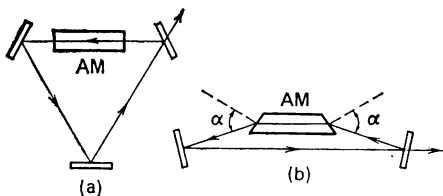


Fig. 2.27 Ring resonator. (a) three-mirror arrangement, (b) two-mirror arrangement; *AM* active material, α Brewster angle

to the resonator optic axis (called a *paraxial ray*). If after a large number of reflections the paraxial ray is observed to diverge from the resonator axis, the resonator configuration being analyzed is characterised by high losses. If, on the other hand, the ray is found to remain close to the optic axis, the resonator is recognized as having a *low-loss configuration*.

Such a stability analysis is performed in general for an arbitrary mirror separation L and arbitrary mirror radii of curvature r_1 and r_2 . The result of this analysis is the *stability condition* generally expressed in terms of two dimensionless quantities, the *g-parameters* of the resonator, defined by the equations

$$g_1 = 1 - L/r_1 \text{ and } g_2 = 1 - L/r_2 \quad (2.1)$$

By convention, the radius of curvature of a mirror is taken to be positive, if the centre of curvature of the mirror lies in the direction of the laser cavity; otherwise r is taken to be negative. For a plane mirror, $1/r = 0$. With this definitions, the stability condition has the simple form

$$0 < g_1 g_2 < 1 \quad (2.2)$$

As long as this relationship is satisfied by the resonator, a paraxial ray continues to remain close to the optic axis, even after many reflections, and the mirror configuration is termed *stable*. In the cases where the product $g_1 g_2$ equals zero or unity, the laser is on the boundary between stability and instability and is termed *marginally stable*.

The stability condition is depicted in Fig. 2.28. In this figure, the stable regions correspond to the shaded area. Each specific resonator is represented by a point on this plane. This plot is referred to as the stability diagram.

Point A on this diagram represents a resonator formed by two plane mirrors (a plane-parallel resonator) for which $1/r_1 = 1/r_2$ and $g_1 = g_2 = 1$. The point at the origin of coordinates corresponds to a confocal resonator. It may be a resonator formed by two concave mirrors of the same curvature whose radii equal the mirror distance $r_1 = r_2 = L$, and consequently $g_1 = g_2 = 0$.

The confocal resonator. This practically important configuration is illustrated in Fig. 2.29. In this figure, the shadowed area represents the section through the volume filled with bouncing light rays. The side surface of this volume is the hyperboloid of revolution of the shown section around the resonator axis. This surface is produced by marginal rays and is termed a *caustic*. The cross section of the beam where the spot size is a minimum is referred to as the *beam waist*. If the apertures of the resonator mirrors are identical, the beam waist is exactly at the resonator mid-point; in this case the radius of the spot (often given as the beam waist

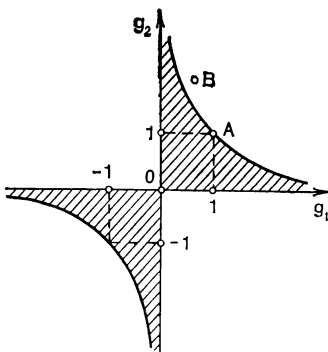


Fig. 2.28 The stability diagram

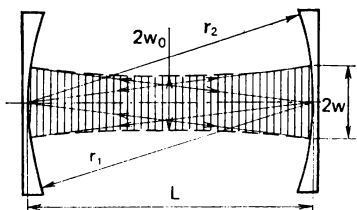


Fig. 2.29 A confocal resonator. The shadowed portion shows the volume filled with bouncing rays

the resonator axis. This surface is produced by marginal rays and is termed a *caustic*. The cross section of the beam where the spot size is a minimum is referred to as the *beam waist*. If the apertures of the resonator mirrors are identical, the beam waist is exactly at the resonator mid-point; in this case the radius of the spot (often given as the beam waist

too) is

$$w_0 = (\lambda L / 2\pi)^{1/2} \quad (2.3)$$

where λ is the radiation wavelength. The spot size radius on a mirror is given by

$$w = (\lambda L / \pi)^{1/2} = w_0 \sqrt{2} \quad (2.4)$$

The position of the beam waist may be controlled by choosing mirrors of different aperture or introducing a diaphragm inside the cavity. We should also note that the light beam inside a cavity has no ideally confining side surface. The caus-

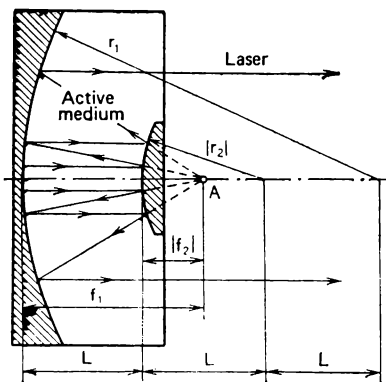


Fig. 2.30 Unstable confocal "telescopic" resonator. f_1 and f_2 focal distances of the mirrors, A common focus of the mirrors

tic represents the volume filled with light in the sense that outside this volume the light intensity of the beam rapidly falls off away from the resonator axis.

The unstable confocal "telescopic" resonator. An example of unstable resonator is shown in Fig. 2.30. This is the so-called "telescopic" resonator. For operation, it is filled with an active medium. This resonator is formed by a concave mirror of $r_1 = 3L$ and a convex mirror of $r_2 = L$. It is an easy matter to see that both mirrors have a common focal point, therefore this is also a confocal resonator. In the stability diagram (see Fig. 2.28) this resonator is represented by point B of $g_1 = 2/3$ and $g_2 = 2$.

The radiant field within the resonator combines two types of light waves — plane waves and spherical waves. The plane wave travels from the concave to the convex mirror, while the spherical wave travels in the reverse direction. The light rays of these waves are illustrated by arrowed lines. Both mirrors are of totally reflecting type. The output beam leaves the resonator upon reflecting from the convex mirror, and therefore is a ring in cross section.

Chapter 3

Control of the Laser Output

Application purposes call for control of the laser output, including such common optical manipulations as deflecting the beam in space, splitting it and focusing on a target. These simple transformations are, however, far from exhausting the requirements for laser output control. On a wider scale, laser output modification assumes that the output will possess a certain energy content or exhibit variable spectral, temporal, and spatial characteristics.

Laser output can be modified in either of two ways — inside the resonant cavity or beyond the cavity. In the first case, the output is controlled by affecting the process of laser oscillation, whereas in the last case, the output is transformed already when it has left the cavity. Sections 3.1 through 3.5 of this chapter will discuss the topics of intracavity control, while the rest sections of the chapter will take up modifications of laser radiation outside the cavity.

3.1 Intracavity Control of Spectral Characteristics

As will be recalled, the spectral characteristics of laser radiation are decided by the active medium. The system of energy levels of the active material gives rise to a specific set of emission lines. By using various types of lasers one may obtain, in principle, coherent output of any wavelength within the range from 0.1 to 100 μm and even of longer wavelengths.

When we come to modifying the laser output we shall focus on the possibility of affecting the radiation frequency for a particular type of laser and a certain active material.

An obvious way of modifying the laser output by means of diverse band filters passing specific bandwidths is of low

importance in this case, as it inevitably incurs high radiant losses. Therefore, more efficient means of practical control involve a variety of intracavity methods influencing the process of laser oscillation. Instead of rejecting by a filter an undesired portion of the output, these methods take care of the laser not to oscillate on those undesired transitions.

Suppressing the undesired transitions. As a rule, the active material possesses a few lasing transitions. For many laser applications, however, it is desirable that the laser oscillate on certain transitions or lase a single line only. An obvious way to produce such an output is to suppress the undesired transitions.

By way of example let us look at the helium-neon laser. The atoms of neon have three laser transitions at 3.39, 1.15 and 0.63 μm (see Fig. 2.12). The initial gain coefficient for this laser increases with the wavelength. On the other hand, most applications use this laser as a source of red light at 0.63 μm . In order to prevent the laser from oscillating in the 3.39 and 1.15 μm lines, the resonator mirrors are covered by materials highly reflective at the shortest wavelength and absorbing the two others. Therefore, laser action occurs only at the wavelength 0.63 μm .

Selection of laser emission lines by intracavity elements. We have seen in the section concerning dye lasers that this type of laser is characteristic of a rather wide transition line (about 0.1 μm). A similar linewidth is also observed in electron-beam controlled high-pressure lasers. These types of lasers lend themselves well for tuning the wavelength of the laser output within the laser transition linewidth.

This gradual selection of monochromatic lines from a multiple-line emission can be achieved by introducing a *wavelength-dependent element* into the cavity. Two popular designs use a dispersive prism and a diffraction grating as such elements. The prism is inserted in the cavity, while the grating replaces one of the cavity's mirrors.

Consider the dispersive prism tuning design in more detail. Assume that a prism inserted inside the cavity is traversed by a beam containing two wavelengths λ_1 and λ_2 such that $\lambda_1 < \lambda_2$. Beyond the prism, the beam splits into the two wavelengths which are bounced back by the cavity mirror as shown in Fig. 3.1a. For a given angular setting of either the prism or the mirror, only one of the wavelengths retraces its

path into the cavity, that is retained for laser action. The other ray is lost. The mirror, however, may be shifted into a position shown by the dashed plate in this figure to reflect the other ray back into the cavity, therefore, a desired line may be selected for laser oscillation. More often the configuration with a rotating mirror is used (Fig. 3.1b). For a given

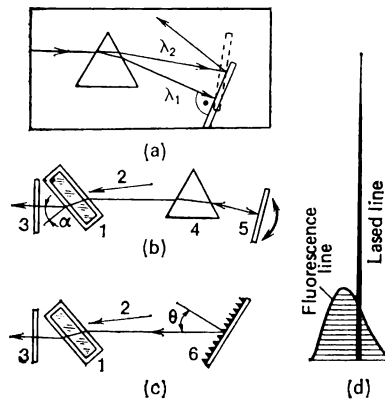


Fig. 3.1 Tunable dye laser system. 1 dye cell, 2 pumping, 3 output mirror, 4 prism, 5 rotating mirror, 6 diffraction grating

orientation of the mirror only one wavelength incident normally on the mirror retraces its path back into the laser cavity, gets amplified by stimulated emission, and emitted as the laser output. Other wavelengths fail to do so and no oscillation is sustained on these wavelengths. Gradually rotating the mirror enables tuning the laser wavelength.

It was only for the sake of simplicity that we spoke above about a selected wavelength. In fact this configuration with a prism and a rotating mirror selects each time not a certain wavelength but a spectral line of 10^{-4} to $10^{-3} \mu\text{m}$ linewidth. This is about one hundredth the laser gain linewidth. Therefore, the rotating mirror selects for lasing one by one the spectral lines from the laser emission linewidth.

Another configuration, shown in Fig. 3.1c, uses a diffraction grating which reflects back into the cavity rays incident on it at an angle of diffraction θ related with the wave-

length λ and the period of the grating d by the formula

$$2d \sin \theta = \lambda \quad (3.1)$$

This relation suggests that for a given angle θ , i.e., at a given angle setting of the grating in the cavity, the laser will oscillate at a wavelength λ defined by (3.1), if this line is within the multiline emission of the laser. Tuning is achieved by rotating the grating through a range of θ angles.

It should be noted that both configurations allow for not only tuning of the laser wavelength but also considerable narrowing of the lased line. This narrowing occurs without a sizeable degrading of the output power. Instead of a relatively wide and not very intense fluorescence line the laser emits a narrow line of high irradiance, shown for comparison in Fig. 3.1d.

The resonators schematized in Fig. 3.1b, c may be called selective resonators as they realize the selection of certain photon states we have discussed in Sec. 1.5. The selected photon states possess energies within a narrow line cut in the transition linewidth. Compared to ordinary cavities, the selective resonators provide a more severe selectivity for photon states.

Single mode operation. When operated in a single longitudinal, single transverse mode, a laser is the closest approximation to a monochromatic light source known. The linewidth of a single laser mode is far smaller than the broadened transition linewidth. Usually, however, there are a number of modes in the laser output, and such a laser is referred to as operating *multimode*.

By placing appropriate devices in the laser cavity one can often modify the laser output. For example, by introducing selective losses for certain transverse modes, one can force a multimode laser to lase with a specific transverse mode pattern. In some lasers, an adjustable iris diaphragm is located on the optical axis of the cavity to suppress all transverse modes except those with TEM_{00} character. This is because other modes, which have some off-axis component, experience more loss with the diaphragm closed down than do the TEM_{00} modes. Thus by increasing the losses for off-axis modes, the laser can be modified to operate only in the TEM_{00} mode. The TEM_{00} mode is attractive because it has lower beam divergence than other modes, and such an output

may be required, for example, if one were to use the laser for an alignment application. In what follows we shall assume that the TEM_{00} output is ensured.

Even when a laser is oscillating on a single transverse mode, it can still oscillate on several longitudinal modes (i.e., modes differing in their value of the longitudinal mode index q). These modes are separated in frequency by $\Delta\nu' = c/2L$, where L is the resonator length. As the resonator length decreases, this frequency separation between the

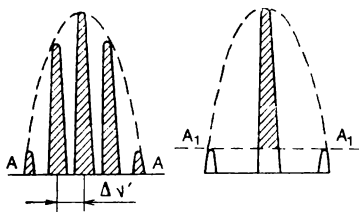


Fig. 3.2 Selecting the central axial mode by the "short-cavity" method

axial modes increases, and they move apart, as it were, on the frequency scale, hence fewer modes remain within the gain curve. Therefore, a possible way to achieve single axial-mode operation is to design the cavity so that only one axial mode is possible within the laser transition linewidth. Normally, it is the central axial mode that is selected in such a manner. In physical terms, the intensity of the central mode exceeds in this separation by far those of the adjacent longitudinal modes which disappear below the threshold level.

The situation is illustrated in Fig. 3.2. On the left it shows a number of longitudinal modes present within the transition line for a certain resonator length L . The line AA represents the threshold level of the cavity. The right portion of the figure shows the same gain curve and the axial modes remained after the resonator length has been halved. The A_1A_1 line shows the new level of losses in the cavity.

This technique of *single-moding* is outstanding in its simplicity. Unfortunately, a shorter length of the cavity means that the active length of the laser is also small, severely limiting the power output. Therefore, more attractive appear to be the techniques based on inserting various reflecting elements inside the cavity. We shall discuss them in the

following paragraphs after a short intermission for the analysis of linewidth achieved with such single-mode selection.

We recall that the linewidth measured in terms of frequency is given by equation (1.56). By assuming the resonator quality factor $Q = 10^6$, and $\lambda_0 = 1 \mu\text{m}$ ($v_0 = c/\lambda_0 = 3 \times 10^{14} \text{ Hz}$) we obtain $\Delta v_c \approx 10^9 \text{ Hz}$. To convert this linewidth in wavelength units one may refer to the expression

$$\Delta\lambda_c = -\lambda_0^2 \Delta v_c / c \quad (3.2)$$

It gives for the linewidth $\Delta\lambda_c$ of a single axial mode an order of magnitude estimate of 10^{-5} to $10^{-6} \mu\text{m}$.

Another method for obtaining increased single axial-mode output from a TEM_{00} laser is to introduce large losses for

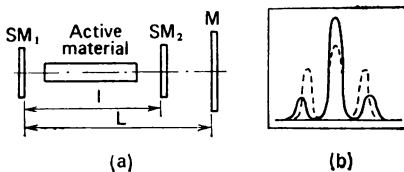


Fig. 3.3 Single-moding by introducing an additional mirror in the cavity

all but one of the modes. This can be done by introducing one or a few additional mirrors within the laser cavity which thereby is transformed essentially into a set of coupled resonators. The interference of light waves produced by these resonators brings about a redistribution of light power between the oscillating longitudinal modes. A suitable choice of reflectivity and position for the additional mirror builds up the intensity of the desired axial mode and the losses for the other axial modes. Collectively these methods of single-moding may be referred to as *interference techniques*.

By way of illustration consider the resonant cavity shown in Fig. 3.3a. Of the three mirrors involved only mirror M is totally reflective ($R_3 = 100\%$). The semitransparent mirror SM_1 is the output mirror of the resonator and SM_2 is the additional mirror. Fig. 3.3b shows the lineshape for the longitudinal modes within the transition linewidth, as related to the modified resonator (solid lines) and to the initial resonator without mirror SM_2 (dashed lines). These results are plotted for the specific case of $l/L = 3/4$ and $R_2 = 65\%$.

3.2 Methods of Q-switching

In the early chapters of this book we have learned that the cavity Q shows the ability of the cavity to store energy. A high Q means that high energy can be stored in the cavity, while a low Q implies that the cavity will rapidly dissipate its energy. For certain applications the time dependence of laser light is of much higher importance than its frequency characteristics, i.e. monochromaticity. In this section we look at some techniques for obtaining high power pulses from a laser by means of varying this ability of the resonator to store energy, known as Q -switching or Q -spoiling techniques.

The rotating reflector method using mechanical shutters. Imagine a resonant cavity where one of the mirrors is replaced with a total reflection prism which spins rapidly around its axis set at right angles to the resonator axis (Fig. 3.4a). As the prism revolves, it faces the cavity with its reflecting side and makes the cavity's Q high for only a short time. When the prism is out of this position for an angle of only one angular minute, the cavity Q drops by half below the maximum value. At still greater angles the Q falls off very rapidly to a minimum. It is quite obvious that laser action can occur when the prism is brought into alignment with the cavity, whereas away from the alignment the cavity losses rapidly grow too high to enable lasing action (low Q) and the oscillation ceases.

If the rotating reflector revolves at 1000 revolutions per second the time in which the Q of the resonant cavity switches from its maximum to minimum value amounts to about 10^{-7} s.

Electrooptical shutters. These exploit suitable electro-optical effects of altering the refractive index of a cell by applying an electric field. Here we look at two such effects, a square law (*Kerr*) effect and a linear (*Pockels*) effect. In the former, the refractive index varies as the square of the electric field intensity, while in the latter it is proportional to the first power of the field. The Pockels effect exists only in crystalline media.

Consider electrooptical Q -switching of the resonant cavity which exploits the Pockels effect. We mention here that a crystal cell based on the Pockels effect (Pockels electrooptic modulator, or cell) is a device which, when subjected to an

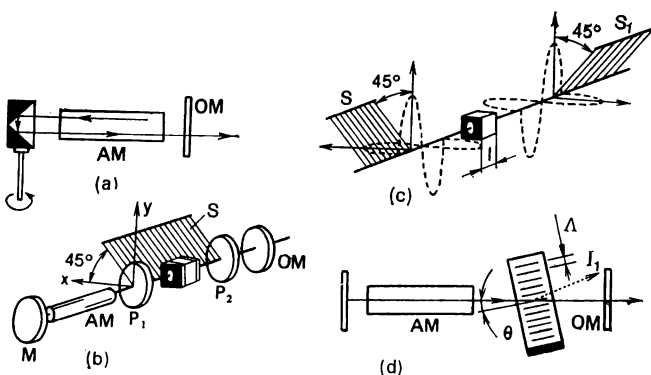


Fig. 3.4 Methods of active *Q*-switching. (a) rotating reflector method
(b) electrooptic method, and (c) acoustooptic method

applied dc voltage, becomes birefringent. In birefringent crystals, as will be recalled, a light wave splits into two waves travelling at different velocities, that is, the crystal offers different refractive indices for differently polarized light. In a Pockels cell, this induced birefringence is proportional to the applied voltage.

Figure 3.4b shows a laser arrangement designed for *Q*-switching with a Pockels cell. Here *AM* is the active material, *TM* the totally reflecting ($R = 100\%$) mirror, and *OM* the output mirror. Between the active material and the output mirror, there are two polarizers oriented in the same sense, i.e., transmitting light polarized in the same plane, *S*. The Pockels cell placed between the polarizers is a crystal confined in an electric capacitor whose plates have windows for light.

In this polarizer-Pockels cell-polarizer combination, any light travelling to the cell has to pass a polarizer and, therefore, becomes polarized in the *S* plane. For the sake of analysis we represent this polarized radiation as consisting of two waves, one polarized in the *x* direction, the other polarized in the *y* direction (see Fig. 3.4c). Within the Pockels cell, the first wave will travel at a velocity corresponding to refractive index n_1 , while the second wave will travel at a velocity corresponding to refractive index n_2 . Polarizer P_1 and the cell are oriented so that the *x* axis is at 45° to plane *S*.

As a result, if the wavelength of this light in a vacuum is λ_0 , it will emerge from the cell of thickness l as two waves $\Delta\phi$ out of phase

$$\Delta\phi = 2\pi l (n_1 - n_2)/\lambda \quad (3.3)$$

The refractive indices n_1 and n_2 linearly depend on the electric field strength in the cell (the Pockels effect)

$$\begin{aligned} n_1 &= n_0 + n_0^3 r E / 2 \\ n_2 &= n_0 - n_0^3 r E / 2 \end{aligned} \quad (3.4)$$

where n_0 is the refractive index when the field is absent, and r is an electrooptic constant of the cell crystal. Hence,

$$n_1 - n_2 = n_0^3 r E \quad (3.5)$$

Obviously, when the field is absent, $n_1 = n_2$ and $\Delta\phi = 0$.

Substituting (3.5) into (3.3) and observing that $El = V$, the dc voltage applied to the cell, yields

$$\Delta\phi = 2\pi n_0^3 r V / \lambda \quad (3.6)$$

The voltage may be adjusted so that $\Delta\phi = \pi$. Then the cell functions as a half waveplate since the emerging beams are 180° out of phase with each other, or shifted by half wavelength. The resultant polarization is still linear, but the polarization vector is rotated, as can be readily seen from Fig. 3.4c, into plane S_1 orthogonal to plane S . Since the new plane of polarization is at right angles with the orientation of polarizer P_2 , it will not pass the light to the output mirror.

Thus, with no voltage applied to the Pockels cell (the cell is off) light traverses the system of polarizers and the cell almost without any losses, except the absorption loss suffered in these components. When the cell is on, the light passage is blocked. Saying it another way, the cavity Q is a maximum with the Pockels cell off, and a minimum with the cell on. The switching rate depends on the frequency of the voltage applied to the cell. The switching time is as low as about 10^{-9} s which is appreciably smaller than that with the mechanical shutters.

To summarize, a Pockels cell performs in the arrangement with polarizers as a shutter operating at a very high speed. Hence the term *electrooptical shutters* is used for the systems of this type.

Note. With no voltage applied to the Pockels cell, $n_1 = n_2$. This implies that a beam of light incident on the cell is no longer sorted into two components travelling through the crystal at different velocities. This is valid, however, provided that the crystal is oriented with respect to the incident beam so that its optic axis is parallel to the beam direction.

Acoustooptic Q switches. For modulation of the cavity Q , these switches rely on the diffraction of light on a phase grating produced by an ultrasound wave. This wave is launched in a medium (solid or liquid) by a piezoelectric transducer (PET). Due to the presence of the ultrasonic wave, the material acts like a phase grating. In fact the strain induced by the ultrasonic wave results in local changes of the material refractive index (*photoelastic effect*). The grating has a period equal to the acoustic wavelength Λ and an amplitude proportional to the sound amplitude. A light beam incident on such a three-dimensional grating partially undergoes diffraction, i.e. is deflected in part from its previous direction. The proportion of the light being diffracted out may be increased by increasing the high frequency driving voltage applied to the PET.

An arrangement with the laser Q being switched by an acoustooptic modulator is shown in Fig. 3.4d. Inside the acoustooptic modulator, also referred to as acoustooptic shutter, the light wave forms with the diffraction grating, induced by an acoustic wave an angle θ which must satisfy the diffraction relationship:

$$2\Lambda \sin \theta = \lambda \quad (3.7)$$

where λ is the wavelength of light in the graving's medium. To meet this condition, the shutter is suitably oriented relative to the resonator axis. The angle θ is referred to as the Bragg angle. Note that the relation (3.7) is a modification of (3.1).

When the PET is off, no ultrasound wave is launched into the shutter medium, and the incident light beam traverses it without any losses. When the PET is on, the modulator will diffract a portion of the incident light beam of irradiance I_0 into a diffracted beam of irradiance I_1 , shown by a dashed line in Fig. 3.4d. The closer the efficiency I_1/I_0 of

the shutter to unity, the less light it transmits in the axial direction of the cavity and the lower the cavity Q .

The switching time of the acoustooptic shutters is in the order of 10^{-7} s. In order to decrease this time of Q -switching, the light spot at the shutter should be decreased in size, i.e., focused on the device. Then the time it takes the ultrasound wave to cross the light beam diminishes, and the time the diffracted beam takes to emerge and vanish is cut down. One should not overlook, however, that this focusing of the light beam impairs the efficiency I_1/I_0 of the shutter, i.e., increases the portion of light passing through when the shutter is on, or closed.

Passive Q -switching using saturable absorbers. The modulation or Q -switching techniques we have discussed so far are referred to as *active* to emphasize that the control of cavity losses is exercised from the outside. Conversely, *passive* Q -switching is one where losses in the cavity rise and fall "automatically", with no command from the outside.

A simple passive Q -switching modulator consists of a nonlinear element inserted into the cavity. This is an absorber which absorbs light at the laser wavelength but is saturated very soon and becomes transparent for the light, as if bleached, and therefore called a *bleachable cell*. The cell usually contains absorbing species (atoms or molecules of solved organic dyes) capable of absorbing light at the laser wavelength, that is, possessing among their energy levels those exactly matching the laser transitions.

The process of bleaching is illustrated in Fig. 3.5. Suppose for simplicity that the absorbing species has only two energy levels, the upper and the lower levels. Denote their population densities by n_1 and n_2 . Then we may write the resonant absorption coefficient for the transition between these levels as

$$\alpha = \sigma_a (n_1 - n_2) \quad (3.8)$$

where σ_a is the cross section of the stimulated processes in this transitions. Equation (3.8) immediately follows from (1.36) for the small signal gain coefficient upon the appropriate change of sign to account for the absorptive nature of the transition. Accordingly, a signal gain may be treated as a negative absorption. Equation (3.8) indicates that resonant absorption is due to the processes of absorption being dominated over that of stimulated emission,

In the initial state, when laser oscillation has not yet commenced, all the absorbing species are in the lower level, therefore $n_2 = 0$. This state of the cell is unbleached, it is characteristic of the maximum absorption. Assume that a pumping pulse has excited the active centres in the active material and has inverted the populations of the lasing levels. As yet laser action cannot occur in spite of the high population inversion because of high losses introduced by the unbleached cell. Some of the excited active centres can meanwhile spontaneously fall to the lower laser level and

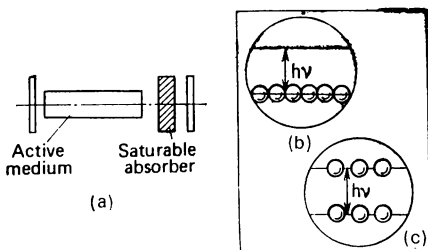


Fig. 3.5 Passive Q-switching by the saturable absorber (bleachable dye cell)

initiate by means of the emitted photons new transitions in the active material, which cause the emission of small avalanches of secondary photons. Some of these avalanches propagate along the cavity to be absorbed by the bleaching cell. The absorbing species in the cell are raised from the lower into the upper level, so that n_2 builds up, is saturated and the absorption ceases. The cell is bleaching. This process facilitates further photon avalanches. As a result, the system arrives at a state when the cell bleaches rapidly and completely, the cavity switches to its high- Q condition and a giant pulse develops.

Figure 3.5 shows the population of the levels in the absorbing species when in an unsaturated state, in part (b) and in a completely saturated, bleached, state, in part (c). In the bleached condition $n_1 = n_2$, and therefore $\alpha = 0$. This implies that the processes of absorption and stimulated emission of light between the energy levels of the absorbing species now mutually compensate each other, and the cell

neither absorbs nor amplifies the beam at the laser wavelength.

Once the laser pulse has been emitted, the absorbing species in the cell begin gradually decay to the lower level through spontaneous emissions and the cell returns in its unbleached state. The characteristic time the cell takes to return to an unsaturated state is referred to as the relaxation time of the cell.

Most often the bleachable media are solutions of organic dyes — cyanine dyes (phthalocyanine and cryptocyanine) and polymetine dyes. Cyanine dye solutions are employed for ruby lasers, while polymetine dye solutions are employed for *Q*-switching neodymium lasers.

3.3 Pulsed Lasing

Currently available lasers are able to produce light pulses of various duration, from milliseconds (10^{-3} s) to nanoseconds (10^{-9} s) and even to picoseconds (10^{-12} s). Oscillating techniques are in existence, which yield giant single pulses and pulse trains whose repetition rate may be varied in a wide range, up to about 10 MHz, i.e., 10^7 pulses per second (pps). In the mode-locking operation (which will be our concern in the next section) the pulse repetition rate may be as high as 0.1 to 1 GHz, i.e., 10^8 to 10^9 pulses per second.

Free oscillation regime. In fact this regime involves a few modes of operation. What all of them have in common is the absence of any control of oscillation, that is, any influence on lasing action by means of extraneous signals or nonlinear elements inserted within the cavity, i.e., the ones whose behaviour varies with the irradiance produced by the active element. Specifically, they are denuded of any type of *Q*-switching, either active or passive.

Pulsed pumping produces in a free-oscillating laser a pulse of duration corresponding to that of the excitation pulse. For solid state lasers, the pulse length is 0.1 to 1 ms; for dye lasers pumped by shorter pulses, the pulse length may be as short as 1 μ s. The radiated output pulse exhibits a fine structure: its initial portion consists of a series of spikes about 0.1 μ m in width. These spikes, shown in Fig. 3.6, represent the decay of the population inversion typical for the onset of oscillation. Nondecaying spiking may also take

place due to the unstable resonator behaviour and nonlinearities in the cavity.

Production of giant pulses. Short pulses of high peak power can be produced in pulse pumped lasers by using active or passive Q -switching. Consider first the case of active Q -switching. By using one or another type of control for the cavity Q , the level of cavity losses is deliberately driven rather high to raise the threshold of oscillation. This builds up a considerable population inversion for the lasing levels. Then the cavity is switched into a low- Q state, causing the oscillation threshold to drop rapidly to the lowest possible level. As a result, the initial population inversion turns out to be appreciably high above this new low-loss threshold, and a giant pulse is lased. Its peak power is higher, the more the initial buildup of inverted population, achieved under the low- Q condition, exceeds the threshold inversion corresponding to the high- Q of the cavity. The duration of such giant pulse of gigawatt range is from 10 to 50 nanoseconds, although the minimum pulse length may be 1 to 3 ns.

Figure 3.7a shows the time evolution of a giant pulse in a Q -switched laser with a shutter which rapidly switches the cavity Q from its minimal to the maximal value. The plots shown in the figure represent four time-varying functions: irradiance $I(t)$, population inversion $N(t)$, quality factor $Q(t)$, and threshold population inversion $N_{\text{th}}(t)$. We note in passing that N_{th} varies in inverse proportion to Q . At $t = 0$, $N(t)$ crosses $N_{\text{th}}(t)$ to start the oscillation process. Since this process begins, as have been already noted, from spontaneous transitions that give rise to cavity noise, it develops slowly. It can be readily seen that the irradiance power increases at first slowly, linearly with time, the linear portion, t_1 , being relatively long, on the order of 100 nanoseconds. Almost all the energy of the pulse is emitted during the next, relatively short (about 10 ns) nonlinear interval, t_2 . Within the time interval t_1 , the population inversion of the laser levels remains practically unaltered, whereas du-



Fig. 3.6 Structure of a light pulse lased in the free oscillation mode

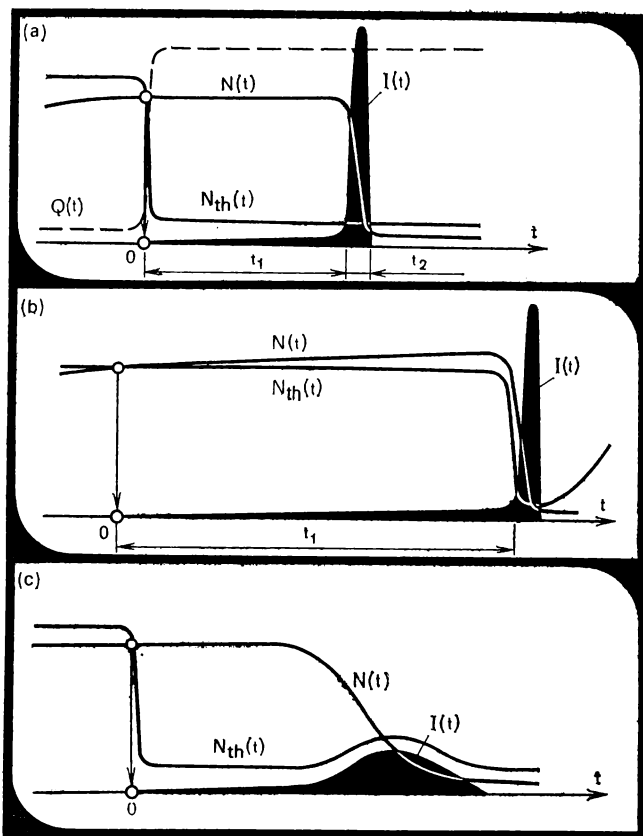


Fig. 3.7 Evolution of a Q -switched laser pulse. (a) active Q -switching, (b) passive Q -switching, (c) active Q -switching with negative feedback

ring t_2 this function $N(t)$ sharply falls off as all the population stored in the upper level during the low- Q condition is emitted in one giant pulse.

Such pulses may also be produced with passive Q -switching methods, employing saturable absorbers (bleaching dye cells) with relatively high density of absorbing species and a relatively long relaxation time. In addition, the cross section of stimulated transitions of the cell must appreciably exceed that of stimulated transitions in the active material.

The time evolution of a high-power short pulse in a laser Q -switched by a bleaching dye cell is presented in Fig. 3.7b. The process begins at a time instant when the population inversion $N(t)$ increased by pumping grows over the threshold level $N_{\text{th}}(t)$. The latter reflects the temporal behaviour of the bleaching dye. In contrast to the case of active Q -switching, here the linear development of a pulse occurs not under low-loss but rather under high-loss conditions, as the dye cell is effectively bleached in fact only during the nonlinear pulse development (simultaneously with the fast drop of $N(t)$). Therefore, the length of the linear pulse development t_1 appears with passive Q -switching to be about an order of magnitude longer ($t_1 \approx 1 \mu\text{s}$) than with active Q -switching. The length of nonlinear pulse development stage, t_2 , which is essentially the pulselength of the output radiation, and the peak power of the pulse remain the same as in the case of the active Q -switching procedure.

Expanding the pulselength by negative feedback. Suppose we control the loss of the cavity in the following pattern: when the power being emitted increases, it brings about higher losses, and conversely, as the power falls off, the losses also abate. This pattern is typical for configurations with a negative feedback control.

Negative feedback hampers the development of stimulated emission. Therefore, a population inversion in a system with an amount of negative feedback decays longer. This implies that it takes a longer time to produce an output pulse. As a result, the pulselength increases, while the pulse peak power decreases.

Negative feedback can be applied by a number of diverse means. One of them relies on the two-photon absorption process in a semiconductor material. Assume that a plate of semiconductor with a band gap E_g such that $h\nu < E_g < 2h\nu$ is inserted in the cavity of a laser emitting at frequency ν . By way of example, for neodymium lasers this condition is satisfied by using GaAs and CdSe semiconductor plates. At relatively low intensities, the radiation at frequency ν traverses such semiconductor plate without being absorbed because the photon energy $h\nu$ is insufficient to raise its electron from the valence band into the conduction band. However, when the irradiance grows in intensity there appears a possibility for an electron in the valence band to absorb already

two photons and, being raised in energy by $2hv$, to jump into the conduction band.

The probability of the two-photon absorption increases as the radiation power grows. This implies that an increase in the irradiance power incurs (automatically) an increase in the loss of the cavity due to the semiconductor plate growing more "opaque".

Figure 3.7c shows the time evolution of a developing pulse in a pulse-pumped, actively Q -switched laser whose cavity, besides an electrooptic shutter, contains a semiconductor flat that grows opaque at the laser wavelength. Owing to the automatic negative feedback applied to this system, the giant pulse it emits spreads in time to a duration of 0.1 to 1 microsecond. The peak power of the pulse abates accordingly.

Production of pulse trains at high repetition rates. Many applications require emissions in the form of regular trains of pulses following at a rather high repetition rate. Such trains are produced by continuously pumped lasers. First attempts at pulse train generation in continuously pumped lasers, Q -switched with rotating reflectors, turned out to be of low consequence because of poor amplitude stability of pulses in the train due to a poor positional reproducibility of the shutter reflective plane. More successful have appeared to be the systems with acoustooptic modulators introduced later.

A typical repetition rate of the pulse trains produced by acoustooptically Q -switched cw pumped lasers is 10 kHz with a peak pulse power of 1 kW and an average power of 1 to 10 W.

A higher repetition rate in this case is prevented by a relatively long time needed for each pulse evolution (see Fig. 3.7). Unless special measures are taken to cut down the linear period in the pulse development, the maximum possible repetition rate lies around 50 kHz.

A considerably higher repetition rate may be realized in continuously pumped lasers operating in the *cavity dumping mode*. These lasers employ high- Q cavities with both mirrors being totally reflective. The cavity contains a fast-operating shutter which, when externally triggered, dumps a portion of the irradiance energy off the cavity within short time intervals.

Now suppose that the shutter is off while pumping excites

the laser. In the circumstances, the energy density in the resonator builds up due to the processes of stimulated emission dominating over those of absorption. The continuously operating pump nevertheless keeps the inverted population above the oscillation threshold. Actually, oscillation has already started but the radiation is confined within the cavity. When the shutter is switched on for a short time, a short pulse is emitted and the resonator dumps a portion of the stored radiation.

Compare the active Q -switching and the cavity-dumping modes. In the first mode, the radiation field density inside the cavity is low in the initial state when the Q is low, so the laser is below the oscillation threshold. When the cavity Q is switched to the high condition, oscillations set in and the output pulse is formed to be emitted through the semi-transparent output mirror. The pulse buildup here begins from the level of noise, which inflicts a long period of linear development.

Unlike the Q -switching mode, the cavity-dumping mode is characterized by a high- Q in the initial state: the laser is above the gain threshold. Even before output pulse shaping begins, oscillations are taking place and the cavity is filled with photons. We emphasize that whereas in the Q -switching mode oscillations begin after the shutter has received a control signal, in the cavity-dumping mode the dumper is switched on in the laser that has already been oscillating. This cuts down considerably the time taken for the formation of the pulse as it lacks the period of linear development. As a result, a possibility opens up to realize higher repetition rates for pulse trains.

The typical characteristics of cavity dumped outputs are as follows: pulse repetition rate 100 kHz to 10 MHz, pulse duration 10 to 100 ns, average power 1 to 10 W.

3.4 Mode Locking for Ultrashort Pulses

The technique of mode locking allows the generation of laser pulses of ultrashort duration (from a fraction of a picosecond to a few tens of picoseconds, i.e., 10^{-12} to 10^{-11} s) and very high peak power (a few gigawatts, i.e., 10^{12} W).

Mode-locking defined. In Chapter 1 we have learned that longitudinal modes are uniformly spread on the frequency

scale, the spacing between the adjacent modes being constant and equal to $\Delta v' = c/2Ln$. The linewidth Δv of the transition line accommodates $m = \Delta v/\Delta v'$ longitudinal modes. The output of an ordinary laser, as a function of time, depends on the relative frequencies, and amplitudes of these modes. All these parameters, however, are time-varying and the output fluctuates randomly. If an external perturbation forces the various mode oscillations to maintain fixed phases with respect to each other, the modes will produce a

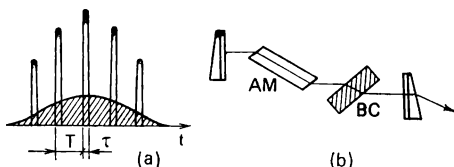


Fig. 3.8 (a) Comparison of a giant pulse and a train of mode-locked spikes, (b) resonant cavity preventing axial mode selection; *AM* active material, *BC* bleaching dye cell for passive mode locking

constructive interference pattern and the output becomes repetitive. Such a laser is then said to be "mode-locked" and its emission is regularly spaced pulses of high peak power.

These pulses are of extremely short duration. The duration of an individual pulse, τ , is decided by the linewidth of the gain curve, in other words, by the number of locked modes which the transition line can sustain

$$\tau \approx 1/\Delta v \approx 1/m \Delta v' \quad (3.9)$$

The peak power of an individual ultrashort pulse is about m times the output power without mode locking. The period of the pulses may approximately be found as

$$T \approx 1/\Delta v' = 2Ln/c \quad (3.10)$$

For solid state neodymium lasers, the linewidth of the transition line is about 10^{10} Hz, and for organic dye lasers it is about 10^{12} to 10^{13} Hz. Letting $\Delta v' \approx 10^7$ Hz yields that the maximum possible number of axial modes these lines can sustain equals 10^3 and 10^5 to 10^6 , respectively.

Figure 3.8a gives an approximate comparison of the profiles of a giant pulse (shadowed in the figure) and a mode-locked pulse train produced in the same pulse pumped laser.

Methods of mode locking. An essential requirement for mode locking is the active medium providing a rather broad emission profile. Examples of such a medium are glass or crystal doped by neodymium, or, a still better choice, solutions of organic dyes. Then, precautions must be taken to prevent mode selection from occurring, as in this case multimode operation is of principal importance. A selection of modes may occur due to interference which always takes place in ordinary resonators owing to the presence of additional reflectors such as the ends of the active material, mirror substrates, etc. These sources of reflected waves must, therefore, be eliminated. For this purpose, mirror coatings are deposited on wedge-shaped plates, and the ends of the active material are cut at the Brewster angle, so that a geometry similar to that in Fig. 3.8b may result.

Last but not least, the modes themselves must be locked in phase. The most commonly used mode locking methods belong to one of the following two categories: (i) mode locking by an active modulator driven by an external signal (*active mode locking*), and (ii) mode locking by means of a suitable nonlinear optical material (*passive mode locking*).

Of the active mode-locking techniques, configurations involving acoustooptic shutters are most widely used. These shutters use the same principle of diffraction on an acoustic phase grating as in the shutters used for *Q*-switching, except that this time the grating is produced by a standing, rather than running, ultrasonic wave. The fixed phase relationship is accomplished by varying the loss of the laser cavity at a frequency equal to the intermode separation. The shutter modulates the losses practically by the sine law with the period defined by (3.10). The resultant amplitude modulation at the frequency $1/T$ converts a mode at frequency ν to the three synchronously phased modes at ν , $\nu + 1/T$, and $\nu - 1/T$. The sideband modes at $\nu \pm 1/T$ coincide with the modes that have been adjacent to the basic mode at ν . As a result, the modes become locked in phase.

Passive mode locking is provided by saturable absorbers that are incorporated in the laser cavity to mode lock, as shown in Fig. 3.8b. When an intense pulse of light passes through the saturable absorber inside the laser cavity, the low power wings of the pulse are attenuated because of absorption of the dye molecules. The high power peak of the

pulse, however, is transmitted because the dye is bleached. In order for this to occur, it is essential that the saturable absorber must recover in a time which is short compared with the duration of the pulse. Because of this nonlinear bleaching mechanism, the shortest and most intense fluctuations grow at the expense of the weaker ones. It may be shown that the use of such dye cell brings about, as in the case with active mode locking, a time-periodical amplitude modulation of

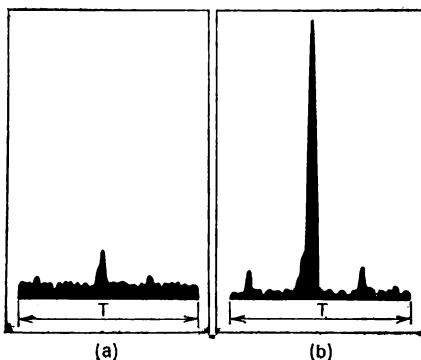


Fig. 3.9 Typical noise field profile over the resonator round-trip period (a), and the final field profile (b)

the radiation in the cavity as the result of which the modes become locked in phase. Below we shall see the process of passive mode locking in more detail.

Growing a high-power pulse from spontaneous emission noise. There exists a rather straightforward explanation of how ultrashort light pulses emerge in a laser with passive mode locking effected by a rapidly recoverable dye cell. In the initial stage preceding the formation of the mode locked pulse, the laser medium forms within the cavity a radiation field whose temporal profile contains numerous fluctuations of intensity of various amplitude. This profile recurs approximately over a time interval equal to the round-trip time for this radiation in the cavity. Equation (3.10) suggests that this round-trip time is exactly the parameter T , called the period of the cavity.

A typical initial energy density field over the resonator period is presented in Fig. 3.9a. It is seen to contain one pulse more intense than the surrounding noise. It is this

pulse that will pass through the bleaching dye cell and gets amplified in its round trip through the active medium. If the cell recovers fast, it will be shut immediately behind this pulse and stay ready for being saturated by the next fluctuations of the field. As these are less intense proportionally they will suffer greater attenuation in the absorber. Therefore, the strongest pulse will grow faster than the others, and after many round trips the situation depicted in Fig. 3.9b will eventually result, where a single intense mode-locked pulse remains.

Thus, a fast-recoverable saturable absorber inserted in the cavity is able to select and enhance the most intense fluctuations in the initial energy density and, conversely, to suppress the other, less intense, fluctuations. As a result the profile of the initial radiation field deforms with each next round trip. The energy contained in diverse fluctuations is redistributed, accumulating in one stronger pulse. This pulse grows in power and becomes shorter in duration.

To summarize in loose terms, the presence of a rapidly recoverable saturable absorber inside the cavity launches a single light pulse bouncing back and forth (from one mirror to another) within the cavity. At first the pulse grows in magnitude, then, when the pump energy given to the active material is exhausted, gradually declines in power. At regular intervals of time T this pulse arrives at the output mirror and is partially emitted. As a result, the laser output is a regular train of pulses following each other with the pulse repetition time T , as shown in Fig. 3.10a.

In actual conditions, however, the ideal pattern depicted above may not take place. For one thing, the shutter may not relax fast enough to "close" before a less intense pulse trailing the major pulse. The result will be an output train

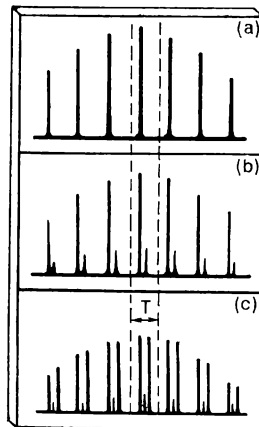


Fig. 3.10 Trains of ultrashort pulses enveloped in the gain profile at (a) complete and (b, c) incomplete mode locking

of pulses plotted in Fig. 3.10b. For the other thing, the initial noise may provide two or more identically intense initial pulses which the dye cell will enhance in the same extent. Therefore, the resonator period will contain two or more intense pulses of short duration (Fig. 3.10c).

By way of a remark we note that the description given above for the mode locking of ultrashort pulses in a laser with a saturable absorber may be called a treatment in the *time domain*. Indeed, this description presents the development of mode-locked pulse trains as the process of regular (recurrent with a period T) lasing of a portion of an intense fluctuation spike selected and enhanced from the stimulated emission noise in the cavity by the bleachable dye cell. A similar pattern of an intense pulse bounced back and forth within the cavity may be invoked in a treatment of active mode locking. We recall that the losses incurred by the acoustooptic modulator are modulated in time with period T . In its round trips, the pulse will pass through the shutter each time at the instant consistent with the lowest level of losses.

In other texts, similar description but in the *frequency domain* may be encountered. This treats the process of mode locking as the result of interference of a large number of modes uniformly spaced on the frequency scale and forced to oscillate with synchronous phases.

3.5 Modifying the Spatial Structure of the Laser Output

Selection of the fundamental mode. We use the term “spatial structure of the light field” to mean the distribution of the beam irradiance over the beam cross section. We have seen earlier that this structure is defined mainly by the transverse modes sustained in the cavity. A number of light field structures produced by various transverse modes are illustrated in Fig. 1.18 by light spots the beam produces on the resonator mirror.

Often it is desirable that only the fundamental mode, TEM_{00} , be present in the beam, as this produces a more uniform distribution of irradiance over the beam cross section and the least divergent beam due to the absence of

off-axial modes. As can be seen from Fig. 1.18, the TEM₀₀ mode is concentrated around the resonator axis, therefore it can simply be selected by introducing an axial diaphragm (a screen with a hole aligned with the resonator axis) in the cavity.

A diaphragm placed in the cavity introduces certain losses in the emission process. These losses are lowest for the fundamental mode because almost all of it passes through the diaphragm hole. By selecting a suitable aperture and position for the diaphragm one can provide selective oscillation of the fundamental mode and suppress oscillation of the other transverse modes.

Use of unstable resonators for mode selection. It was believed at one time that unstable resonators were unsuitable for laser action because such resonators were not able to confine radiation. Subsequent research has demonstrated, however, that lasers with unstable resonators are feasible when the active medium provides a rather high gain per pass (round-trip power gain) of at least 10–20%. Moreover, these resonators offer a number of advantages.

One of these advantages concerns the enhanced selective behaviour of unstable resonators as the result of which they are capable of yielding highly coherent light beams. When the selection of the fundamental mode is at stake, more attractive seem to be the cavities with high diffraction losses, since diffraction implies losses and the suppression of oscillation for high-order transverse modes. In unstable resonators, diffraction losses are always large and qualified as radiation losses. It is not surprising, therefore, that the laser with an unstable cavity sustains laser action in the fundamental mode only. More often than not such operation results in a light beam of exceedingly small divergence defined by the aperture of the beam and said to be at the diffraction limit:

$$\varphi_d = 1.22\lambda/d \quad (3.11)$$

where φ_d is the angle of beam divergence, λ the wavelength of the radiation, and d the beam diameter.

As an example of the unstable resonator, Fig. 2.30 shows a confocal “telescopic” resonator. This resonator emits radiation with a practically plane wavefront, accurate to the diffraction limit.

Apodizing diaphragms. Diffraction of light beams at the edges of objects of limited size, whether it be a diaphragm or the end of the active material rod, may cause considerable disturbances of irradiance over the spot size of high power outputs. Interference patterns may occur with the associated local waves of irradiance. For this to occur, the use is made of apodizing diaphragms, or "soft" apertures which are inefficient in a smooth transmission behaviour at their edges, in contrast to the jump-wise behaviour in ordinary "hard" apertures. Apodizing diaphragms are prepared by depositing an absorbing material in a layer of variable thickness on a substrate.

A similar effect is achieved in unstable resonators by means of mirrors with "smoothed" edges, i.e., ones exhibiting a gradual decline in reflectivity at the edges. Such mirrors appreciably decrease the diffraction effects at the edge of the output mirror in the unstable resonator.

3.6 Frequency Transformations in Nonlinear Media

Nonlinear polarization of the medium. At the time of the prelaser optics it was reasonably believed that the medium characteristics are independent of the intensity of light passing through this medium. Prelaser light sources produced light field intensities not exceeding 10^5 V/m. Recalling that the intra-atomic fields are characterized by intensities of the order of 10^8 to 10^{12} V/m makes it evident why light waves of such sources could not produce a somewhat detectable effect on the atomic fields and, consequently, on the medium behaviour. Therefore, the medium response, in the form of polarization P , to the external perturbation, in the form of a light wave electric field E , turned out to be linear

$$P = \chi E \quad (3.12)$$

where χ is the dielectric susceptibility of the medium. This relationship coined the term "linear optics" used in relation to the prelaser (incoherent) optics.

Laser sources of light have radically changed this situation. The high degree of coherence involved in laser radiation has made possible extremely high concentrations of

light powers. In practice it is realized owing to small divergence of laser beams and availability of pulsed outputs with enormously high peak powers. Available lasers yield light fields with intensities as high as 10^{10} to 10^{11} V/m. These electric field strength are comparable with those within the atom. Now the dielectric susceptibility of the medium becomes a function of the light field intensity.

For high light powers, theory suggests that the susceptibility can be presented as a sum of rapidly diminishing terms

$$\chi(E) = \chi_0 + \chi_1 E + \chi_2 E^2 + \dots \quad (3.13)$$

where χ_0 , χ_1 , etc. are the medium parameters which define its polarizability. For practical purposes, it will be sufficient to retain in (3.13) the two leading terms only. With this model for χ equation (3.12) becomes

$$P = \chi(E) E = \chi_0 E + \chi_1 E^2 \quad (3.14)$$

We note that this equation is nonlinear in the light field intensity. This implies a nonlinear response of the material to high light powers and gives birth to such terms as "nonlinear optics" and "nonlinear media". The nonlinear term

$$P_{NL} = \chi_1 E^2 \quad (3.15)$$

in equation (3.14) describes the nonlinear polarization of the medium, χ_1 being the nonlinear susceptibility.

Interaction of light waves in nonlinear media. Let a plane monochromatic light wave of frequency v travel at velocity v_1 in the z direction of a nonlinear medium (exhibiting a nonlinear polarization for this wave). The electric field strength of this wave may be defined as

$$E_1(z, t) = E_{01} \cos [2\pi v(t - z/v_1)] \quad (3.16)$$

Substituting (3.16) into (3.15) and observing that $2\cos^2 \beta = 1 + \cos 2\beta$ we obtain

$$P_{NL}(z, t) = \frac{1}{2} \chi_1 E_{01}^2 + \frac{1}{2} \chi_1 E_{01}^2 \cos \left[4\pi v \left(t - \frac{z}{v_1} \right) \right] \quad (3.17)$$

The second term of this equation indicates that there is a wave of polarization propagating in the medium in the same direction and at the same speed, but this wave oscillates at the twice higher frequency $2v$, rather than v . This wave of polarization may be thought of as the kind of "radiation aeri-

al" traversing the medium at velocity v_1 . Under certain conditions this "aerial" may cause emission of a new light wave at the frequency of the wave of polarization. We put the equation for this generated wave as

$$E_2(z, t) = E_{02} \cos [4\pi v(t - z/v_2)] \quad (3.18)$$

The amplitude of this wave E_{02} may be expressed in terms of E_{01} , the nonlinear susceptibility χ_1 , and other parameters of the medium. The velocity v_2 of the generated wave differs from the velocity of the incident wave v_1 because the refractive index is a function of frequency; in accord with (1.2)

$$\begin{aligned} v_1 &= c/n(v) \\ v_2 &= c/n(2v) \end{aligned} \quad (3.19)$$

Hence, in a nonlinear medium, a strong light wave of frequency v can beat with itself by means of the nonlinear polarization and give rise to a new light wave at frequency $2v$, the so-called *second harmonic*, accordingly this process is called *second harmonic generation*.

Consider now the case with two waves, one at frequency v_1 and the other at frequency v_2 , being launched into the nonlinear medium. The superposition of these waves gives the e.m. field

$$\begin{aligned} E(z, t) &= E_{01} \cos [2\pi v_1(t - z/v_1)] \\ &\quad + E_{02} \cos [2\pi v_2(t - z/v_2)] \end{aligned} \quad (3.20)$$

Substituting this expression into (3.15) yields

$$\begin{aligned} P_{NL}(z, t) &= \chi_1 E_{01}^2 \cos^2 [2\pi v_1(t - z/v_1)] \\ &\quad + \chi_1 E_{02}^2 \cos^2 [2\pi v_2(t - z/v_2)] \\ &\quad + 2\chi_1 E_{01} E_{02} \cos [2\pi v_1(t - z/v_1)] \cos [2\pi v_2(t - z/v_2)] \end{aligned} \quad (3.21)$$

Observing further the relationships $2\cos^2 \beta = 1 + \cos 2\beta$ and $2\cos \beta \times \cos \alpha = \cos(\beta + \alpha) + \cos(\beta - \alpha)$ we conclude that the wave of nonlinear polarization described by (3.21) is the superposition of waves at frequencies $2v_1$, $2v_2$, $v_1 + v_2$, and $v_1 - v_2$. Thus, the interaction of light waves at frequencies v_1 and v_2 launched in a material with the nonlinear polarization (3.15) may cause generation of new light waves at sum ($v_1 + v_2$), difference ($v_1 - v_2$) and double $2v_1$ and $2v_2$ frequencies.

Second harmonic generation in nonlinear crystals. We have mentioned above that under certain conditions the wave of nonlinear polarization (3.17) may give birth to the second optical harmonic, a generated light wave at frequency 2ν given by equation (3.18). In what follows, we shall disclose these conditions.

We recall that the polarization wave propagates in the medium at the velocity $v_1 = c/n(\nu)$, while the second harmonic propagates at the velocity $v_2 = c/n(2\nu)$. For the transfer of energy from the polarization wave to the new light wave to be efficient, the waves must be matched in velocity. This leads to the condition

$$n(\nu) = n(2\nu) \quad (3.22)$$

referred to as the *phase-matching condition*.

How could this condition be met? The answer to this question has appeared to be rather interesting. It relies on the fact that the refractive index depends on the direction in the anisotropic crystal. We have already mentioned that a light wave launched in an anisotropic crystal splits into two waves travelling at different velocities. In a large group of anisotropic crystals, called uniaxial crystals, one of these light waves is called the *ordinary wave*; its refractive index is independent of the direction of propagation. The other light wave is called the *extraordinary wave* and the corresponding refractive index depends on the direction of propagation. When we speak of the direction of propagation of a light wave, we imply the direction of its wavevector which is the normal to the wavefront at its any point.

The different refractive index behaviour in an anisotropic crystal is usually described in terms of the so-called *index ellipsoid*. Fig. 3.11a shows a section through the surfaces of refractive indices for the ordinary (sphere) and extraordinary (ellipsoid) waves. The ellipsoid axis OA is the optic axis of the uniaxial crystal. As can be seen, the refractive indices are the same along the optic axis, therefore a light wave travelling in this direction does not split into the ordinary and extraordinary waves. In case the wavevector forms an angle θ with the crystal optic axis OA , the "splitting" does take place, as away from the axis the ordinary refractive index is n^o and the extraordinary refractive index is $n^e(\theta)$. The extraordinary wave is polarized in the plane

passing through the wavevector and the optic axis (exactly this plane is shown in Fig. 3.11a), whereas the ordinary wave is polarized normally to this plane.

The section through the surfaces of refractive index, shown in Fig. 3.11a, corresponds to a certain frequency of the incident light. Suppose now that this frequency doubles. The

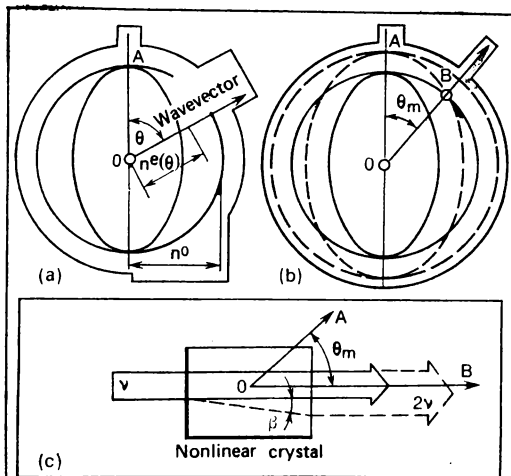


Fig. 3.11 Second harmonic generation in a nonlinear crystal

refractive index normally increases with frequency. Therefore, the dimensions of the refractive-index sphere and ellipsoid increase accordingly. Fig. 3.11b shows for comparison the sections through these surfaces plotted for a frequency v (solid lines) and the doubled frequency $2v$ (dashed lines). The dashed ellipse is seen to intersect with the solid circle; one of the points of intersection is point B . This means that for light waves propagating in the OB direction (i.e. close to the cone where OB is a generating element) the phase-matching condition is satisfied

$$n^o(v) = n^e(2v) \quad (3.23)$$

The cone angle θ_m is obviously the phase-matching angle. For all directions lying on this cone the ordinary refractive index at frequency v equals the extraordinary refractive index at frequency $2v$.

To summarize, the phase matching condition is met for light waves travelling in the crystal at an angle θ_m to its optic axis and provided the fundamental wave is polarized normally to the plane passing through its wavevector and the optic axis of the crystal, i.e., it is an ordinary wave. Consequently, the crystal must be cut as illustrated in Fig. 3.11c (OA is the optic axis, OB the wavevector direction) and also one must take care of the incident light being respectively polarized. The plane of the page contains both the wavevector and the crystal optic axis; the second-harmonic wave

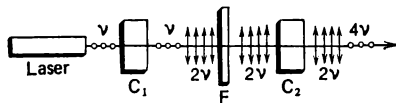


Fig. 3.12 Arrangement for fourth harmonic generation

is polarized in this plane, while the fundamental wave is polarized normally to this plane. The solid arrow shows the beam at the fundamental frequency v and the dashed arrow represents the radiation at the second-harmonic frequency $2v$.

Birefringence causes the light beam of the second harmonic to experience a certain lateral shift characterized by an angle β , called the anisotropy angle (in spite of this shift the second-harmonic wavevector has the same sense as the wavevector of the fundamental wave—along the line OB). This shift, however, causes a decrease in the ratio of the second harmonic to fundamental mode powers, referred to as the *conversion efficiency*. The shift is absent ($\beta = 0$) at 90° phase matching when $\theta_m = 90^\circ$.

Fourth harmonic generation. The fourth harmonic can be derived by doubling the frequency of the second harmonic in the arrangement schematized in Fig. 3.12. A linearly polarized laser beam at frequency v passes through the crystal C_1 to give rise to the second harmonic at frequency $2v$. This radiation enters the rejection filter F which passes through only the second frequency harmonic and rejects the radiation at the fundamental frequency v . The filtered beam then arrives at the second crystal C_2 where the fourth harmonic at frequency $4v$ is generated. The polarization planes of extraordinary waves in the crystals C_1 and C_2 are at right angles. If the fundamental wave is polarized

normally to the plane of the page, then the optic axis of C_1 must be in this plane too, whereas the optic axis of C_2 must belong to the plane orthogonal to the page.

In passing we note that nonlinear crystals may be employed to generate not only even harmonics but also odd harmonics of a fundamental frequency. For example, the second harmonic may be made to beat with the fundamental frequency to triple the fundamental frequency: $2\nu + \nu = 3\nu$. In principle, nonlinear crystals can be used to generate harmonics of any order. It should not be overlooked, however, that the intensity of higher-order harmonics rapidly declines. To illustrate, if the conversion efficiency for the second harmonic is 20%, the figure for the fourth harmonic, produced in the configuration shown in Fig. 3.12, is never above 4%. This implies that the power output for the fourth harmonic is only 0.04 from the power of the radiation launched at the fundamental frequency.

Optic harmonic generators. Harmonic generation (optical frequency multiplication and sum-frequency generation) has been developing as an individual optical discipline for 15 years already. A variety of optical harmonic generators are commercially available. Their fabrication takes advantage of the well developed industrial technology for the production of diverse and efficient nonlinear crystalline materials offering a second-harmonic conversion efficiency of 20 to 50%. These crystals exhibit considerable birefringence which allows for the phase matching of the fundamental radiation in a rather wide spectral range. They also are transparent over considerable bandwidths and demonstrate good power handling capacity, i.e., resistance to high powers. A family of such crystals is given below.

Material	Symbol	Formula
Potassium dihydrogen phosphate	KDP	KH_2PO_4
Ammonium dihydrogen phosphate	ADP	$\text{NH}_4\text{H}_2\text{PO}_4$
Cesium dihydrogen arsenate	CDA	CsH_2AsO_4
Cesium dideuterium arsenate	D-CDA	CsD_2AsO_4
Lithium niobate	—	LiNbO_3
Lithium iodate	—	LiIO_3
Barium-sodium niobate	—	$\text{Ba}_2\text{NaNb}_5\text{O}_{15}$

Considerable progress in the development of efficient optic frequency multipliers has been achieved with commercially available Nd : YAG lasers. These lasers operate at the wavelength 1.064 μm which has been found to be highly suitable for efficient harmonic generation in the visible range (second harmonic, $\lambda = 0.532 \mu\text{m}$) and in the ultraviolet end (fourth harmonic, $\lambda = 0.266 \mu\text{m}$) of the e.m. spectrum. The sum-frequency radiation extracted from a Nd : YAG laser and an organic dye laser makes it possible to produce coherent beams in the practically important blue-violet portion of the spectrum, where traditional means of powerful coherent radiation are difficult.

Intracavity harmonic generation, with a nonlinear crystal being placed in the cavity of the laser producing the fundamental frequency, also undergoes extensive development. For continuously pumped lasers with output powers sizeably lower than that inside the cavity, this technique allows considerable enhancement for second-harmonic conversion efficiency.

Frequency tuning by parametric oscillation. In the previous paragraphs we have demonstrated that two light waves at frequencies v_1 and v_2 interacting in a nonlinear medium can bring about a new wave at the difference frequency $v_1 - v_2$. Phase matching for this process requires that the sum of wavevectors at v_2 and $v_1 - v_2$ be equal to the wavevector at v_1 . We assume that all the three wavevectors are in one direction and observe that a wavevector k of a wave at frequency v is defined as

$$k = 2\pi v/v = 2\pi v n(v)/c \quad (3.24)$$

Then the aforementioned phase matching condition takes the form

$$v_2 n(v_2) + (v_1 - v_2) n(v_1 - v_2) = v_1 n(v_1) \quad (3.25)$$

Note. Second harmonic generation may be viewed as the beat of two light waves at the same frequency v . Phase matching in this case implies that the sum of the wavevectors at frequency v should be equal to the wavevector at frequency $2v$. Assuming that all wavevectors are in one direction and observing (3.24), we may write the phase matching condition for second harmonic generation in the

form similar to that of (3.25), namely $v n(v) + v n(v) = 2 v n(2v)$. This again leads to the familiar equality (3.22).

Let us place the nonlinear crystal inside the cavity and orient it so that the phase-matching direction for the frequency combination concerned, v_2 and $v_1 - v_2$, coincide with the optic axis of the cavity. In this arrangement, the photon states with energies $h v_2$ and $h(v_1 - v_2)$ become selected states (according to the terminology of Sec. 1.5). Imagine now that a laser wave at frequency v_1 (the *pump* frequency) is launched along the resonator axis. This pump wave should be intense enough to induce the nonlinear behaviour of the crystal and to exceed the level of losses for the selected photon states. In addition, phase matching requires that the pump wave be either extraordinary or ordinary for this crystal, i.e., it should be appropriately polarized. When all these requirements are met, the energy of the pump will be converted into coherent light waves at frequencies v_2 and $v_1 - v_2$.

The wave at frequency $v_1 - v_2$, referred to as the *idler* wave, is the result of the strong pump wave at v_1 interacting with the weak *signal* wave at v_2 , which is selected from noise always available in the cavity. Accordingly, the amplification of the weak signal wave at frequency v_2 made at the expense of the strong pump wave at v_1 is the result of the pump wave interacting with the weak idler wave at frequency $v_1 - v_2$, also present in the noise field. Such a process is *parametric generation* of light: the pump wave at frequency v_1 is converted into two other light waves at frequencies v_2 and $v_1 - v_2$.

Practical parametric oscillators afford maximum 40 to 50% of the pump wave power to be converted to the signal and idler outputs. In close similarity to lasers, the generation of both signal and idler frequencies starts from the noise level as these frequencies are selected by the cavity. We note that the generated waves exhibit a certain polarization. For example, a situation is possible when the pump wave is an extraordinary wave as is one of the generated waves while the other is an ordinary wave.

Parametric oscillation is a convenient tool for tuning the output frequency. Indeed, the pump frequency v_1 is fixed as this is the frequency of laser oscillation. As far as the signal

frequency v_2 selected by the cavity is concerned, it may in principle have any value within a certain frequency range whose upper limit is the pump frequency v_1 itself. Imagine that we are in a possession of a facility capable of adjusting the phase-matching direction corresponding to variable v_2 and $v_1 - v_2$ with respect to the optic axis of the resonator. For this we may lightly rotate the nonlinear crystal to alter the angle θ between its optic axis and the optic axis of the resonator. Corresponding to each value of θ , there is a unique combination of v_2 and $v_1 - v_2$ for which the resonator axis

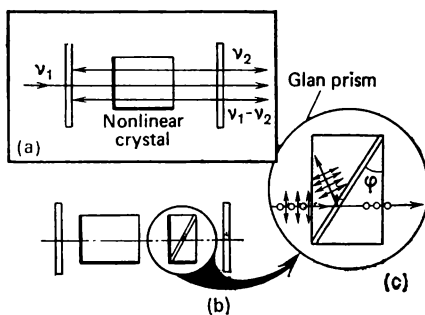


Fig. 3.13 (a) Singly resonant and (b) doubly resonant parametric oscillators, (c) Glan-Foucault prism

coincides with the phase-matching direction. By gradually changing θ , one may smoothly tune the signal frequency v_2 and, consequently, the idler frequency $v_1 - v_2$.

A number of diverse configurations of parametric oscillators are known. One of them is depicted in Fig. 3.13a. Both resonator mirrors are transparent at frequency v_1 . For the lower frequencies, the left mirror is highly reflective while the right mirror has some optimal reflectivity. This system is categorized as a *doubly resonant oscillator* to emphasize the fact that it simultaneously generates two light waves, at the signal and idler frequencies.

The *singly resonant parametric oscillator* produces only one wave, say at frequency v_2 . To suppress generation at the idler frequency $v_1 - v_2$, the losses for this wave are deliberately raised. This can be achieved, for instance, by introducing a Glan-Foucault prism inside the cavity (in case the polarizations of the two waves being generated are differ-

rent, i.e., when one of them is an ordinary wave and the other an extraordinary wave). The optical system of such parametric oscillator is shown in Fig. 3.13b. In this arrangement, the Glan-Foucault prism passes the signal wave at frequency ν_2 , but deflects the idler wave at $\nu_1 - \nu_2$. In fact, it does not come to deflection, as the idler wave simply fails to grow to a reasonable intensity.

The Glan-Foucault prism (or the Glan prism if in US and UK literature) is essentially a birefringent crystal composed of two Iceland spar (CaCO_3) prisms separated from each other by a uniform air gap, as shown in Fig. 3.13c. The optic axes of both prisms are at right angles to the plane of the page, $\varphi = 38^\circ 30'$. The prism transmits a light wave polarized normally to the plane of the page but reflects at its air-gap interface a wave polarized in the plane of the page.

Currently used parametric oscillators are built around nonlinear crystals of lithium niobate pumped by neodymium laser output. By way of example, a parametric oscillator on this crystal pumped by the second harmonic from a Nd : YAG laser (at $0.53 \mu\text{m}$) is tunable in the range from 0.5 to $3.5 \mu\text{m}$ with the conversion efficiency 40% .

On the history of nonlinear optics. Nonlinear phenomena in optics cover those due to the reversible variations in medium behaviour induced by the passage of intense light beams. They involve, specifically, harmonic generation and parametric amplification we have considered above. Other nonlinear phenomena include bleaching, considered in Sec. 3.2 and 3.4 in connection with saturable absorbers, and opaque behaviour of media taken up in Sec. 3.3 in an example of two-photon light absorption in semiconductors.

The first nonlinear-optical experiment was made in 1925 when the Soviet physicists S. I. Vavilov and V. L. Levshin, experimenting with light of high intensity from a spark gap, observed a decrease in the absorption coefficient of uranium glass. This experiment was the first demonstration of bleaching in a medium, induced by incident light. At the time, however, one could not expect extensive research in this field because of the absence of powerful sources of coherent light. In spite of these deficiencies, S. I. Vavilov gave much thought to possible studies of optical nonlinear phenomena. His brilliant scientific intuition and ability to foresee far

ahead have their full measure in the book "Microstructure of Light" published in 1951. In this work Vavilov formulated with an astonishing thoroughness the principal problems and indicated the direction of development for a new branch of optics which he referred to as nonlinear optics.

The development of laser revived, and in fact gave its actual birth to, nonlinear optics. In 1961, P. A. Franken, an American physicist, observed in a quartz crystal second harmonic generation for a ruby laser. Soviet physicists R. V. Khokhlov and S. A. Akhmanov established in 1962 the conditions for various phenomena of nonlinear optics—specifically, harmonic generation—to proceed with reasonable efficiency. They also devised and established the idea of parametric amplification. Simultaneously, American physicists J. A. Giordmaine and R. W. Terhune studied the possibility of phase matching in crystals.

In the period from 1961 to 1963, much fundamental research was done into nonlinear optics by a team of Soviet scientists leaded by R. Khokhlov and their American colleagues headed by N. Bloembergen. By 1965, nonlinear optics has developed into a substantial and independent branch of modern optics.

3.7 Wavefront Correction of the Laser Output

In this section we shall look at another application of nonlinear optics providing automatic correction of the laser wavefront.

Problem formulation. Let us imagine a laser producing highly coherent radiation with an almost plane wavefront but of relatively low power. To boost this power, the laser output is passed through a number of quantum amplifiers, i.e., active components in which pumping creates a population inversion. As the laser output traverses these quantum amplifiers, they build up its power but markedly degrade the degree of coherence. The inhomogeneity of material properties in these amplifiers and deformations induced in these components by mechanical and heat stresses, to name only the principal factors, introduce distortions in the initially almost plane wavefront. As the number of amplifying stages increases, the output receives ever higher

boost and the distortion of the wavefront grows simultaneously.

Such distortions are unavoidable in transmitting a light beam through any optic communication channel. The latter may be a series of amplifying stages, though it may be air or water through which optic signals are tried to be transmitted. In these media, the wavefront distortions will be incurred by eddies and inhomogeneities intrinsic in any natural medium.

A question arises whether the wavefront distortions accumulated in propagating through optic channels can be corrected. This question has been answered positively in fact only a decade ago, after the discovery of *wavefront reversion*, or *phase conjugation*, in nonlinear media. This discovery initiated an intensive development of new field called *adaptive optics*.

Note. Adaptive optics deals with the development of optical systems which are able to adapt to the changing environment by altering their behaviour, operating regimes and even the structure. Adaptation improves the system performance or optimizes its behaviour in variable conditions.

Generally, adaptive systems include all optic systems with feedback, capable of correcting the characteristics and performance of the systems. More specifically, adaptive systems are taken as ones that perform wavefront correction for light beams experiencing front distortive effects.

Wavefront reversal by nonlinear mirrors. For the sake of consideration we assume that the laser emits a beam with an almost plane wavefront. This beam traverses the active material of the amplifier and then is reflected backward by a plane mirror. When the beam passes through the amplifier it undergoes wavefront distortions. Fig. 3.14a shows the profile of such wavefront (by a dashed curve) near the mirror surface. The rays corresponding to this wavefront (recall that by definition they are normal to the wavefront) are indicated by dashed arrows. Each ray is reflected by the mirror according to the law of reflection, saying the angle of incident and reflected rays make equal angles with the normal to the reflecting surface. The reflected rays are indicated by solid arrows.

Suppose now that the plane mirror is replaced by a reflecting surface which is exactly the shape of the oncoming wavefront, as shown in Fig. 3.14b. Such a mirror having the surface which in each moment of time matches the profile of the arriving wavefront may be called the adaptive mirror. Upon the reflection from the adaptive mirror each ray is backscattered in the same line—experiences a 180°

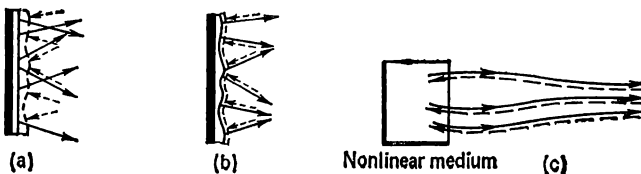


Fig. 3.14 Reflection from a plane (a), adaptive (b), and "nonlinear" (c) mirror

turn—and a reversal of the wavefront occurs. In terms of ray phases, the reversed rays acquire the conjugated phases, therefore this process is also referred to as *phase conjugation*.

Because ray paths are reversible in optical systems, each ray mirrored in such phase conjugated manner will return to the laser in exactly the same path it has traced in its forward trip. Hence, upon a round trip through the amplifier the light beam will regain the same wavefront it had as lased from the laser. By reversing the wavefront the adaptive mirror performs the necessary correction, offsetting the distortions introduced by the amplifier. The net result is a more powerful beam with the initial wavefront, i.e., intense radiation of high coherence.

The crucial problem that remains is how to prepare such an adaptive mirror capable of offsetting the distortions of wavefront obtained in the particular optic channel. It turned out that such a mirror could be realized in a rather simple manner by invoking certain nonlinear-optical phenomena. The point is that the nonlinear medium is able to reverse the wavefront of a beam launched in this medium. In other words, under certain conditions, the nonlinear medium can function as an adaptive mirror. It is essential that in this case there is no need to reveal what distortions the wavefront has suffered. The "nonlinear mirror" automatically

accounts for these distortions, since each ray launched in this medium will be retraced in exactly the same path it has travelled on its way down the medium (see Fig. 3.14c). Virtually, the self-correction of the wavefront takes place. The term "nonlinear mirror" is conditional to a certain extent, since actually no reflecting surface is present and the reflection is effected in the bulk of the nonlinear medium.

Nonlinear-optical phenomena for wavefront reversal. In this text we take up only two such phenomena. One is stimulated scattering of light on acoustic waves, referred to as *stimulated Brillouin scattering* (SBS), or stimulated Mandelshtam-Brillouin scattering if in the Soviet literature on the subject. Launched in a medium, a light wave undergoes scattering on acoustic waves induced by thermal motion of molecules in the medium; this process is termed *spontaneous* Mandelshtam-Brillouin scattering. It is remarkable that when a light wave is scattered on an acoustic wave travelling in the same direction, the frequency of the scattered wave appears to be decreased by the frequency of the sound wave. This component of scattered light is referred to as the Stokes satellite named in deference to the British physicist George G. Stokes. Conversely, when the light wave is scattered by a countercurrent sound wave, the frequency of the scattered wave increases. This component is called *anti-Stokes*.

Spontaneous scattering of light gives rise to both scattered components, Stokes and anti-Stokes, but their power is insignificant compared to that of the fundamental beam. A different pattern is observed in stimulated Brillouin scattering which occurs at rather high intensities of incident light. The modifier "stimulated" implies that this time the light wave is scattered on the acoustic waves that it has induced in the medium by means of electrostriction. Now the intensity of scattered waves may grow significantly so that an appreciable Stokes (be sure to notice that) component will be observed. Under certain conditions, the spatial structure of the backscattered Stokes component (180° reversal) will have the wavefront reversed with respect to the front of the fundamental wave.

The other nonlinear-optical phenomenon of the two aforementioned is the familiar interaction of light waves in non-

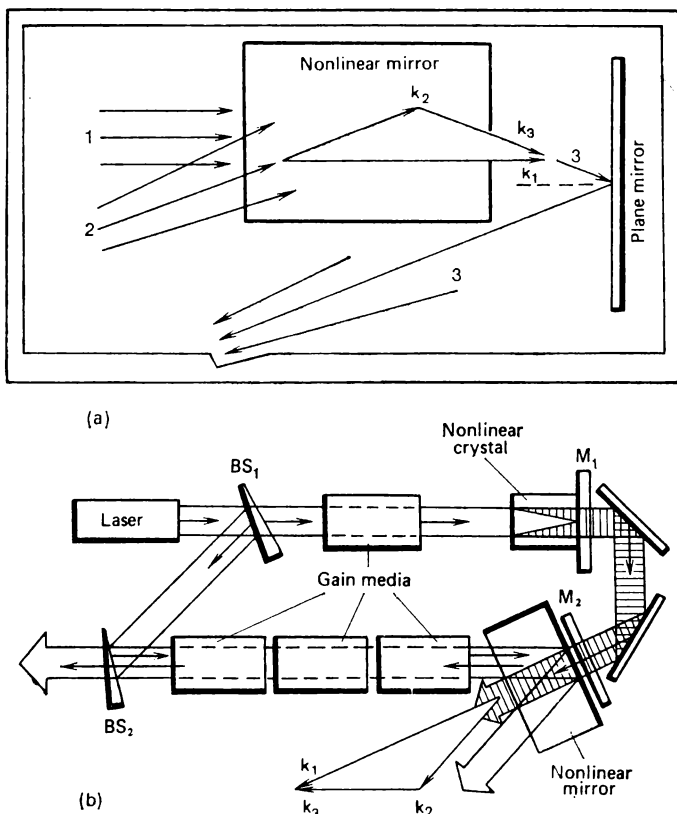


Fig. 3.15 Wavefront reversal achieved by making light waves interact in a nonlinear medium (a), and an example of laser adaptive system (b)

linear media. Referring to Fig. 3.15a for illustration, plane wave 1 of wavevector k_1 at frequency 2ν interacts in a nonlinear medium with a spatially inhomogeneous light wave 2 of wavevector k_2 at frequency ν . As the result of this interaction, the nonlinear medium generates a wave 3 of wavevector k_3 at frequency ν . After reflection from a plane mirror orthogonal to k_1 , the last wave is converted to a wave with the wavefront reversed with respect to that of wave 2. The wavevectors are related in accordance with the phase-

matching condition

$$\mathbf{k}_1 - \mathbf{k}_2 = \mathbf{k}_3 \quad (3.26)$$

As an example of the system exploiting this principle consider a laser adaptive system capable of yielding high-power outputs of highly coherent light. The optical configuration of this system is depicted in Fig. 3.15b.

The prime source of radiation is a low-power laser emitting highly coherent beam at frequency ν . The beamsplitter BS_1 splits the beam into two parts of different irradiance. The more intense beam passes through, while the less intense beam is reflected. The first beam is amplified in the amplifier and then excites the second harmonic (at frequency 2ν) in the nonlinear crystal. The mirrors M_1 and M_2 are totally reflective ($R = 1$) for the light at ν but transmittive at 2ν . As a result the second harmonic travels with almost no losses into the nonlinear medium which here plays the part of the nonlinear mirror. It is this wave that is denoted as wave 1 (frequency 2ν , wavevector \mathbf{k}_1) in Fig. 3.15a.

The second light beam reflected by BS_1 undergoes one more splitting at the beamsplitter BS_2 , passes through the amplifying stages and upon traversing once the nonlinear medium it is reflected by mirror M_2 to this medium again. This beam represents wave 2 (frequency ν , wavevector \mathbf{k}_2) in diagram (a) of Fig. 3.15. Waves 1 and 2 interact in the nonlinear medium to produce a new light wave 3 at frequency ν , defined by wavevector \mathbf{k}_3 connected with \mathbf{k}_1 and \mathbf{k}_2 by the relation (3.26). Wave 3 propagates counter to the wave approaching from BS_2 through the amplifiers and has the wavefront reversed with respect to the countercurrent wave. As a result, the output leaving the system through BS_2 is an amplified beam at frequency ν with an almost ideal wavefront.

3.8 Light Beam Manipulation

General. A light beam may be deflected by appropriately set mirrors, prisms, diffraction gratings, etc. Some applications require that the beam is not just deflected, but assumes new position very fast. Moreover, the deflection must be made recurrent and performed according to a certain pattern, say, scanning deflection. Rotating mirrors and prisms can no longer suit the purpose as their motions are relatively

slow. To serve the purpose, non-mechanical techniques of laser beam control are employed.

Devices providing deflection or scanning of light beams are called *optical deflectors*. They can deflect the light beam continuously or according to a certain *discrete pattern*. The first are called analog deflectors and are used for continuous scanning, while the second, known as digital deflectors, for discrete scanning. The latter are useful for orienting the beam in certain directions or for parallel shift of the beam position in space.

Most popular groups of deflectors are electrooptic and acoustooptic deflectors. The electrooptic deflectors harness the electro-optic effect which consists in controlling the refractive index of the medium by an electric field. In the acoustooptic deflectors, the refractive index of the medium is controlled by setting in mechanical stresses in the medium by means of an acoustic wave launched into it. We recall that both electrooptic and acoustooptic effects were treated in Sec. 3.2 in connection with the methods of *Q*-switching discussed there.

Analog electrooptic deflectors. A simple example of continuously operating deflectors is an ordinary triangular prism with metal electrodes placed at its ends to apply a variable voltage. These ends are shadowed in Fig. 3.16. Assume for simplicity that the incident beam hits the prism normally to its face. Then the angle of deflection θ from the initial direction is defined as

$$\theta = \arcsin(n \sin \Phi) - \Phi \quad (3.27)$$

where Φ is the angle of the prism, and n the refractive index of the prism. Since the refractive index of the prism is a function of the external electric field the value of the index and θ can be varied by applying variable voltage.

Two such prism deflectors set in tandem and at right angles to each other provide for two-dimensional reflection and scanning.

Electrooptic prism deflectors are made from materials of high transparency in the desired range of wavelengths and

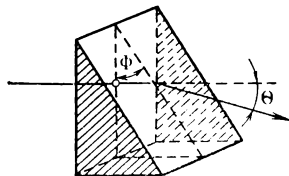


Fig. 3.16 A continuous electrooptic deflector

which exhibit sufficient electrooptical effect. A sufficient variation of the refractive index with the electric field is offered by such crystals as potassium tantalate-niobate (symbol KTN, chemical formula $\text{KTa}_x\text{Nb}_{1-x}\text{O}_3$, where x varies from 0 to 1) and barium titanate (BaTiO_3). Also useful are crystals KDP and D-KDP (KH_2PO_4 and $\text{KH}_{2(1-x)}\text{D}_{2x}\text{PO}_4$). The operational speed of these deflectors is conditioned by the minimal time they take to sweep the beam from one extreme position to the other and normally is on the order of 1 μs .

Analog acoustooptic deflectors. Deflection of a light beam by the acoustooptic deflector may be treated as the

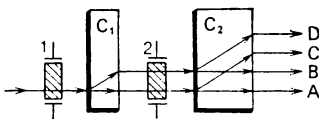


Fig. 3.17 A discrete electrooptic deflector (two-stage configuration)

result of the diffraction of light by the ultrasound wave launched in the medium. In agreement with (3.7) the angle of deflection in such a device is

$$\theta = \arcsin (\lambda/2\Lambda) \quad (3.28)$$

This angle can be gradually varied by altering the frequency of the ultrasound wave and, hence, the spacing of grating Λ .

The ultrasound deflectors are made of transparent materials with a relatively high refractive index and reasonably high photoelasticity. In this respect, promise is held by such materials as lead molybdate (PbMoO_4) and paratellurite (TeO_2).

The speed of these devices is limited by the time $\tau = d/v$, where d is the diameter of the deflected beam, and v the velocity of sound. For $d = 1$ cm and $v = 2 \times 10^3$ m/s, $\tau = 5 \mu\text{s}$.

A digital electrooptic deflector. Fig. 3.17 shows the optical arrangement of an electrooptic deflector capable of changing the spatial position of the light beam by parallel transfer in 1 μs . The arrows represent the directions of light rays; C_1 and C_2 stand for two identically oriented birefring-

ent crystals (say CaCO_3), 1 and 2 for Pockels cells which rotate the polarization plane of the beam through 90° with an external electric field (recall that the field in both cells must be set at 45° to the polarization plane of the initial beam; see Sec. 3.2). The orientation of C_1 and C_2 is such that the incident beam is for them an ordinary beam (it is polarized orthogonally to the plane containing its wave-vector and the optic axis of the crystal).

When both cells are deenergized, the light beam is not deflected in traversing C_1 and C_2 as it is an ordinary beam for both of them. So it leaves the system in position *A*. When both cells are energized, the polarization plane of the beam undergoes 90° rotation in cell 1 and the beam becomes extraordinary for C_1 and is deflected in it. Having turned its polarization plane in cell 2, the beam is handled by crystal C_2 as ordinary and experiences no deflection in it. The resultant beam leaves the system in position *B*.

It is an easy matter to argue that with cell 1 off and cell 2 on, the beam will leave the deflector in position *C*. Finally, when cell 1 is on and cell 2 off, position *D* is realized.

For the sake of simplicity we confined ourselves in this treatment to a two-stage system. With N stages, the number of possible positions of the beam is 2^N . Current deflectors of this type stably realize 1024 states which corresponds to 10 stages in the scheme.

Chapter 4

Applications of Lasers

First of all we should note that the studies into interaction of laser radiation with matter are of extreme scientific significance. Lasers are widely used for fundamental studies in physics, chemistry and biology. They have numerous applications in electronics and medicine.

Research in nonlinear optics gives a vivid example of such studies. We have learned above that high-power laser radiation can alter, in a reversible manner, the physical behaviour of material and bring about diverse nonlinear-optical phenomena.

The laser makes possible high concentration of light power within rather narrow bandwidths and frequency tuning over considerable ranges. Therefore, lasers are useful light sources in investigations of optical spectra of materials. Laser spectroscopy is advantageous in exceedingly high accuracy and resolution.

Tunable lasers present an extremely attractive proposition for selective excitation of various desired states of wanted atoms or molecules or for selective rapture of certain chemical bonds. This opens up the possibility for initiating the desired chemical reactions, controlling these reactions, and studying their kinetics.

Picosecond pulses available from lasers have initiated studies into a number of fast processes in materials, specifically, in biomedicals. We note as an example the fundamental studies of photosynthetic processes. These processes are of a rather complicated variety, in particular because they are very fast—their time scales being in the picosecond range. The use of ultrashort light pulses provides a unique possibility to follow the development of such processes and even to model separate steps of these processes.

Lasers play a tremendous role in the current fundamental research. An elaborate discussion on this subject would call

for consideration of a number of special theoretical questions and needs a more fundamental physical background from the reader. Therefore, our later discussion will be focused on purely practical, particularly industrial, applications of lasers.

The numerous fields of laser applications may be broadly categorized into two groups. One involves applications where laser beams—as a rule of high power—are exploited to produce a targeted effect on material. These applications include material working (say, welding, heat treatment, cutting, hole burning, etc.), isotope separation, medical diagnosing, etc. The other group involves data transmission and processing, measurements, and quality control.

In our discussion of these most significant applications of lasers we will place main emphasis on the principal aspects of the particular application of system, rather than on the specific technical features of the systems or their design subtleties.

4.1 Material Working

Effects of strong laser radiation on materials. The optic system of focusing can focus a laser beam into a light spot of only $10\text{-}100 \mu\text{m}$ in diameter on the surface of a material. As a result, a very high irradiance is available within a small spot on the surface. If the 1-kW output of a cw laser is focused in a spot of $100 \mu\text{m}$ diameter, the resultant irradiance will be 10^7 W/cm^2 .

Let us look at the physical processes that occur in the material irradiated by a laser beam of high irradiance. When the irradiance increases to the value in the order of 10^5 W/cm^2 , the material starts melting. With more light energy influxed in the material, the boundary between the liquid bath and the solid (the melt interface) gradually protrudes inside the material (Fig. 4.1a). The surface of the melt also increases, hence the heat transfer by thermal conduction into deeper layer of material also intensifies to reach finally a steady-state surface.

At still higher levels of irradiance, up to $10^6\text{-}10^7 \text{ W/cm}^2$, incoming to the material, it starts boiling and an intense evaporation occurs. The material being evaporated leaves a pit in the surface, which grows into a hole as the evaporation goes on (Fig. 4.1b).

When the beam irradiance grows to 10^9 W/cm^2 , the vapour will be ionized by the light to produce a high temperature plasma. The plasma is highly absorptive for light, hence it will prevent the beam from entering the material (Fig. 4.1c). Therefore, in material working it is essential that plasma should not occur. Accordingly, power densities realized in material working systems are not very high.

So far we have discussed concentration of light power in space. The amount of energy delivered by the beam to the

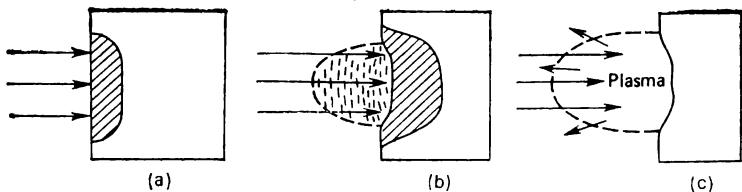


Fig. 4.1 Effects of the increased power density in a powerful laser beam on material. (a) material melts, (b) material melts and evaporates, (c) plasma barring the beam path to the surface

surface depends also on the power concentration in time. The temporal profile of the laser output can be controlled by varying the length of single light pulses or the repetition rate in the pulse train. Assume that the irradiance of the output is high enough to bring about not only melting but also intense evaporation of the material. Let the output consist of short pulses, say 10^{-7} to 10^{-8} s long. Such a pulse brings into the material a large amount of energy in a very short time. For the time of the pulsed width the melt interface fails to penetrate deeper in the material, and most of the energy goes into the evaporation of the already existent melt. Thus, if the energy content of the pulse is fixed, the duration of the pulse should be adjusted so that there be enough time for the melt interface to penetrate in the material.

Diverse material working processes and the properties of specific materials necessitate the use of laser outputs with certain energy contents and temporal profiles. Whereas relatively low peak power but durable pulses (10^{-3} to 10^{-2} s pulsed width) are suitable for welding applications, more intense and short pulses (of 10^{-4} to 10^{-3} s) are required for perforation and hole cutting where intense evaporation of

the material is essential. The spectral characteristics of the laser output are also important here, as the wavelength of the beam governs the portion of light power reflected, rather than absorbed, by the surface of the material. Apart from that, a beam of shorter wavelength may be focused into a smaller light spot.

Laser welding. This type of welding competes well with such familiar welding techniques as arc welding, resistance welding, and electron beam welding. Moreover, it offers a number of advantages which make it preferable in many

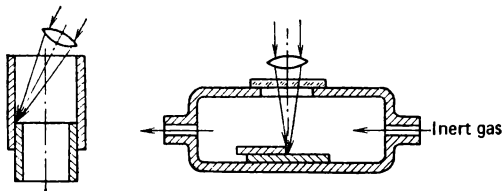


Fig. 4.2 Inert gas laser welding for otherwise inaccessible locations

circumstances and even the only possible welding technique. This welding is contactless, therefore there is no possibility for introducing deleterious impurities in the weldment. Unlike electron-beam welding running in a vacuum, laser welding is performed in the atmosphere. It offers a possibility to weld in inaccessible regions, too. In practice, any region which can be seen (even though it may require some optical system to permit observation) can be processed by a laser.

Particular mention should be made of the application of the laser for welding microelectronics components inside a chamber filled with an inert gas to preclude oxidation reactions. Laser welding is capable of a fast and highly accurate local melting at a given point or along a line. The heat affected area is very small. This is a significant feature in those situations where welding is to be made in the vicinity of heat sensitive components, as is the case in microelectronics. Two specific examples of welding in otherwise inaccessible regions are depicted in Fig. 4.2.

Laser welding has passed through two stages in its development. Spot welding has been the first to develop on the base of limited and moderate powers of pulsed solid lasers,

such as ruby and Nd:glass lasers. Then high power CO₂ lasers and Nd:YAG lasers have made continuous and pulsed-train outputs available for the development of seam welding with melting depths of a few millimetres. The largest currently available melting depth is 2 cm in one pass of the laser beam.

Spot welding is especially suitable for precision welding in a thermally sensitive environment. Examples of this application are the connection of a nickel lead to a nickel alloy tap in the transistor base, welding of thin copper wires to each other or to leads, connecting microelectronic components.

Seam welding uses output powers of several hundred watts to seal cases of diverse devices, joining tips to blades of gas turbines, fastening cutting steel edges to metal cutting saws, connecting circalloy tips to fuel elements of nuclear reactors, and so on. Achievable welding velocities are as high as 1 to 3 m/min, weldment widths are 0.3 to 0.6 mm.

A comparatively recent addition to the industrial applications is seam welding with 1 to 10 kW strong beams. The associated weld width runs into a few millimetres and the strength of the weldments is the same as that of the parent materials. Laser welding lends itself well to automatic processes in automotive production lines, for joining titanium and aluminium sheets in ship building, for trunk pipe lines construction works, to name a few. Welding of nonmetallic materials is also an interesting application of lasers. Common glasses are welded by lasers of 100 W output, while quartz needs 300 W to be welded.

Laser heat treatment. A powerful laser output rapidly warms up the surface layer in an item it hits. As the beam moves away to other areas the heated spot cools down as rapidly. This procedure is used for heat treatment of surface layers of metal items, which considerably enhances the item strength. Laser heat treatment is advantageous in that it provides selective treatment of the desirable areas, say those subjected to the more intense wear. In the automotive industry, for example, this treatment is used to strengthen cylinder blocks, valve guides, gears, camshafts, etc. The heat treatment is effected at considerable speed, with high strengthening efficiency and least distortions of shape and size of the item being processed.

Laser power may also be employed to surface alloy various items. The alloying powder is applied on the surface and when the laser heats the surface the powder melts as does the surface layer of the piece and mixing occurs in a thin surface layer.

The laser most widely used for heat treatment is the 1-kW CO₂ laser operating in the continuous wave mode.

Laser cutting. In this application field, lasers offer the following advantages:

- wide range of processed materials (paper, cloth, plywood, glass, sheet asbestos products, ceramics, sheet metal);
- possibility of fine and precise cuts;
- minimal amount of mechanical distortion and thermal damage introduced in the material being cut;
- chemical purity of the cutting process;
- possibility of cutting in two and even three dimensions according to a complicated profile;
- easy automation of the process and high production rates.

The laser output power required for cutting depends on the material being cut. For example, 50 mm thick boards may be cut with a 200-W CO₂ laser, the width of cut being 0.7 mm, whereas sheets of plywood are processed with an 8-kW CO₂ laser at a cutting velocity of 1.5 m per minute. Cutting glass of 10 mm thickness requires already 20 kW of output power.

Metals can be cut with output powers of only 100 to 500 W provided that the beam-heated material is blown with a jet of oxygen, so that gas-laser cutting results. The configuration of such a cutter is schematized in Fig. 4.3. Considerable portion of energy required for cutting is supplied in this case by exothermal reactions between metal and oxygen (burning of metal in the oxygen jet). The oxygen jet also blows away and removes cutting products and melt from the cutting area, at the same time cooling the adjacent edges of the cut metal. Therefore, oxygen blow reduces laser power requirement, increases the depth and velocity of cutting, and produces quality-cut edges.

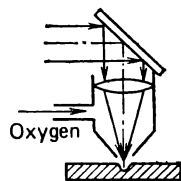


Fig. 4.3 An arrangement for a gas-laser cutter

To demonstrate the range of laser cutting applications, we give two examples from different areas. One of them concerns laser cutting of cloth in garment factories. The cutting system includes a CO₂ laser capable of 100 W of continuous output, facilities for focusing and direction control of laser beam, a computer, and fixtures for cloth tension. The laser cuts the cloth at a velocity of 1 m/s. The beam is focused into a spot of 0.2 mm diameter. Such a system is able to prepare cut pieces for 50 suits during an hour. The pieces are cut with a high precision and a good quality of cut edges.

The other example relates to metal cutting. Laser cutting is a technology widely used in the aero space industries, specifically in the fabrication of spacecraft. Lasers automatically cut sheets of titanium, steel, and aluminium. A continuous CO₂ laser of 3 kW output cuts titanium sheets of 5 and 50 mm thickness at a velocity of 3.5 and 0.5 m/min respectively. The use of oxygen blow in gas-laser cutting allows for similar processing rates with considerably lower powers (100 to 300 W).

Drilling and perforating holes. Hole perforating by the laser relies on the intense evaporation of material heated by powerful light pulses (one or a few) of 10^{-4} to 10^{-3} s duration, developing on the material surface power densities in the order of 10^6 to 10^7 W/cm². The power density 10^7 W/cm², for example, can be achieved by focusing a 100 μ s pulse of 1 J into a light spot of 0.3 mm diameter. The CO₂ laser is equally suited to working on metallic and nonmetallic (plastic, ceramic, glass) materials. The Nd:YAG laser beam is only appreciably absorbed by metallic materials, and therefore finds wide use for hole perforating in metals only.

Laser perforation offers a number of advantages over traditional tools. Freedom from wear in the case of a laser tool eliminates the problem of wear and broken drills. Moreover, lasers perform drilling with extremely high precision and in any desired direction. Very large aspect ratios (l/d) are possible; for example, lasers can perforate very small diameter (0.2-0.5 mm) holes to extremely high depths. Drilling of hard materials is also possible. One of the first laser drilling applications was laser drilling of diamond dies for drawing thin wire. We note that ordinary drilling of ceramic materials, very brittle when burned, has to be performed

prior to firing. Naturally, firing changes the size of drilled items and the dimension and position of the holes may change. Laser drilling is carried out after burning and is free from size variation problems. Further advantage comes from the possibility of drilling holes in close vicinity with each other and near the item edge.

Microelectronic applications. Lasers find ever wider application in processing microelectronic components, e.g., laser welding is used in the fabrication of microcircuit components, material evaporation by a focused laser output is used for the fabrication of electronic circuit elements and for fine trimming of components of integrated circuits (resistor trimming). In the component manufacturing, a focused laser beam trims off by evaporation a portion of metal or semiconductor film deposited on the dielectric substrate. An accurately controlled laser beam may prepare a complete thin-film circuit including all its resistors and capacitors. The laser may also be utilized for the preparation of photo-masks employed in the light exposure of photosensitive substrates of integrated circuits to produce then a certain pattern by etching.

By way of example of a system suitable for such applications we point to a pulsed Nd:YAG laser capable of 1 kW of peak power in 200-ns pulses with a 400-Hz repetition rate. The beam of this laser is focused in a 10- μm diameter spot. When the beam travels at 2 mm/s it evaporates a narrow strip of metal film about 1 μm thick deposited on a sapphire substrate. The strips on the substrate appear to be totally denuded of the metal.

4.2 Lasers in Medicine

Already first lasers have been studied for their effects on biological materials. A great deal of experimental evidence is now acquired on laser use in medicine. Commercial laser systems find their way in many clinics.

Laser surgery. The focused laser beam proved to be a unique scalpel, capable of bloodless surgery, since the beam not only cuts but also "welds" blood vessels being cut. Apart from that, this surgery is outstanding in its high sterility, as no contact of tissues with surgical tool takes place. And, last but not least, laser surgery is painless because operat-

ions are very fast and there is not enough time for the patient to respond to the incision and sense pain.

It is now common for laser surgical units to fix the laser scalpel in a facility which provides the possibility of certain movements of the beam and its rotation. Fibre optics (see Sec. 4.6) has put the laser scalpel into the surgeon's hand: flexible optic fibres lead the beam to the radiator in the hand. The radiator contains a lens system for beam focusing.

Laser radiation is efficient in haemorrhage control due to cauterizing action of the laser beam on the blood vessels. Therefore, lasers are used for reduction of hematic losses, which is especially important for patients with poor blood coagulation. Laser surgery became a routine procedure in the treatment of liver and lungs, and for elimination of moles and tumors developing on the skin tissues. Most common sources for these applications are CO_2 and argon lasers.

A separate medical field for laser surgery is ophthalmology where the laser (usually Ar^+) has already been in use for several years to treat the detachment of the retina. The beam is focused on a certain point of the retina after it has passed through the lens of the eye and the vitreous chamber without being absorbed in them. The green beam of the laser is strongly absorbed by the red blood cells of the retina and the consequent thermal effect leads to re-attachment of the retina. The operation is carried out by a 0.01-s pulse and, being very short, is virtually painless. Of other illnesses treated by the focused laser beam, mention should be made of cataract, varied tumors, and glaucoma. In the last case the laser pulse is used to destroy plugs in blood vessels feeding the eye. Most popular ophthalmological systems involve also neodymium and ruby lasers.

Lasers are now finding increasing use in therapy. The He-Ne laser has produced curing effect on trophic ulcers, poorly healing wounds, and bone fractures. Relatively rapid healing effect has been observed for all these cases after a few radiative treatments.

Stomatology is another field in medicine where the laser has also been found useful. It has been proved capable of destroying selectively those tissues of the tooth affected by caries, that is, the laser can replace dental drills. In this

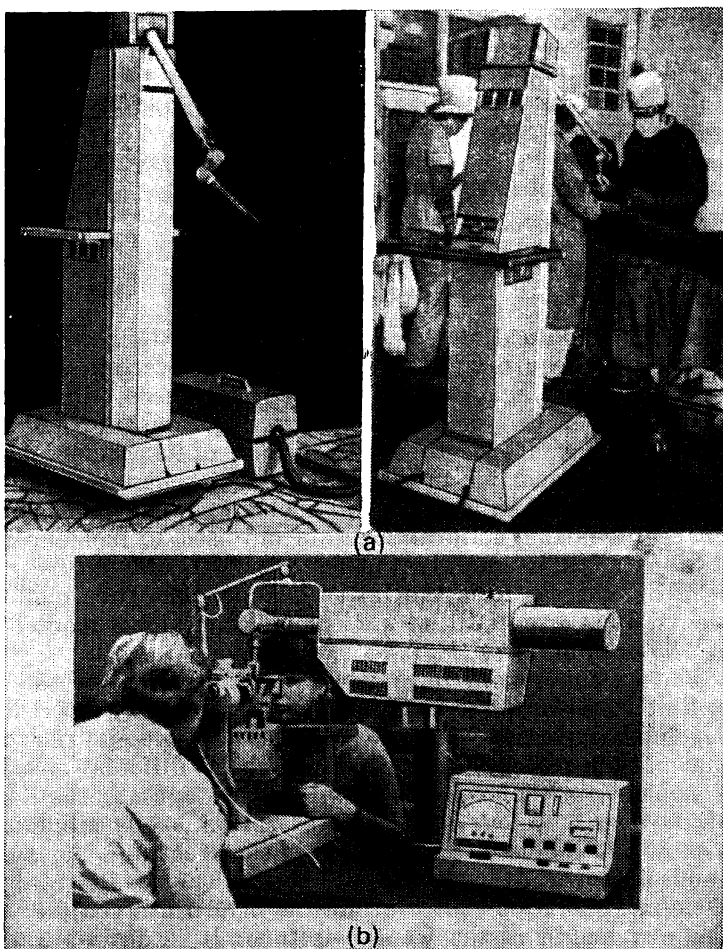


Fig. 4.4 (a) Two views of the laser surgery unit Skalpel-1, (b) ophthalmologic surgery with the Yatagan-2 facility

function it has demonstrated a much higher performance and operated without pain.

Figure 4.4a shows, as an example, a unit for laser surgery, Skalpel-1, developed at the Elektronika Central Research Institute, Moscow, for soft tissue incisions. It incorporates

a 10-W CO₂ laser. The unit is widely used for plastic surgery, including burns treatment, gynaecologic operations, and treatment of festering wounds.

Figure 4.4b shows the process of an ophthalmologic operation with the Jatagan-2 facility (developed by the same establishment). The facility is built around a *Q*-switched ruby laser. It is designed for the microsurgery of the front tissues of the eye.

4.3 Isotope Separation

Numerous applications in the industry, medicine, and research field require substances enriched in a certain isotope (say deuterium against hydrogen). These needs stimulated techniques of isotope separation, which are supposed to separate the wanted isotope with the aim of its accumulation or a higher proportion in the final product. These techniques are of immense importance for nuclear power engineering. The point is that natural uranium ore used to fuel nuclear stations contains mainly the isotope ²³⁸U and only 0.7% of ²³⁵U, whereas it is the latter isotope that fires nuclear plants. It is essential that nuclear fuel contained about 3% of 235-uranium.

The most promising in the family of separation techniques is that based on laser excitation or dissociation, feverishly developed in recent years. Laser separation exploits the fact that various isotopes of an element exhibit different absorption bands in their spectra, i.e., each isotope absorbs light of its own wavelength. These absorption bands are fairly narrow and lie close to each other in the spectrum. To excite one isotope without "touching" the other, one has to irradiate their mixture by a source of narrow bandwidth centered on the wavelength of the wanted isotope. It is desirable also that this source be tunable so that the radiation may be tuned to the desired wavelength. This opportunity is offered by tunable lasers.

Let us assume that we have a mixture of two isotopes one of which is desired to be separated. To achieve the goal we irradiate the mixture by a powerful output of a laser operating at the absorption wavelength of the wanted isotope. The excited atoms of this isotope are raised to the upper level, while the other isotope remains in the ground state. Now we

apply another radiation to the mixture and such that will be absorbed by the excited atoms only to ionize them. As a result, we obtain the desired isotope in the form of ions easily separable by applying a dc electric field. This is essentially the idea of one of the laser separation techniques, called two-step photo-ionization.

Another approach uses selective dissociation of molecular compound (such as uranium hexafluoride in uranium isotope

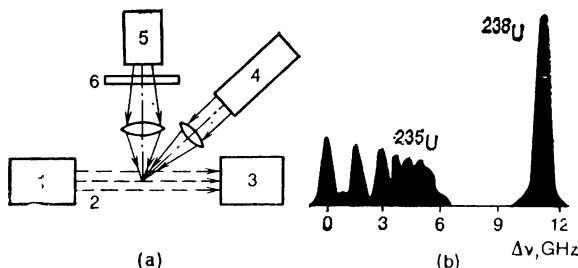


Fig. 4.5 (a) Schematic of a uranium isotope separation facility, (b) absorption spectra of the uranium isotopes: 1 furnace, 2 uranium atoms beam, 3 mass spectrometer, 4 dye laser, 5 mercury lamp, 6 bandpass filter

separation) having first been selectively pumped to an excited (vibrational) level. This compound is subsequently dissociated as a result of further optical pumping. The dissociated atoms enter then in a chemical reaction with purposefully introduced molecules so that the product contains only the wanted isotope. This product is separated for further treatment. Still another technique is such that the atoms or molecules containing the desired isotope enter in certain chemical reactions upon laser excitation to form an easily separable compound.

The two-step photo-ionization technique appears to hold the greatest promise for uranium isotope separation. The configuration of a system using this principle is shown in Fig. 4.5a. The beam of uranium atoms emitted from a heated uranium-rhenium alloy is pumped by a continuous dye laser tuned to a desired wavelength ($\lambda = 0.59154 \mu\text{m}$) and then is additionally excited by ultraviolet radiation from a mercury lamp ($\lambda = 0.21$ to $0.31 \mu\text{m}$) to be ionized. The beam of the ^{235}U ions is separated from ^{238}U in a mass spectrometer.

Fig. 4.5b shows the absorption bands for both uranium isotopes. The frequency spacing between the bands is seen to be more than 5 GHz. Because the dye laser has a bandwidth of only 0.1 GHz, it readily tunes for pumping the wanted isotope alone.

4.4 Holography

Holography is a revolutionary technique which allows three-dimensional (i.e., complete) pictures to be taken of a given object or scene. The word is derived from the Greek words "holos" (complete) and "graphos" (writing). The technique became a practical proposition and really demonstrated its potential only after the invention of the laser. In this section we shall look at the principles and uses of holography.

Suppose we wish to obtain an image of an object on a screen. Then we must illuminate the object so that the reflected light entered the screen. Moreover, the reflection is to be such that the rays reflected from different points on the object surface come to different points on the screen; in other words, the travel of rays from the object to the screen must be "ordered" to produce a certain pattern. This is achieved normally by lens systems. The result is the familiar photographic method of imagery. The invention of laser brought about a qualitatively new method of imagery without lens systems—optical holography.

The principle of holography. We place an object illuminated by a coherent source of light in front of a photodetector (a screen covered with a photosensitive layer, most commonly a photographic emulsion, and therefore capable of permanent hold of images). The light wave incident on the object is a component of a single monochromatic beam of light split into two components, one of which is directed toward the object while the other to the recording medium. The component that is incident on the object is scattered by it, and this scattered radiation, now called the *object, or signal, wave*, impinges on the recording medium of the photodetector. The wave that proceeds directly to the recording medium is called the *reference wave*. In Fig. 4.6a it arrives at the photodetector at an angle α . Since the object and reference waves originate from the same source they are mutually coherent and form a stable interference pattern when they meet at the recording medium. The

detailed record of this interference pattern constitutes the *hologram*.

Notice that in this arrangement we have made no attempts to control the rays in the object beam with some optical elements, such as an aperture or a system of lenses. It is not surprising therefore that the developed photographic plate with a holographic record looks like an ordinary

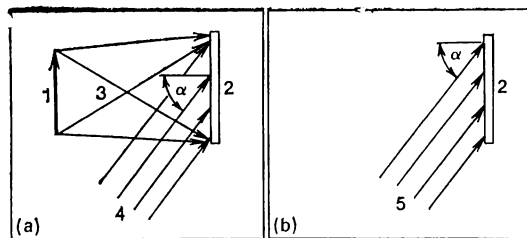


Fig. 4.6 Principle of holography. (a) production of the hologram, (b) reconstruction from the hologram: 1 object, 2 hologram, 3 object (signal) wave, 4 reference wave, 5 reconstructing wave

exposed negative—even the sharpest eye cannot reveal anything resembling the object in this photoplate. Nevertheless this exposed negative, the hologram, contains a complete record of the original object. It is coded in the fine and complex pattern of interference fringes, produced by the two waves, object and reference. This pattern is very fine indeed, the spacings between its interference fringes may be as small as 0.001 mm.

Now suppose that the developed plate is returned to the position it occupied while being exposed and the object under examination is removed (Fig. 4.6b). The reference beam now interacts with the interference fringes on the photographic plate and reproduces beyond the plate a diffracted beam which is exactly the same as that originally scattered by the object in Fig. 4.6a. An observer looking at the plate from the right side on the page will therefore see the object beyond the plate as if it were still there. This process is called the *reconstruction of the primary object wave from the hologram*. The beam that illuminates the hologram for reconstruction must be similar to the reference beam, but its wavelength may be different. This will affect the dimension of the three-dimensional image reconstructed from this hologram.

Thus, the holographic method of optical imagery is a two-step method. In the first step, the hologram of the object is recorded, whereas in the second step the image is reconstructed from this hologram. The hologram recording is based on interference of coherent waves, and the reconstruction relies on diffraction of waves. We note that the "ordering" of light rays necessary for the reconstruction is provided automatically by the *reconstructing (illuminating) wave*.

Holographic imagery requires highly coherent radiation. If L is the maximum difference of pathlengths that the two

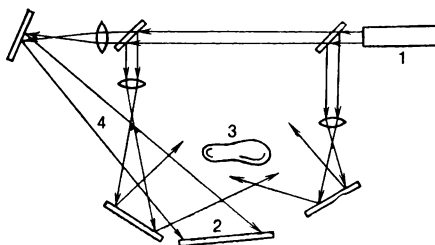


Fig. 4.7 An optical arrangement for hologram recording. 1 laser, 2 hologram, 3 object, 4 reference beam

components of a light beam gain proceeding toward the hologram as the object and reference waves, then the time of coherence (introduced in Sec. 1.2) must be such that

$$c\tau \gg L \quad (4.1)$$

Gas discharge lasers are more widely used for holographic applications as they lase in the visible portion of the spectrum (the He-Ne laser, for example).

The fine structure of interference fringes on the hologram requires photographic materials with a high spatial resolution. This is defined as the largest number of parallel lines written within a unit length—usually within a millimetre—that the examined material is able to resolve. The spatial resolution of the photographic materials used for hologram recording must be at least 1000 lines per millimetre. This requirement is met by certain photomaterials offering resolutions of about $2 \times 10^3 \text{ mm}^{-1}$.

We note that the photographic materials relate to "irreversible" recording media, since once recorded on a photo-

plate a hologram cannot be erased to record another hologram. There exist also "reversible" recording media, for example, photochromic materials, such as specially doped glasses, or organic polymers capable of altering their colour or transmittance when irradiated by certain wavelengths.

To conclude, we refer to Fig. 4.7 which shows an optical arrangement for hologram recording. A single laser is here

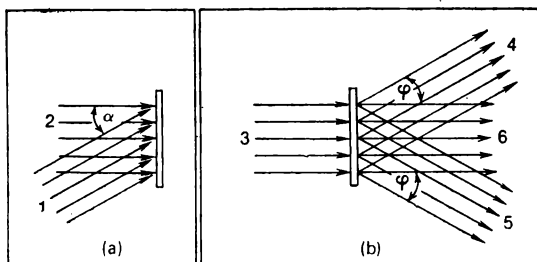


Fig. 4.8 (a) Interference of light waves in hologram recording, **(b)** diffraction of light in hologram reconstruction: 1 object beam, 2 reference beam, 3 reconstructing wave, 4 and 5 diffracted beams, 6 transmitted beam

the source of all the beams, multiplied by beamsplitters and mirrors. We have mentioned above that lenses are not necessary for holographic recording and reconstruction. This arrangement uses lenses to expand the beams only, that is, the lenses perform secondary roles.

The principal identity. Let two monochromatic mutually coherent plane waves making an angle α with each other (Fig. 4.8a) impinge on a photographic plate in recording a hologram. These waves will interfere to bring about an interference pattern consisting of a set of parallel strips spaced from each other by the distance

$$d = \lambda / \sin \alpha \quad (4.2)$$

where λ is the radiation wavelength, and α is the angle of interference.

When in the reconstruction of the object wave from this hologram it is illuminated by wave 3 in Fig. 4.8b, this wave is diffracted to give rise to two diffracted waves making an angle φ with the direction of the illuminating wave. We

will call it the diffraction angle. It is defined as

$$d \sin \varphi = \lambda \quad (4.3)$$

where d is the period of the diffraction grating, i.e., the same d that enters equation (4.2). Comparing (4.3) and (4.2) yields

$$\varphi = \alpha \quad (4.4)$$

This identity is of principal consequence—*the angle of diffraction equals the angle of interference*.

In the general case of nonplane wave, the angle of interference varies over the hologram from one point to another.

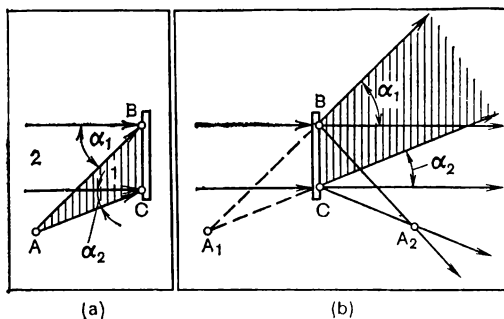


Fig. 4.9 Holography of a point object. (a) recording of the hologram, (b) reconstruction of the object wave

The angle of diffraction varies accordingly. It is essential, however, that at each point of the hologram the angle of diffraction equals the angle of interference.

Holography of the point object. Fig. 4.9a shows the scheme of hologram recording for a point object. The nomenclature is the same as in Fig. 4.8. The angles of interference for rays AB and AC are α_1 and α_2 respectively. The illumination scheme in hologram reconstruction is shown in Fig. 4.9b. The diffraction at point B will be at the angle α_1 , whereas in point C at the angle α_2 , in agreement with (4.4). This principle leads to the geometry of Fig. 4.9b which produces two images of the object—one is the *primary or virtual image* A_1 , the other is the *conjugate or real image* A_2 .

One principle implication is to be emphasized. The object beam scattered from A in Fig. 4.9a is shadowed. As can be

readily seen, one of the beams in Fig. 4.9b is this very beam. No object is present at A when the object beam is reconstructed, but one of the evolving light beams is identical with the beam that would be reflected by the object. In other words, when we reproduce the image we do it by reconstructing the object wave.

Holography of three-dimensional objects. The reconstruction of the object wave from a hologram is obviously independent of whether the object recorded has been a point or three-dimensional one. If a 3-D object is recorded, then upon reconstruction the viewer will see not a plane, photograph-like image of the object, but rather a realistic 3-D image indiscernible from the object so as this could be seen during the hologram recording. If the viewer shifts aside, other objects hidden behind the first one will become visible and new side features emerge. In other words, the viewer will see an absolutely real 3-D scene.

It will be noted that in this arrangement it is the primary, or virtual image, that exhibits the features of the real object. The conjugated, or real, image will appear inverted in depth, i.e., reversed front to back with the features being farther from the viewer in the holographed object appearing closer. This image is called *pseudoscopic*. The situation will reverse in another reconstruction arrangement with the illuminating wave travelling in the direction opposite to that of the reference wave (the hologram is illuminated from the back side), then the real image will have actual appearance, while the virtual image becomes pseudoscopic.

A few words are in order on the types of holograms. We have seen in Fig. 4.8b that when the hologram is illuminated with a beam similar to the original reference wave the transmitted wave divides into three separate components, one of which exactly duplicates the original object wave. If the two interfering beams are travelling in substantially the same direction, the recording of the interference pattern is said to be a *Gabor hologram* or an *in-line hologram*. If the two interfering beams arrive at the recording medium from substantially different directions, the recording produces a *Leith-Upatnieks* or *off-axis hologram*. If the two interfering beams are travelling in essentially opposite directions the recorded hologram is referred to as *reflection hologram* first invented by Y. N. Denisyuk, a Soviet researcher.

Holograms can be classed by the way they diffract light. In an *amplitude hologram*, the varying irradiance distribution of the interference pattern is recorded as a density variation of the recording medium. In this type of hologram, the illuminating wave is always partially absorbed, that is amplitude modulated. In a *phase hologram*, a phase modulation is imposed on the illuminating beam, which in turn results in diffraction of the light. Phase modulation occurs when the optical path (thickness \times index) varies with position.

Any of these hologram types may be recorded as either a *thick* or a *thin hologram*. A thin hologram is one for which the thickness of the recording medium is thin compared to the spacing between the recorded interference fringes. A *thick* or *volume hologram* is one in which the thickness of the recording medium is of the order of or greater than the spacing of the recorded fringes.

Electromagnetic radiation is most commonly used for holography, although acoustic radiation can be used. The most common e.m. radiation employed is light, but holograms have also been recorded successfully with electron beams, x-rays, and microwaves.

To summarize, we emphasize again that the hologram serves to reconstruct not just the image of an object (a three-dimensional one, remember) but rather a real light wave containing all the information originally carried in the light wave reflected from the object proper. It is this property of holography that justifies the meaning of the Greek words which made up the term.

Some history of holography. The idea of holography was proposed as far back as 1920 by Polish physicist M. Wolfke who demonstrated that the diffraction patterns that occur when x-radiation penetrates through the crystal may be used to reconstruct the image of the crystal lattice. Unfortunately, this work failed to find due support in physical quarters at that time.

The principles of holography were reformulated, and in a more thoroughful way indeed, in 1948 by British scientist Dennis Gabor, unaware of the Wolfke work. Gabor made the fundamental contribution to the development of holography and coined the term itself. He came to the method by trying to solve a rather ordinary problem—it was proposed then

as a means of improving the resolution of electron microscopes.

The spurious development of holography began with the appearance of the laser. In 1961, two University of Michigan research workers, E. N. Leith and J. Upatnieks, developed and used the two-beam method of holography relied on two light beams, the object and reference beams. It is this method that has been employed in our considerations of holography.

In 1962, Y. N. Denisyuk, a Soviet researcher, came up with a holographic technique based on exploiting thick photographic films. The thickness of such emulsions is many times the light wavelength. These holograms are remarkable in that they are reconstructed not necessarily by a laser. The reconstruction may be effected by sunlight or a collimated projector beam.

4.5 Information Related Applications

Much progress have recently been made in a new field of laser application concerning transmission, reception, processing, and storing of information. The systems that deal with this work are known as information systems, and the field is referred to as optoelectronics.

Coherent optical radiation in information systems. The transmission system consisting of a transmitter and a receiver conveys information by means of an e.m. wave, known as the carrier wave, being modulated by the oscillations of the information proper. The modulation depth, i.e. the difference between the carrier amplitude and that of the resultant waveform, depends on the nature of the transmitted information. For example, to transmit a human voice, the carrier is modulated with the sounds of speech occupying the frequency range from 16 to 10^3 Hz, and music expands this range up to 2×10^4 Hz. A much wider frequency interval is required for the transmission of TV signals, about 10^7 Hz.

Because this information modulates the carrier, its frequency must be appreciably lower than the frequency of the carrier wave. Or conversely, the higher the carrier frequency, the wider frequency range can be modulated on it. Light with its high frequency offers unprecedented expansion of frequency band to be transmitted. Available sources of

coherent radiation in the form of lasers operating in the optical range lift the upper boundary of the frequency band to 10^{12} Hz. Because one telephone conversation occupies 10^3 Hz, allocating each line, such a frequency "slot" by means of modulation techniques results in 10^9 simultaneous connections. This possibility of light beam to handle extremely wide modulation bandwidths indicates the immense information capacity of laser trunk lines. Currently operating light modulators are capable of handling bandwidths up to 10^{10} Hz.

The laser holds promise not only for transmission systems but also for data processing. In this connection we recall that in the radio frequency band, first the transmitter modulates a high frequency carrier which is then transformed by an aerial in a radiated signal. The modulated waveform varies in time only. A principally new possibility is realized in the optical range, where the radiated wave itself is modulated. It is remarkable that here the waveform is characterized not only by temporal but also by spatial variables so that the spatial modulation of the light wave results, a specifically optical concept.

Whereas in temporal modulation the characteristics of the radiated waveform vary in time, in spatial modulation the characteristics of the radiation vary over the plane orthogonal to the direction of wave propagation. This variation is described by a function $s(x, y)$ in the coordinates of the plane (x, y) , referred to as the spatial signal. It is specified within the area confined by the light beam aperture (cross section).

The spatial signal is first written in the material of a transparency whose optical characteristics can be controlled making them vary over its area according to the desired law. Assume that this transparency is a plate whose transmittance varies in accordance with $s(x, y)$. Then a light wave travelling through this plane will be spatially modulated, i.e., its field intensity will vary over the beam aperture as $s(x, y)$. Now assume that the transmissivity of the transparency is the same over its area but its refractive index varies as $s(x, y)$. Then the pathlength of the rays traversing the transparency in different points will vary by the same law. Consequently, a coherent light wave passing through this transparency will experience various phase shifts in

various points of the beam aperture, and these shifts will vary by the law $s(x,y)$. In both these situations the transparency plays the role of the spatial light modulator.

When the laser light traverses or, in some arrangements, is reflected from the spatial modulator, the beam becomes a carrier of the spatial signal written in the material of the modulator (Fig. 4.10). Various types of spatial light modulation in use, such as amplitude, phase, or polarization modulation, differ from each other and are named by the property of light wave they exploit to carry the spatial signal. Time-variable spatial modulation is realized through the control of the optical characteristics of the transparency. Among the media used to prepare controllable transparencies are electrooptic and photochromic materials, magnetic films, thermoplasts, liquid crystals, and the like.

The liquid crystal transparency, for example, changes its transmittance in a reversible way as a function of an applied electric field. Liquid crystals are organic dielectrics which in a certain temperature interval exhibit properties intermediate between that of crystal and liquid. The area of such a transparency is composed of individual cells each separately controlled by an electric field. Under the influence of an applied electric field turbulent currents occur inside the cell and its transmittance sharply reduces. A $10 \mu\text{m}$ thick layer of liquid crystal biased by 10 V reduces the intensity of transmitted light more than ten times.

Written into characteristics of the laser beam, the signal arrives at the optical system for processing. The methods of optical data processing are gaining considerable momentum. This fact is associated with a number of advantages offered for data processing in optic field. Whereas electric signals are unidimensional—they are functions of only one variable, time—optical spatial signals are two-dimensional, and even three-dimensional, when time-variable. This is highly beneficial for multidimensional information processing, such as image analysis, and reading of plots and

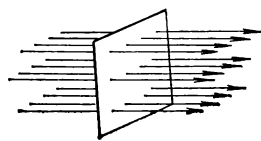


Fig. 4.10 Spatial modulator impresses a signal on a laser beam

drawings, and for simultaneous parallel (multichannel) data processing.

The large information capacity of optical signals is worth separate mentioning. It is not only due to the high carrier frequency but also due to the spatial nature of such signals. For example, 1 cm² of a spatial signal can carry up to 10⁸ bits of information. Moreover, optical signals can be processed, i.e., subjected to various mathematical operations, in a rather simple optical arrangements, composed of optic elements without complicated electronics. And, last but not least, the optical systems may involve holographic techniques.

Applications of holography. The use of holography in information systems appears to be highly promising. Some most advantageous applications will be taken up below.

Data storing systems. In the previous section we have seen that in holographic recording the information about each point of the object surface is recorded over each area of the hologram. Therefore, removing a part of the hologram will not cause part of the object in the image to disappear. Experience in this field indicates that up to nine tenth of a hologram may be removed or spoiled without much harm to the image, except for a somewhat degraded resolution (contrast) of the image.

This behaviour is not surprising, in fact the hologram serves to reconstruct not just an image but rather the real object wave. The available area of the hologram determines the area of the reconstructed wavefront, i.e., a reduction in the hologram area reduces the size of the wavefront.

Hence, hologram recording is a reliable way of storing information. In addition, the same hologram may carry a number of individual data packages separately written onto it for separate readout. To produce such a record, different data frames should be holographed, each at different angle of incidence for the reference wave. The orientation of the hologram in the reference beam may be altered to achieve this goal. Then, to reconstruct the desired frame one needs to set the hologram in the appropriate orientation with respect to the illuminating beam. According to estimates, a hundred square centimetres of a hologram may accommodate as much information as a volume of *Britanica encyclopaedia*, and in a perfectly readable form.

This outstanding capacity of the hologram backed by the reliability of the store makes it an attractive proposition for data storage facilities. One of the schemes of holographic memory will be discussed later.

Associative information search. Associative search is one of the underlying principles of the human memory. We often recall a scene by a detail of it, or by an associative feature which helps the memory recover the entire scene or object. To state this differently, associative search is the reconstruction of the whole by a single feature. Holography is just a suitable method to realize associative information search technically.

Suppose that in recording a hologram the reference wave is absent. Can such a hologram be used to reconstruct the image of the object? It may surprise you, but it can. This hologram may be treated as an interference pattern produced by the interference of waves reflected by different parts of the object. We may take one wave reflected, say, from the tail of the bird in Fig. 4.11 to be the reference wave, and the wave reflected from the other features of the object to form collectively the object wave. In reconstructing, it will suffice then to illuminate this hologram by the wave reflected from the selected detail, in other words it will suffice to produce this detail. This procedure gives a clue to associative search. Indeed, if this hologram is used to record a number of various objects or scenes, only that will be reconstructed to which the feature produced in the reconstruction relates.

Thus, the holographic techniques are highly suitable for the realization of both random access and associative memory systems.

Information coding. The hologram stores information in the form of an interference pattern, i.e. in an encoded form, and can be decoded only by a coherent light wave with the same wavefront as that of the reference wave. Accordingly, the wavefront of the reference wave is the key enabling the reconstruction of the hologram. To achieve a special encod-

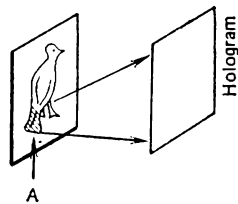


Fig. 4.11 Associative reconstruction of a hologram by producing a specific feature of the object

ing, the reference wave is passed through an encoding mask to gain a special wavefront. Without this mask, even the most skillful decoders will be unable to read (decode) this hologram.

Pattern recognition. How can a wanted letter be recognized in a text? a non-standard product in a sequence of similar items? an expected signal among those arriving at the input? All these problems are solved by a branch of science known as pattern recognition theory. Holography is one of the promising means for practically solving such problems.

We look at the pattern recognition procedure handled by holographic means by taking a letter-and-text example. Let

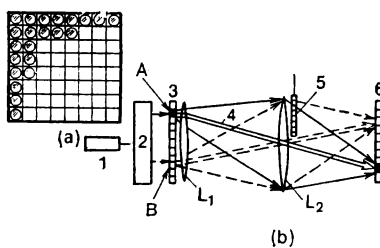


Fig. 4.12 (a) Holographic matrix, (b) schematic diagram of a holographic memory system: 1 laser, 2 digital light deflector, 3 auxiliary holographic matrix, 4 nondiffracted beam, 5 transparency imposing spatial modulation (page composer), 6 holographic matrix store

the letter to be recognized in the text be "A". A hologram is recorded of the size of letter A in the given text. The reference wave is the one reflected from an A, while the object wave is the one emitted by a bright point source of light. A scanning device moves the hologram over the lines in the text. As soon as the hologram meets an A in the text, the detector records a bright flash which is an image of the point source reconstructed by the wave reflected from the A.

A holographic memory system. The key element of such a memory system is a holographic matrix medium. This is an array of small holograms of only 2 to 5 mm in diameter (Fig. 4.12a). Each of these holograms may store a considerable massive of data, from 10^3 to 10^4 bits. The interference pattern of the hologram is produced by a reference wave and a wave modulated by a certain spatial signal. For associ-

native memory, this interference pattern is the result of the interference of the object wave and the wave modulated by the signal of an interrogation feature (associative feature).

The optical arrangement of this holographic memory is shown in Fig. 4.12b. The electrically governed deflector directs the laser beam into the particular hologram in the auxiliary holographic matrix. Each of these holograms, when illuminated, reconstructs a diverging light wave. The light beam transmitted by the hologram without dif-

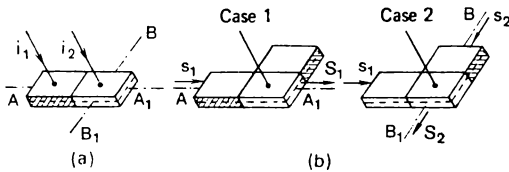


Fig. 4.13 (a) Double laser diode, **(b)** NOT logic exercised by optically coupled injection lasers

fraction is deflected by the lens L_1 , traverses without deflection the central area of the lens L_2 (placed in the focal plane of L_1) and impinges on one of the holograms in the memory matrix. Here it interferes with the wave which has been divergent and becomes convergent after L_2 . The latter wave on its path to the holographic matrix has passed through the transparency, called page composer, and has been converted into a carrier of the respective spatial signal.

The solid-line arrows in the figure correspond to the case when the deflector directs the laser beam in position A , and the dashed arrows show the situation with the beam in position B . By making the deflector alter the initial position of the beam and changing simultaneously the spatial signal written in the transparency, one may gradually fill with the desired information all the cells of the matrix memory.

Optically coupled injection lasers. These lasers are fabricated in a single chip with a common $p-n$ junction but with separate pumping circuits. Fig. 4.13a illustrates schematically two optically coupled injection lasers, often called dual laser or strip diode. Here i_1 and i_2 designate the pumping currents for the left and right diodes respectively, the dashed line shows the common $p-n$ junction, and the shadowed face shows the diode end which cannot serve as a resonator

mirror. This diode can lase in the AA_1 direction, and the right component can also lase in the BB_1 direction. Simultaneous lasing in both directions is impossible as a lasing action in one direction suppresses oscillations in the other.

Optically coupled injection lasers may be used in the function of memory cells (switching time down to 10^{-9} s). As an example of such an application, Fig. 4.13b shows a triple diode performing as a NOT logic element. It is made up of a common active portion, where pumping current is directed, and two passive components. Two switching situations are possible. *Case 1*: an optical signal s_1 is applied to the input A to initiate lasing action in the AA_1 direction and produce an output S_1 at the output A_1 . In this case the component transmits information from A to A_1 . *Case 2*: simultaneously with the input s_1 at A another signal s_2 is impressed on input B . The emission at A_1 vanishes and a signal S_2 appears at the output B_1 . The B input is therefore called disabling, because when this input receives a control signal the data transmission from A to A_1 through the NOT device is blocked.

4.6 Optical Communications

We have already emphasized the large information capacity of optical communications channels. It will be recalled that an increase in frequency of the carrier wave expands the frequency bandwidth available for transmission. Additionally, higher carrier frequencies offer better directivity for communications, higher powers being concentrated in the signal, hence provide for higher efficiencies of communications systems. Finally, the use of light beams for transmission purposes warrants the message best of all from interception and makes it immune to distortions by interference.

The optical communication systems using lasers as light sources divide naturally into two groups: those where signals are transmitted through free (unguided) space, and those where they are carried by light guides.

Communications through open space. Open space in which optical signals propagate may be either in space beyond the Earth or in the Earth's atmosphere and water. Schematically this transmission line is illustrated in Fig. 4.14a. The laser beam with a modulation impressed on it in the modulator

becomes an optical signal carrying certain information. The targeting (beaming) device sends this signal toward the receiver through a medium in which the signal is to traverse a certain optical path. A special collector acts as the aerial for the signal. It recovers the expected signal from the multitude of diverse signals arriving at the aerial and focuses the received emission on the receiver input.

In open space, laser communications can be established between satellites, satellites and aircraft, and satellites and stations on the ground. Unguided communications can

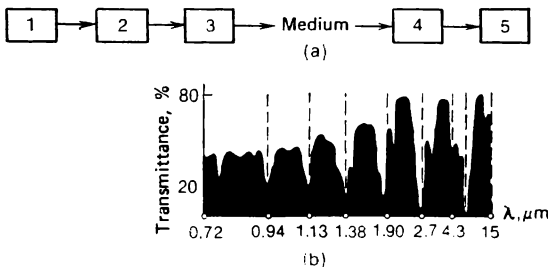


Fig. 4.14 (a) Components of a laser communication line, (b) atmospheric transmittance as a function of wavelength: 1 laser, 2 modulator, 3 directional beaming facility, 4 receiving "aerial" (telescope), 5 optical signal receiver

exist also between stations on the Earth's surface and under water. For communications in space and long-distance transmissions on Earth (within kilometres and tens of kilometres) wide use is made of CO₂ and Nd:YAG lasers. For short distance ground communications, GaAs injection lasers are frequently employed.

When optical radiation travels through a medium it is scattered or absorbed by the species of the medium, i.e. attenuated, and its wavefront is distorted by the scattering and eddies in the medium. To cope with attenuation, the wavelength of the transmitter is selected such that provides sufficiently high transmissivity in the particular medium. For the Earth's atmosphere, the transmittance of the surface layer as a function of wavelength is shown in Fig. 4.14b; wavelength is plotted in the logarithmic scale. The dashed lines separate the so-called atmospheric windows of higher transmittance. It will be seen that the emission of CO₂

lasers ($\lambda = 10.6 \mu\text{m}$) and Nd:YAG lasers ($\lambda = 1.06 \mu\text{m}$) is just within these windows.

To cope with wavefront distortions, the directivity of the radiation is increased, and transmissions are carried out in favorable weather conditions. All these measures, however, are able to extend the range of terrestrial communication links only as far as 20 km. The situation is expected to change

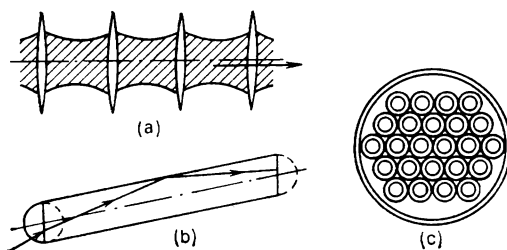


Fig. 4.15 Lens waveguide (a), dielectric fibre guide (b), and optical cable (c)

by the incorporation of adaptive optics techniques in laser communication systems, which are capable of appropriately correcting the radiation wavefront.

Optical waveguides. Fig. 4.15 shows two types of optical guides: (a) a lens waveguide, and (b) an optical fibre light guide. The light guides with optical fibres have found the widest use. Research in this field brought about a new scientific and engineering discipline called fibre optics.

Figure 4.15b shows the reflection of a light ray launched inside the fibre and incident on its surface from inside; this is the familiar phenomenon of total internal reflection. It is ensured in optical fibres technologically so that the radiation injected in a fibre is confined, as it were, inside it. The beam will experience multiple reflections from the fibre walls and propagate to its end following all the fibre bends.

Today optical fibres are finding increasing use for transmission at distances from a few metres to several kilometres. It is quite obvious that long optical fibres should exhibit very low light absorption. According to modern requirements, the attenuation of light power in optical fibres should

not exceed a few decibels per kilometre of fibre length (for the case of long fibres available nowdays). To provide for internal reflection these fibres are made of two types of glass with different refractive indices: one goes to make the core and the other of smaller index to make the cladding of the fibre. For example, a glass fibre with a core of germanium doped quartz glass exhibits an attenuation of only 0.7 dB/km at a wavelength of 1 μm .

Optical fibres may carry not only time-variable waveforms, but also spatial signals, i.e., images, two-dimensional (2-D) pictures. For this purpose fibres are stranded into cables. Fig. 4.15c shows the cross section of an optical-fibre cable containing a relatively small number of fibres. Practical cables may include as many as hundred thousand fibres. Each fibre has a cladding preventing its light energy from penetrating into the adjacent fibres of the cable. The principle of 2-D pattern transmission through an optical cable is rather simple. Light rays emitted, or reflected, by an element of the transmitted scene enter into the respective fibre of the cable, travel over all the length of the cable to produce this element at the output. Loosely speaking, the ray emitted by an element of the scene is captured by an optical fibre and is conveyed to an appropriate place. If at the output of the cable the relative arrangement of the fibres is kept the same as at the input, then the pattern launched into the cable at the input will appear at the output.

Optical fibre lines in computer systems. A very sensible place to errors in modern computers is their communication lines, carrying input and output signals, connecting the processor with memory units and other hardware facilities. These communications systems are complicated strands of many wires, called busses, which are sensitive to noise currents, and may be the place where interference enters to spoil the signal. It is this place where the setback intrinsic to all wire communication systems manifests itself—it is impossible to isolate input from output systems, and make the wires immune to a variety of pickups. Optical communication lines, on the other hand, are free from this disadvantage. Therefore, use of laser communication lines based on fibre optics is particularly attractive in modern computer communication lines and computer networks.

For better efficiency, computers are now connected into computer networks. To effect data flow in such networks it is essential that the communication between computers be rapid, directional, and multichannel. All these requirements may be satisfied by laser communications over optical cables.

4.7 Ranging and Measurement

Strong and weak points of the laser radar. Lasers gave birth to the optical radar. Similar to the ordinary microwave radar, the optical radar, also called rangefinder by militaries, has been designed to detect distant objects and retrieve information about these objects from the portion of radar signal reflected from these objects. High carrier frequencies, possibility of extremely narrow directivity of the radiation, operation in the range of nanosecond and picosecond pulses, all these features predetermine a number of advantages of optical radar systems over ordinary radars. Optical rangefinders afford more accurate ranging and velocity measurement. The high resolution of the method makes possible the determination of the size and shape of the object and its orientation.

For velocity measurements, laser rangefinders apply to the Doppler shift $\Delta v = 2vv/c$ in the signal frequency v due to the velocity component of the ranging object v colinear with the laser beam. Evidently, the higher the carrier frequency v , the greater the detected Doppler shift, and the accuracy of velocity evaluation.

In a range-Doppler system, the transmitter radiates a signal which typically is a pulse or a sequence of pulses. A portion of the signal reflected from an object is returned to the radar, which then becomes a receiver. By measuring the round-trip delay time, the range of the object is readily ascertained. The range resolution improves as the pulse is made shorter. On the other hand, the Doppler frequency resolution is $1/T$, the reciprocal of the pulse duration. Therefore, if the pulse is shortened to improve the range resolution, the Doppler resolution is degraded by a similar degree, so that the product of the two resolutions remains unchanged. As far as the other spatial coordinates of the object are concerned, i.e., its dimensions, shape and orientation, their

derivation is enabled by means of directivity as the key factor.

The optical rangefinders are also not free from disadvantages. First of all, the same high directivity of the beam hampers a straightforward detection of the object, the time of scanning over the monitored zone is rather long. Therefore, optical rangefinders are preferably exploited in parallel with the ordinary radar. The latter provides for a comparatively fast scanning and target detection, while the optical rangefinder derives the target parameters. Secondly, the laser wavefront is degraded and attenuated in the medium where it propagates, and one has to invoke adaptive optics methods to cope with this drawback.

Pulsed radar systems. These laser systems are nowadays in wide use in space and geodetic research. An example of such a system is the laser radar complex of the P. N. Lebedev Physical Institute, Moscow. It measures to a very high accuracy (within 1 m) the distance to the five reflectors placed on the Moon surface. This accuracy enables solving a number of unique problems of scientific and applicational significance. They include in particular the study of the Earth's poles motion and evaluation of their instantaneous coordinates accurate to within several tens of centimetres; the study of continental drift, and refinement of the Moon orbit and the peculiarities of its orbital motion.

The laser system of this complex is mounted on the Crimea observatory telescope. It is built around an electro-optically *Q*-switched ruby laser yielding giant pulses amplified in a ruby amplifier. Every three seconds the system produces a 2.5-J pulse of 10 ns duration and 10' divergence.

The development of space laser radar is one of the subjects of the international Interkosmos research programme. Under this programme, a new satellite tracking station was made operational in Cuba in 1977.

Another laser system deserving special mentioning concerns the radar for the mutual orientation and ranging of docking spacecraft. The radar is installed on one of the craft. It operates from a passively *Q*-switched CO₂ laser producing a pulse sequence at a pulse repetition rate of 30 μs. The beam is scanned with a certain location area.

Still another practically important class of devices includes laser altimetres. These devices enable accurate naviga-

tion of aircraft at low altitudes. A device of this class was used in the American space programme Appolo to map the Moon surface during Appolo missions.

CW laser rangers. Many applications such as geodetic, construction of large precision-sensitive structures, optical system alignment, and certain physical studies, call for the distances of tens of metres to several kilometres to be measured accurate to within millimetres and even fractions of a millimetre. These measurements are easily handled by laser rangers emitting in a continuous wave mode.

The laser of such a ranger produces continuous radiation whose intensity is modulated by a sinusoidal law with a frequency f . As a result, the instantaneous beam intensity varies along the beam propagation with the spatial period c/f . The radiation traverses the path to be measured, is reflected, goes back and enters the phase detector. The phase shift between the emitted and return beam incurred in this round trip is used to infer the measured distance.

By way of example, we note the Soviet-made geodetic ranger Kvarts operating on a helium-neon laser ($\lambda = 0.63 \mu\text{m}$) with the following performance data: radiation power, 2 mW; modulation frequency, 753.02 MHz; range, up to 1 km; accuracy, within 0.2 mm. Gallium arsenide injection lasers are a feasible alternative for He-Ne lasers in laser rangers.

Interferometric distance measurement. Modern engineering is ever more often in demand of diverse large-size items manufactured to extremely high accuracy. Such jobs naturally impose severe constraints on tool operation accuracy. As an example of such a job we point to milling tools with a carriage travel of 10 m used for spar milling in aircraft construction. These situations call for distance measurements from a metre to several tens of metres accurate to within 10 μm . Measurements of this type can be ensured by one of the laser interferometric techniques with a frequency-stabilized He-Ne laser operating in the central longitudinal mode. This technique controls tool motions, automatically compensating for the errors due to wear, facilitates marking-off of points of engagement for a cutting tool on the surface to be machined, precisely aligns fixtures in aircraft engine manufacturing, and facilitates a number of similar jobs.

Figure 4.16a shows, as an example, an optical arrangement which can be used to measure workpiece travel in machining. The laser beam is divided by a beam splitter into a *measurement beam* and a *reference beam*. The reference beam is reflected by a fixed mirror while the measurement beam is reflected by a retro-reflector fixed to the object being measured. The two reflected beams are then recombined so as to interfere, and their combined amplitude is measured

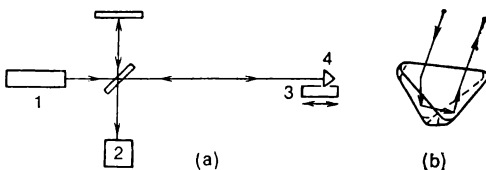


Fig. 4.16 (a) Measuring distance by laser interferometry, **(b)** corner retro-reflector: 1 laser, 2 photodetector, 3 moving workpiece, 4 cube corner reflector fixed to the work

by a detector. When the position of the object is changed along the beam direction by $\lambda/2$, where λ is the laser wavelength, the interference signal will go from a maximum through a minimum and back to a maximum again. An appropriate electronic fringe counting device can therefore give information on the displacement of the object.

The reflector fixed to the moving object is the so-called cube corner reflector. The outstanding feature of this device is that it reflects the incident light beam exactly in the direction of incidence, and is capable of back reflecting in a wide range of incidence angles. It is essentially a truncated triangular prism where an incident light ray is twice internally reflected and redirected as shown in Fig. 4.16b. It will be noted that the retro-reflectors placed on the Moon surface and used in the laser ranging experiments, mentioned earlier, also were corner retro-reflectors.

Flow velocity measurements. The high degree of monochromaticity makes it possible to use lasers for velocity measurements. Consider a two beam flow velocity measurement technique schematized in Fig. 4.17a. The laser beam is split into two beams converging at an angle α . The measurement system is arranged so that these beams meet each other at a location in the flow where velocity is to be measur-

ed. The interfering beams produce a sequence of interference fringes distanced

$$D = (\lambda/2) \sin(\alpha/2) \quad (4.5)$$

apart, where λ is the laser wavelength in the liquid.

Let a liquid parcel cross these interference fringes. The light scattered by the parcel and detected by a photodetector, rises in intensity when the parcel moves through an

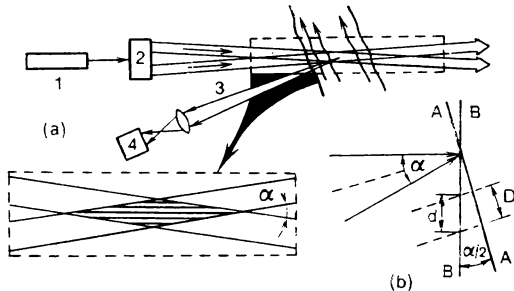


Fig. 4.17 (a) Schematic of a dual-beam mode arrangement for laser fluid velocimetry, (b) beam geometry; the dashed insert shows the interference pattern generated by the superposition of the two beams at a small angle α . 1 laser, 2 beam splitter, 3 scattered light, 4 detector

illuminated stripe and drops when in a dark stripe. As a result the photodetector records an electric signal modulated with the frequency

$$f = 2v \sin(\alpha/2)/\lambda \quad (4.6)$$

where v is the velocity component in the direction perpendicular to the fringes. This frequency is measured to infer the velocity component of the flow.

When the measuring system is installed near the flow (within a few tens of centimetres), they depend for their measurements on helium-neon lasers with output of about 10 mW. When velocity measurements are made for distant flows, the system normally relies on argon lasers of about 1 W output.

It should be noted that equation (4.5) could be derived from (4.2), observing that $D = d \cos(\alpha/2)$. The geometrical construction presented in Fig. 4.17b brings forth the difference between these expressions: (4.5) describes the distance

between fringes as measured in plane *AA* whereas (4.2) in plane *BB*.

Angular velocity measurement. The laser gyroscope. A particular velocity measurement that can be made by a laser is that of angular velocity. The instrument designed to do this is called the laser gyroscope. It consists of a laser whose resonant cavity has a ring configuration shown in Fig. 2.27. This laser supports oscillation both for light travelling clockwise and anticlockwise around the ring. The resonant frequencies for these two directions of travel are obtained from the condition that the length of the ring resonator be equal to an integer number of wavelengths. Assume now that the ring is rotating around the axis perpendicular to its plane. Then in the time needed for the light to complete a round trip, the resonator mirrors will move by a very small, but finite, angle. The beam, that is rotating in the same sense as the resonator does, will see an effective resonator length slightly greater than seen by the counterrotating beam. The frequencies of the two oppositely rotating beams are thus slightly different, and their difference frequency is proportional to the angular velocity of the resonator. By beating the two beams together one can measure the angular velocity.

The laser gyros have been found useful for attitude control of satellites and orbiting spacecraft. Modern laser gyros allow the measurement to be made with a precision in the order of 10^{-3} deg/h and are capable of tracking very small angular velocities. This precision is comparable with that available using the most sophisticated (and expensive) conventional gyroscopes.

4.8 Environmental Measurements. Quality Control

Laser monitoring of the environment. Another field in which the laser properties of directionality and monochromaticity are put to good use is that of ambient measurement of the concentration of various atmospheric pollutants. These above all include oxides of nitrogen, carbon monoxide, sulphur dioxide, and a variety of particular matter, such as dust, smoke, and flyash. Conventional techniques of pollution control require collection of the sample for

chemical analysis. These techniques cannot, therefore, give real-time data and some of them are incompatible with automatic measurements in fixed locations. The laser techniques, on the other hand, perform these measurements by remotely sensing the composition of the atmosphere with a light beam without the necessity of sample collection or of any chemical processing. The results of the measurements can be available immediately and there is no distortion of the quantities being measured. Consequently, these techniques yield real-time data and are extremely suitable for sounding time variations of the atmosphere, i.e. for environmental monitoring.

The basic method of laser monitoring involves sending a beam of laser radiation through the sample of atmosphere to be investigated and monitoring either the transmission or the scattering of the light. According to the monitoring technique employed there exist a few versions of laser pollution control, of which we take up the three most widely used.

Ranging pollutant areas by optical radar. This method relies on light scattering from the pollutants in the atmosphere. The optical radar techniques used for the purpose are often referred to as LIDAR, which stands for light detection and ranging. Lidar operates in a manner similar to radar. In its basic form lidar employs a pulsed laser simply as a source of light energy. Light that is back-scattered is detected by a photodetector. The distance to the scattering congestion of particulate matter is inferred from the time the light pulse takes to go to this congestion and return back, in a manner similar to that of a radar ranging system. Lidar, therefore, is very useful in determining *concentrations* of particulate matter and usually gives no information on the nature of the scattering particles. Lidar systems have been used most often for applications in which the total concentration of particulate matter is desired. They have the capability of determining this concentration as a function of distance from the measuring station. Therefore, they provide distributions of atmospheric pollutants in different vertical sections, and monitor variations in these vertical profiles.

Absorption techniques. Absorption techniques are extremely sensitive in detecting specific gases in the atmospheric

sample. The usual procedure is to transmit the laser beam through the studied sample and record with a detector on the opposite side of the sample from the transmitter the attenuation of intensity of the light due to the absorption in the sample. The chemical resolving power of the technique relies on the fact that each chemical compound absorbs at characteristic wavelengths, hence, can be detected by measuring the atmospheric transmittance at one of these wavelengths.

For example, to detect atmospheric methane (CH_4), a frequency-doubled dye laser can be used, operating at $0.372\ \mu\text{m}$. The same laser may be used to detect lower oxide of nitrogen (N_2O) absorbing at $0.389\ \mu\text{m}$. In both cases the sounding range extends for a few hundred metres.

Raman backscattering. The Raman effect involves scattering of light by molecules of gases accompanied by a shift in the wavelength of the light. For a particular gas, the Raman effect involves the appearance of additional spectral lines at a wavelength near the original wavelength. This effect exploits the fact that atoms in a molecule oscillate in a number of certain frequencies, and when a beam of monochromatic light is incident on a gas sample including these molecules, the light output will also contain two sidebands shifted from the original light frequency on either side by a molecular oscillation frequency.

Because the Raman shifts are individual for each molecular species, analysis of backscattered laser light immediately reveals the constituents of the gas sample by their characteristic shifts. To detect sulphur anhydride (SO_2), for example, the atmospheric volume of interest may be scanned by frequency-doubled ruby laser light at $0.347\ \mu\text{m}$.

The frequency of laser radiation in this technique is not subject to limitations. However, the intensity of the Raman return signal appreciably increases when the original frequency is near the resonant absorption of the particular molecular species. Therefore, tunable lasers will be of much greater use for this application; relative increases of several orders of magnitude are possible.

Holographic interferometry for inspection and quality control. Holographic interferometry is the area in which the most significant industrial applications of holography have occurred. In holographic interferometry, the wave-

front stored in the hologram is released by the reconstruction of the hologram and is used to interfere with some other wavefront, so as to form dark and bright fringes in regions of constructive and destructive interference. The two wavefronts can therefore represent the same object at different instants of time.

To have a better insight into the procedure, consider a specific example. The object will be a plate of metal fixed



Fig. 4.18 Interferograms revealing the nature of internal stress occurred in a deformed object (a), and the presence and location of internal defects in an object (b)

in a test bench. We record a hologram for this plate in the normal way. Then, without changing the plate position on the bench, induce a stress to deform the plate. Record this deformed plate on the same hologram with the former reference beam. In reconstructing, this hologram will yield two object waves, one due to the undeformed and the other due to the deformed plate. These waves will interfere to produce familiar pattern of interference fringes covering the image of the plate (Fig. 4.18a). From the width and placement of these fringes one may infer the degree and nature of deformation in various locations of the plate surface. This double-exposure technique is in wide use for the evaluation of stresses that occur in deformation.

Modern production flow lines manufacturing precise items demand accurate control of item parameters both for a ready product and during manufacturing. These parameters include dimensions, shape accuracy, internal flaw evaluation, load critical areas, stress concentrators, and the like. More often than not it is undesirable or just impossible to interfere in the fabrication process with gauges, templates and similar mechanical means of accuracy control. These measurement problems must be solved by non-destructive testing techniques. Holographic interferometry is one such technique.

Holographic inspection of size and shape of items in production can be established by considering the interference of two light waves, one of which is reflected from the item under study and the other is reconstructed from a hologram where the reference item has been recorded.

How internal stress of a loaded item can be brought to light we have learned in general from the aforementioned

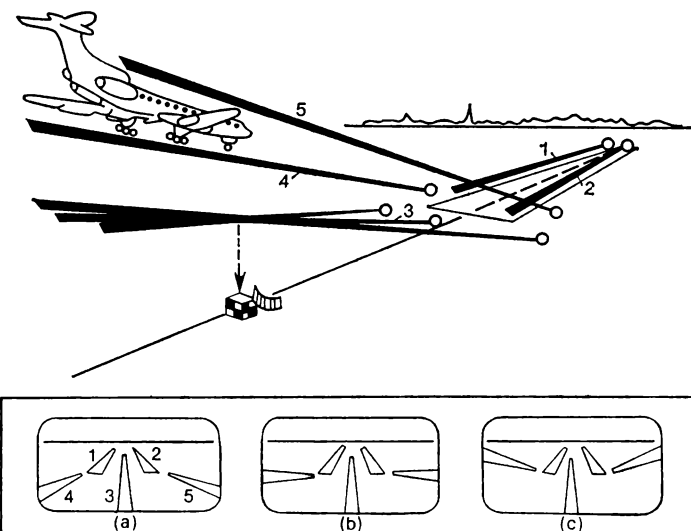


Fig. 4.19 Aircraft landing assisted by the Glissada laser guiding system

particular example of a deformed plate. The evaluation of internal stress is important not only for mechanically loaded structures but also for members subjected to significant and sharp temperature gradients. The object may also contain invisible internal defects, such as flaws, voids, poorly filled welds and the like. If the object is metallic then x-ray testing will be of low help. Acoustic sounding also is able to handle not all defects at all. Here holographic interferometry may come to help—the tested object is subjected to a mechanical load to reveal then by means of a holographic interferogram the presence of internal defects, their size, shape and location.

Consider a specific example of an object constituted by two plates of different metals welded together. The search is for a possible invisible defect of welding—flaws in the weldment. Upon loading and the second exposure, the interferogram, shown in Fig. 4.18b, gives a clear-cut evidence of the presence of invisible defects in the areas where the fringes depart from a regular pattern.

Laser landing system. To facilitate landing safety for modern jet aircraft, Soviet engineers have developed an instrumental landing system for aircraft guiding in night conditions. Continuous He-Ne lasers of this system are placed at certain points along the runway. Lasing in a certain pattern, the beams of the lasers (visible at dusk and night time) provide for the pilot a linear guiding corridor tied in with the runway. The system conveys to the pilot navigation parameters as follows: the heading (heading plane), descent glide path (glide slope), side boundaries of the runway, and distance to the runway. Fig. 4.19 conveys the idea of the Glissada landing system, where rays 1-3 indicate the heading plane, while rays 4 and 5 show the glide slope. The insert shows three views to the runway for three types of approach. In all the three cases the aircraft descends accurate to the heading, but in (a) above the glide path, in (b) accurate to the glide path, and in (c) below the glide path.

4.9 Thermonuclear Fusion

It is already for a quarter of century that intense research has been going on the peaceful harnessing of thermonuclear fusion which nowadays is seen as the controlled production of energy from fusion reactions of light nuclei in a high temperature plasma. The solution of this problem would provide mankind with a virtually inexhaustible source of energy.

According to modern physical concepts, thermonuclear fusion would be easiest to realize in a hot plasma containing heavy isotopes of hydrogen (deuterium, D, and tritium, T). The plasma must have a sufficiently high temperature ($T \approx 10^8$ K) for the highly exothermic fusion reaction to take place



where n indicates a neutron.

The huge temperatures of the plasma are supposed to be achieved by means of powerful laser beams. The idea of laser-assisted nuclear fusion is illustrated in Fig. 4.20. It schematizes a microsphere (glass pellet) a fraction of a millimetre in diameter containing liquid deuterium and tritium. This pellet is irradiated by a laser of sufficiently high

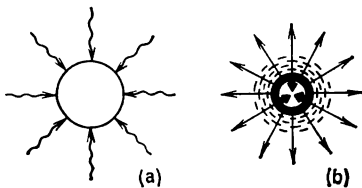


Fig. 4.20 Illustrating the process of thermonuclear microimplosion

energy and short duration so as to induce the $D + T$ reaction (microexplosion). The pulses of 1 ns duration develop at the pellet surface a power density of about 10^{18} W/cm^2 .

Complex calculations have shown that the efficient generation of thermonuclear energy in this system requires not only the heating of the pellet to a very high temperature but also its compression to a density ten thousand times greater than that of the liquid phase. This requires a spherically symmetric heating, and a specially tailored time profile of the firing laser pulses. Upon irradiation of the microsphere the following sequence of events takes place. First a laser pre-pulse, split into a number of beams directed onto the pellet from many directions, heats the pellet so that a low density plasma is generated around the sphere by ablation of its outer material. This low density atmosphere is then irradiated by a second and more intense laser pulse. The absorption of energy in the atmosphere of the pellet leads to a strong material ablation due to surface evaporation.

This rapidly exploding atmosphere causes, by momentum conservation, a violent compression (implosion) of the inner microsphere. At the time of maximum compression, the most intense part of the laser pulse should arrive to produce a significant fusion reaction in the compressed and heated microsphere.

Because the pellet is rather small, the radiation to be focused on it should be fairly coherent, otherwise an effective focusing cannot be achieved. The powerful radiation of high coherence is produced in most laboratories by the master oscillator power amplifier (MOPA) scheme. The laser pulse originates in a low power oscillator where its spatial and temporal characteristics can be accurately controlled. This light is then divided by beamsplitters into several beams each being amplified in a separate channel of a few amplifying stages.

Large laser fusion projects have been under development in several countries, but most notable in the USA and the USSR. In the USA, laser systems giving pulses with an energy of about 10 kJ and peak power of $20-30 \times 10^{12}$ W (terawatt range) have already been constructed. These involve Nd:glass and CO₂ laser systems with the number of beams being 6 for the CO₂ laser (Helios system) and 20 for the Nd:glass (Argus and Shiva systems). Advanced systems giving an order of magnitude more energy and power are also under testing or construction: the Nova system based on Nd:glass amplifiers, (10 beams) and the Antares system based on CO₂ laser amplifiers. In the USSR, a Nd:glass system with 256 beams (Delphin system) has been constructed. The original pulse from a master oscillator is split here and launched into 256 separate chains of laser amplifiers. As a result, each channel yields a light pulse of about 50 J and 1 ns duration. All these beams are simultaneously focused on the target, into a 50 μm diameter spot to develop a power density of 2×10^{15} W/cm².

Calculations indicate that perhaps 10^{14} W may be necessary in a subnanosecond duration pulse in order to achieve scientific breakeven in thermonuclear reactors. Scientific breakeven is defined as the level at which the thermonuclear energy release equals the laser energy input. However, the results are still far from this level. One of the weak points revealed for the aforementioned laser systems concerns the rapid loss of coherence in the amplifying chains. The distorted wavefront prevents the pulse from being adequately focused on the pellet. A way out is seen now in the restoration of the wavefront by methods of adaptive optics.

Exercises**Problems**

1. What frequency range corresponds to the interval of light wavelengths from 0.1 to 10 μm ?
2. What is the photon energy for a light wavelength of 0.6 μm ?
3. The quality factor of an optical resonator is $Q = 2 \times 10^7$ at 0.6 μm wavelength. Compute the loss coefficient for this Q .
4. Suppose we have doubled all the linear dimensions of the resonator, i.e. cavity length and mirror curvature radii and apertures. Will the new resonator be equivalent to the original one?
5. Suppose we have increased two times the aperture of the cavity mirrors. How should the other parameters of the passive resonator be altered to make the new resonator equivalent to the original one?
6. Derive the optimal reflectivity for the output mirror in an 0.5-m long cavity with the loss coefficient 0.081 m^{-1} (except radiative losses) and the initial gain coefficient 0.1 m^{-1} .
7. Find the frequency spacing between two adjacent axial modes for a ruby laser (a ruby rod with polished ends acting as mirrors), given the rod length is 0.6 m and the ruby refractive index is 1.76.
8. Assume that all the pumping power of the pumping lamp is being absorbed by the active species of the ruby laser (chromium ions) which are raised to the 4F_1 state to fall then to the upper laser level. Referring to Fig. 2.4, estimate the efficiency of this laser.
9. The ruby lasers are known to possess efficiencies below 1%, that is appreciably lower than the value obtained in the previous problem. Why?
10. Prove that at the Brewster angle of incidence, the reflected and refracted rays are mutually orthogonal.
11. Describe the geometry of the optical resonator, specified on the stability diagram (see Fig. 2.28) by $g_1 = g_2 = 2$.
12. What is the geometry of the optical resonator producing the g -values $g_1 = 1$ and $g_2 = 1/2$ on the stability diagram (see Fig. 2.28)?

13. Referring to Fig. 2.29, estimate the angle of divergence for a light beam of $0.5 \mu\text{m}$ wavelength leaving the 0.5-m long resonator.

14. Estimate the speed (switching rate) of a fused silica acoustooptic shutter for a light beam of 1.2 mm diameter, given the velocity of sound in the shutter material is $6 \times 10^3 \text{ m/s}$.

15. Compute the peak power of a pulse, given that the laser operates at a pulse repetition rate of $f = 1 \text{ MHz}$ (a cavity dumping mode) yielding pulses of $\tau = 20 \text{ ns}$ duration with an average power of the train being $P = 10 \text{ W}$.

16. The gain profile linewidth of a ruby laser is 6 GHz. Use the result of problem 7 to compute the maximum possible number of longitudinal modes for this laser.

17. Estimate the pulse peak power for a laser operating in a giant-pulse mode, given: pump pulse energy, 1 kJ; laser efficiency, 0.5%; giant pulse duration, 10 ns.

Answers

1. From 3×10^{13} to $3 \times 10^{15} \text{ Hz}$.

2. 2 eV.

3. By virtue of (1.26) we get the loss coefficient of 0.5 m^{-1} .

4. It will not. For the new resonator, the Fresnel number is twice as large as that of the original cavity; see (1.32).

5. The resonator length and mirror radii of curvature should be increased four times; see (1.32).

6. From (1.49) the optimal coefficient of radiant losses amounts to 0.009 m^{-1} . By making use of (1.51), where for $x \ll 1$ one may adopt $e^x = 1 + x$, the optimal reflectivity of the output mirror is found to be 99% for this case.

7. According to (1.55), the frequency spacing in question equals $1.4 \times 10^8 \text{ Hz}$.

8. The photon efficiency for this situation is defined as the ratio of emitted to pumping photon energies. Referring to Fig. 2.4, this ratio is approximately $1.5/2.5 = 0.6$. Therefore, the efficiency in question amounts to 60%.

9. In fact, not all of the pumping energy is absorbed by the active species. Besides, a proportion of the excited ions decays directly to the ground level without falling first to the upper laser level.

10. Let β be the angle of refraction, and α the angle of incidence equal to the Brewster angle and to the angle of

reflection; we were to prove $\beta + \alpha = 90^\circ$. Observing that $\sin \alpha / \sin \beta = n$ and $\tan \alpha = n$, we conclude $\sin \beta = \cos \alpha$. In other words, α and β are complementary to 90° , which proves the statement.

11. From (2.1) it follows that the considered cavity's radii of curvature $r_1 = r_2 = -L$. This points to an unstable resonant cavity produced by two convex mirrors whose radii of curvature equal the cavity length.

12. From (2.1) $r_1 = \infty$ and $r_2 = 2L$. These radii are characteristic of a stable resonator produced by a plane mirror and a concave mirror of curvature radius twice the resonator length.

13. With reference to Fig. 2.29 we can conclude that the angle of divergence measured in radians is determined approximately as $2w/L$. By virtue of (2.4) we find that this angle is about 0.001 radian, i.e. 3.5 minutes.

14. The shutter switching time may be estimated as $d/v = 2 \times 10^{-7}$ s.

15. The peak power in this case may be estimated as $P/\tau_f = 500$ W.

16. About 40.

17. The pulse energy is 5 J. Its peak power may be found as the ratio of this energy to the pulsedwidth, whence 5×10^5 kW.

Appendix

Performance Data for Selected Soviet-made Commercial Lasers

Table A1 Free-oscillating Solid State Lasers

Soviet type designation	Material	Pulse energy, J	Pulse duration, ms
ГОР-100М	Ruby	100	1
ГОР-300	Ruby	300	0.5
ГОС-301	Nd : glass	300	0.8
ГОС-1000	Nd : glass	1000	20
ЛТИ-4	Nd : YAG	0.1	0.04

Table A2 Solid State Q-switched (Giant Pulse Mode) Lasers

Soviet type designation	Material	Pulse energy, J	Pulse duration, ns	Peak power, kW
ОГМ-20	Ruby	0.42	20	2×10^4
ЛТИПЧ-4	Nd : glass	2	15	10^5
ЛТИ-1	Nd : YAG	0.01	10-12	10^3
ЛТИ-3	Nd : YAG	0.03	10-12	3×10^3
ЛТИ-5	Nd : YAG	0.05	8-12	5×10^3

Note: The ЛТИ lasers operate in a single pulse mode, and in a repetitively Q-switched mode with pulse repetition rates of 12.5, 25, 50, and 100 Hz.

Table A3 Nd:YAG Q-switched Lasers with Intracavity Harmonic Generation

Soviet type designation	Generated harmonic	$\lambda, \mu\text{m}$	Pulse energy, mJ	Pulse duration, ns	Peak power, kW
ЛТИПЧ-3	2nd	0.53	3	8-10	300
ЛТИПЧ-4	3rd	0.35	0.45	8-9	50
ЛТИПЧ-5	4th	0.26	0.16	7-9	20
ЛТИПЧ-6	2nd	0.53	5	8-10	500
ЛТИПЧ-7	3rd	0.35	1	8-9	100
ЛТИПЧ-8	4th	0.26	0.5	7-9	50

Note: (i) the ЛТИПЧ-3, 4, 5 models are based on the ЛТИ-3 design; (ii) the ЛТИПЧ-6, 7, 8 models are based on the ЛТИ-5 design; (iii) for the frequency triplers and quadruplers a frequency doubler output is also possible.

Table A4 Continuously Pumped Nd:YAG Lasers: Pulsed and CW

Soviet type designation	$\lambda, \mu\text{m}$	Pump power, kW	Pulse rep. rate, kHz	Average power, W	Pulse duration, μs
ЛТИ-501	1.06	$\leqslant 5$	5-20	$\geqslant 6$	0.3-0.6
ЛТИ-502	1.06	$\leqslant 5$	5-20	$\geqslant 8$	0.3-0.6
ЛТИ-701	0.53	$\leqslant 5$	5-6	$\geqslant 4$	0.3-0.4
ЛITH-401	0.53	$\leqslant 5$	CW	1-2	

Note: (i) all models operate on the fundamental mode; (ii) 0.53 μm corresponds to intracavity second harmonic generation; (iii) pulse trains are provided by acoustooptic Q-switching.

Table A5 Gas-discharge CW Lasers

Model	Type	Power, W	Model	Type	Power, W
ОКГ-13	He-Ne	0.0002	ЛГ-109	Ar ⁺	1
ЛГ-56	He-Ne	0.002	ЛГ-30	CO ₂	5
ЛГ-65	He-Ne	0.02	ЛГ-25	CO ₂	25
ЛГ-38	He-Ne	0.05	ЛГ-43	CO ₂	40

Table A6 Optically Pumped Tunable Dye Lasers

Soviet type designation	Tuning range, μm	Linewidth, nm	Pulse rep. rate, pps	Pulse energy, J
ЛЖИ-404	0.43-0.65	0.4	1/3	0.02
ЛЖИ-406	0.43-0.65	0.2	1/6	0.1
ЛЖИ-408	0.43-0.65	0.2	2/15	0.5
ЛЖИ-409	0.43-0.65	0.2	1/15	1

Note. (i) the linewidth is given for a selective resonator with a reflective diffraction grating; (ii) the pulse energy refers to $\lambda = 0.59 \mu\text{m}$ in a non-selective cavity.

Where to Read More about Lasers

In Russian

L. V. Tarasov: *Lasers—Reality and Hope* (Prosveshchenie, Moscow 1984)

L. V. Tarasov: *Optics Born by the Laser* (Prosveshchenie, Moscow 1977)

Yu. L. Klimontovich: *Quantum Generators of Light and Nonlinear Optics* (Prosveshchenie, Moscow 1966)

V. S. Letokhov, N. D. Ustinov: *Power Lasers and Their Applications* (Sovetskoye Radio, Moscow 1980)

G. V. Venikov: *Optical Computing Systems* (Znanie, Moscow 1976)

In English

O. Svelto: *Principles of Lasers* (Plenum Press, New York 1982)

D. C. O'Shea, W. R. Callen, W. T. Rhodes: *Introduction to Lasers and Their Applications* (Addison-Wesley Publ. Co., Reading, Massachusetts 1977)

J. F. Ready: *Industrial Applications of Lasers* (Academic Press, New York, London 1978)

Index

A

- Acoustooptic Q-switches, 103
- Adaptive optics, 130
- Anti-Stokes component, 132
- Apodizing diaphragms, 118
- Argon laser, 64
- Atomic terms, 60

B

- Band gap, 82
- Beam
 - deflectors, 135
 - diffraction limit, 117
 - manipulation, 134
 - spot size, 92
 - waist, 91
- Beamsplitter, 17
- Birefringence, 123
- Bleachable cell, 104
- Bosons, 12
- Brewster angle, 59

C

- Carbon dioxide laser, 65
 - gas-dynamic, 74
 - longitudinal flow, 66
- Chemical laser, 77
- Coherence, 14
 - degree of, 16
 - time, 17
- CO₂ laser, *see* Carbon dioxide laser
- Conduction band, 82
- Conversion efficiency, 123
- Cube corner reflector, 171

D

- Deuterium fluoride chemical transfer laser, 79
- Diffraction limit, 117
- Doppler
 - ranging, 168
 - velocimetry, 171
- Doubly resonant parametric oscillator, 127
- Dye laser, 53

E

- Einstein coefficients, 22
- Electroionization lasers, 70
- Electronic configurations, 60
- Electrooptical shutter, 100
- Emission line, 38
- Eximer laser, 69

F

- Fermi-Dirac statistics, 13
- Fermions, 12
- Fluorescent line, 38
- Four-level laser, 27
- Fourth harmonic generation, 123
- Frequency multipliers, 125
- Frequency tuning, 125
- Fresnel number, 33
- Fundamental wave, 123

G

- Gain coefficient, 34
- Gain curve, 37
- Gain profile, 38
- Giant pulse generation, 107
- Glass laser, 53
- G-parameters, 90
- Ground level, 25

H

- Harmonic generators, 124
Helium-neon laser, 58, 62
Hologram, 151
 amplitude, 156
 Gabor, 155
 Leith-Upatnieks, 155
 reflection, 155
 thick, 156
Holography, 150
 for coding, 161
 for data storage, 160
 for information search, 161
 for pattern recognition, 162

I

- Image, holographic
 conjugate or real, 154
 primary or virtual, 154
 pseudoscopic, 155
Index ellipsoid, 121
Injection laser, 88
 optically coupled, 163
Interference technique, 99
Interferometric distance measurements, 170
Intracavity elements, 95
Ion laser, 57
Irradiance, 15

K

- Kerr effect, 100

L

- Laser
 applications, 138
 basic principles, 9
 beam waist, 91
 dual, 163
 effect on materials, 139
 gain curve, 37
 historical review, 41
 intracavity control, 94
 oscillation, 27, 36
 output control, 94
 phase conjugation, 130
 pulse, 106
 schemes, 26

- single mode, 97
spot size, 92
wavefront correction, 129
Laser, types
 Ar⁺, 64
 chemical, 76
 CO₂, 65
 dye, 53
 electron-beam, semiconductor, 85

- eximer, 69
 gas-discharge, 45
 gas-dynamic, 73
 glass, 53
 He-Ne, 58
 injection, 88
 Nd : YAG, 51
 photodissociation, 55
 ruby, 49
 semiconductor, 81
 Soviet-made, commercial 184
Laser cutting, 143
Laser environmental monitoring, 173
Laser for information systems, 157
Laser for thermonuclear fusion, 178

- Laser gyroscope, 173
Laser heat treatment, 142
Laser hole perforating, 144
Laser isotope separation, 148
Laser landing system, 178
Laser material working, 139
Laser rangefinder, 168
Laser surgery, 145
Laser welding, 141
Lasing level, 26
Level nomenclature, 25
LIDAR, 174
Light amplification, 23
Losses
 cavity, 31
 diffraction, 32
 radian, 32, 37

M

- Maser, 42
Mode
 asymmetrical stretching, 67
 axial, 40

- bending, 67
 cavity dumping, 110
 fundamental, 40
 longitudinal, 41
 Q-switching, 100
 symmetric stretch, 67
 TEM, 40
 transverse, 41
 vibrational, 67
Mode locking, 111
 active, 113
 methods of, 113
 passive, 113
Molecular laser, 65
- N**
- Nd : YAG laser, 51
 Neutral atom laser, 57
 Nonlinear media, 118
 Nonlinear mirror, 133
 Nonlinear optics history, 128
- O**
- Optical cavity, *see* Resonator
 Optical communications, 164
 Optical deflectors
 analog acoustooptic, 135
 analog electrooptic, 135
 digital electrooptic, 136
 prism, 135
 Organic dye lasers, 53
- P**
- Parametric oscillations, 125
 doubly resonant, 127
 singly resonant, 127
 Phase conjugation, 130
 Phase matching condition, 121
 Photochemical laser, 56
 Photoelastic effect, 103
 Photon, 11
 Piezoelectric transducer, 103
 Plane of polarization, 10
 Plasma laser, 79
 Pockels cell, 100
 Population inversion, 23
 Pulsed lasing, 106
 Pulse plasma laser, 81
- Pulse trains, 110
 Pumping
 chemical, 25
 electrical, 25, 45
 electroionizing, 71
 gas-dynamic, 73
 heat, 25
 level, 26
 optical, 25, 45
 schemes, 25
- Q**
- Q-switching
 acoustooptic, 103
 mechanical, 100
 methods of, 100
 passive, 104
 saturable absorber, 104
 Quality factor, defined, 30
- R**
- Radiant losses, 32
 Raman back scattering, 175
 Resonant collision energy transfer, 63
 Resonator, 29
 confocal, 91
 equivalent, 33
 linear, 89
 modes, 40
 ring, 89
 stable, 90
 unstable, 117
 Ruby laser, 49
- S**
- Second harmonic generation, 120
 nonlinear polarization, 121
 phase matching for, 122
 Semiconductor laser, 81
 Semiconductors
 degenerate, 84, 86
 intrinsic, 83
 transitions in, 83
 Single mode operation, 97
 Singly resonant parametric oscillator, 127
 Small signal gain, 34
 Spatial signal, 158

- Spontaneous emission, 21
Spot size, 92
Stability of optical resonator, 90
Stimulated Brillouin scattering,
 132
Stimulated emission, 20
Stimulated emission cross section,
 24
Stokes satellites, 132
- T
- Transition line, 38
Transitions, 18
 in semiconductors, 83
 lasing, 23
 suppression of, 95
- Valence band, 82
Visibility of fringes, 14
- W
- Wave
 extraordinary, 121
 idler, 126
 object, 150
 ordinary, 121
 pump, 126
 reconstructing, 152
 reference, 150
 signal, 126, 150
- Wavefront correction, 129
Waveguides, 166
Wave trains, 14

TO THE READER

Mir Publishers welcome your comments on the contents, translation, and design of the book. We would also be pleased to receive any suggestions you care to make about our future publications.

Our address is:
USSR, 129820,
Moscow, I-110, GSP,
Pervy Rizhsky Pereulok, 2,
Mir Publishers

